Upcycle Timber

A Design-to-Fabrication Workflow for Free-Form Timber Structures with Offcuts

Bauhaus-Universität Weimar

by Dominik Reisach B.A.

Weimar 2022

Upcycle Timber

A Design-to-Fabrication Workflow for Free-Form Timber Structures with Offcuts

This Thesis is submitted in partial fulfillment
of the requirements for the degree of

Master of Sciences in Architecture

at the Bauhaus-Universität Weimar
Faculty of Architecture and Urbanism

by
Dominik Reisach B.A.

2022

Professor Dr.-Ing. Sven Schneider

Professor Dr. Jan Willmann

Professor Dr.-Ing. Stephan Schütz

Acknowledgements

Abstract

This thesis presents methods for upcycling and designing low-engineered free-form timber structure with offcuts—a waste material from timber production. In particular, the focus is on the development of a complete design-to-fabrication workflow that includes the measuring and assembly of offcuts, thus closing the digital chain. The process is streamlined to minimize material waste and facilitate the disassembly and reassembly of offcut structures. In the end, the workflow provides great flexibility and enables the design and realization of a wide range of architectural and structural typologies. However, these potentials are challenged by (1) the high complexity of the offcuts' non-standard geometries, (2) the spatial relationship between the bespoke elements of an assembly, and (3) the condition of the material.

This research investigated these complex challenges and developed appropriate tools for an architectural design process with upcycled timber. Primarily, these include computational design methods and tools to align and orient offcuts, compute wood joints, and thus to address design-specific parameters. The resulting information was used in integrated data workflows to generate and process fabrication-relevant data. Thereby, it informed and facilitated the handcrafting and robotic fabrication of several prototypes. Together with the strength tests that evaluated the structural capabilities of the waste wood, they validated the concept.

The relevance of this work is demonstrated through the design, robotic fabrication, and collaborative assembly of a 1:1 prototype. It proved that the integrated design-to-fabrication workflow is feasible to construct low-engineered free-form timber structures with offcuts, and, particularly, that these structures are both statically and aesthetically viable. In addition, the material-aware design tool is able to minimize fabrication waste and to conceive structures that follow the principle of design-for-disassembly—further contributing to the sustainability of the concept.

Contents

List of Figures

Listings

Chapter 1
Introduction

1.1 Background

The current debate in the European Union (EU) about sustainable development has implications for a wide range of sectors and industries. That includes the architecture, engineering, and construction industry, which is responsible for an estimated 38% of the waste generation and for 36% of the CO_2 emission in the EU.[1] The proposed strategies to tackle these challenges are manifold. For instance, they include a transition to a circular economic model and the extensive use of materials with a low or negative carbon footprint, e.g., timber.[2] Combined, both strategies imply the reuse and upcycling of timber for architectural and structural applications. The data from life cycle assessments (LCA) support this notion, showing that reused and upcycled timber reduces CO_2 emissions by 44–82%.[3] That reinforces the extension of the lifespan of timber products.

However, there are additional far-reaching implications for the discipline of architecture. It must truly arrive in the digital age to specifically and fundamentally address the sustainability challenges mentioned above. That presumes the coupling of the design, planning, and fabrication processes into interdependent workflows. This holistic approach involves the use of computational design and digital fabrication methods.

In this context, this thesis focuses on the upcycling of timber for architectural and structural applications. To this end, it is relevant to understand the timber industry's supply chains, waste management, and design and manufacturing practices.

1.1.1 Forestry and Timber Industry

The supply chain of timber products begins in the forests when the trees are planted. They form the available stock as they grow and are monitored throughout their lifetime. As soon as they reach a specific size, they are ready for harvesting. The selection of the area to be harvested is somewhat more complex. Primarily, the price of wood per cubic meter determines whether it is worthwhile to clear

---

[1] European Construction Sector Observatory, *Analytical Report: Improving energy and resource efficiency*, tech. rep. (Brussels, 2018).

[2] European Commission, *A new Circular Economy Action Plan: For a cleaner and more competitive Europe*, tech. rep. (Brussels, 2020), 11.

[3] Anders Lendager, *Solution: Circular Buildings* (Copenhagen: Danish Architectural Press Arkitektens Forlag, 2020), 278–94.

an area and sell the tree logs. However, there are circumstances in which this is necessary or even requested, despite economic losses. Specifically, bark beetle infestations are increasingly problematic and require seemingly healthy forests to be cleared prematurely. Areas that are densely grown or difficult to reach facilitate that issue because they are not profitable to harvest. Nevertheless, they pose a threat to other areas because they function as breeding grounds for bark beetles.

After a specific area is selected for clearing, a so-called "harvester" logs and processes the trees on-site. For that, heavy machinery drives on specified forestry roads. Perpendicular to these roads run crop strips called swaths. The maximum range of the harvester determines the distance between the swaths. Thereby, it can drive on them and minimize the densification of the forest soil. After the harvester logs a tree, it removes the branches and cuts the tree log into pieces with a length of five meters. That is the maximum size the trucks can transport. The timber logs are stored in the forest and gradually moved to the fabrication facilities. The branches, leaves, needles, and bark are layered on top of the swaths. These layers act like a pillow for the harvester to drive on. Thereby, there is even less strain on the forest soil. Also, smaller logs, moldy wood, and tree crowns are left in the forest. These leftovers will degenerate to soil and provide the nutrients for the next generation of trees.

Once the tree logs arrive at the fabrication facilities, they are stored until processed. The procedure starts with quality control. On a conveyor belt, each log is peeled, measured, and scanned for deficiencies. Then, the slabs are cut and immediately ground up. From the now rectangular cross-section beams and boards are cut. Finally, these products are dried and stored until they are sold. In that process, 40% of the wood is turned into waste in the form of sawdust and ground bark. From the remaining 60%, only 15–20% are fabricated with high aesthetic surface quality.[4] The rest of the material has blue mold or too many knots and, therefore, lends itself for hidden structural purposes or formwork only. The regulations in the timber industry expect every element to undergo normed quality control. Irrespective of whether an element is a serial product or a product on-demand, it must be inspected. That leads to even more waste. Depending on the product, defective areas are cut or the element as a whole is sorted out.

The timber industry successfully uses a so-called "Cascading Utilization" to extend the lifespan of wood products.[5] This means that at the end of their life cycle they are converted into different products. Usually, the material is downcycled to particle-based products, including medium-density fiberboards (MDF) and oriented strand boards (OSB). Further downcycling processes provide resources for pulp and paper production. However, most of the waste wood produced in the process is not part of the cascading cycle. Rather, it is incinerated to produce energy. This concerns almost 80% of the recovered waste wood.[6] Accordingly, if 40% of the wood from the forests is turned into waste and 80% of the waste is incinerated to produce energy, the process of burning affects up to 32% of the total wood extracted.

To obtain a better understanding of the actual extent of these figures and practices, the timber industry in Thuringia was used as an example in this master's thesis. In the scope of this pursuit, a range of interviews were conducted with relevant stakeholders. These implied the state's forestry agency, the local sawmill association, and two wood manufacturers.

---

[4] These numbers were given in interviews with several stakeholders in the timber industry. They are looking for solutions to recycle the waste material to avoid incineration and, therefore, openly communicate the percentage of waste produced. There is a brochure as a reference as well: https://holzwertplus.de/files/pdf/bmbf_Innoforum_Holzwertplus_7.pdf Furthermore, these numbers align with the findings of various investigations, cf. Adhikari and Ozarska. (Shankar Adhikari and Barbara Ozarska, "Minimizing environmental impacts of timber products through the production process "From Sawmill to Final Products"," *Environmental Systems Research* 7 [2018]: 6, doi:10.1186/s40068-018-0109-x).

[5] The "Cascading Utilization" of wood can be considered a part of the Circular Economy. (Claudia Mair and Tobias Stern, "Cascading Utilization of Wood: a Matter of Circular Economy?," *Current Forestry Reports 3*, 2017, 281–95, doi:10.1007/s40725-017-0067-y).

[6] Karin Höglmeier, Gabriele Weber-Blaschke, and Klaus Richter, "Evaluation of Wood Cascading," in *Sustainability Assessment of Renewables-Based Products: Methods and Case Studies*, ed. Jo Dewulf, Steven De Meester, and Rodrigo A. F. Alvarenga (John Wiley & Sons, Ltd., 2015), 335–46, doi:10.1002/9781118933916.ch22.

1.1.2 Thuringian Context

In general, the forestry and timber industry in Thuringia applies the same processes as described in the previous section (see Chapter 1.1.1). Of particular interest are the local supply chains and the implemented waste management strategies.

Most of the forests are located in the southern mountainous regions of Thuringia. They mainly consist of softwood species. There, Norway spruce (*Picea abies*) is the most widespread, followed by Baltic pine (*Pinus sylvestris)*. To the west and north of the region, there are hardwood forests with significant stocks of European beech (*Fagus sylvatica)* (see Figure 1.1). The apparent homogeneity of the forests in the regions is the result of reforestation measures that began in the 18th century. At that time, the excessive use of wood for energy and construction purposes led to the deforestation of large areas. The lack of sustainable forest management highlighted this trend. To counteract the resulting ecological and economic problems, fast-growing coniferous species—Norway spruce and Baltic pine—were planted. However, these monocultures brought additional challenges, e.g., their susceptibility to bark beetles, droughts, and soil degradation.[7] Global warming poses a further threat to tree populations, as the regional climate is changing faster than trees can adapt. The Thuringian State Forestry Administration is therefore currently converting the state forests into mixed forests with hardwood and softwood species to increase their resilience.[8] However, the current distribution of forests determines the focus of the local timber industry (see Figure 1.1).

In the north and west of Thuringia, the manufacturing companies focus on hardwood, specifically on European beech. On the contrary, the industry in the south works almost exclusively with softwood timber primarily from Norway spruce. Their raw wood comes mainly from local forests. Forestry data reflect this distribution. In Thuringia, Norway spruce is the most available wood with 76.1 million solid cubic meters, followed by European beech with 39.5 and Baltic pine with 25.1 million solid cubic meters. However, the harvested and processed wood is mainly Norway spruce with a share of 60.2%, followed by European beech with 18.7% and Baltic pine with 11.8% (see Figure 1.2). Accordingly, at least 72% of the utilized timber is softwood.[9] Because of this significant trend, it made sense to look at the softwood industry, which also happens to be home to the region's largest manufacturers.

In the initial phase of this work, site visits were made to two different timber manufacturers. Both factories are located in southeastern Thuringia close to softwood forests. It is the most important resource of both companies, even if their products are different. The first company visited produced structural timber elements of various sizes. For this purpose, they lengthen the five meters long logs with glued finger joints. The second company produced standardized timber planks in series. The site visit included a detour into the forest to see a harvester in action.

The insights into the Thuringian forestry and timber industries revealed a range of waste products (see Figure 1.3). Depending on the point in the value chain at which they occur, different recycling mechanisms take place in the cascading cycle. However, most of the products are downcycled. The waste from the timber harvesting, branches, leaves, needles, bark, moldy logs, and treetops, decomposes in the forests. The production waste—sawdust, ground bark, and woodchips—is downcycled into wood insulation, pulp, and bark mulch or compressed into pellets to generate thermal energy. Discarded wooden planks are either sold as low-quality products or burned. Offcuts are burned as well or shredded into woodchips for further processing.

---

[7] Frank Reinhardt and Franz Makeschinr, "Historische Waldumbauversuche mit Rotbuche in Form der „Grünen Augen" im Thüringer Forstamt Hummelshain: Entstehungsgeschichte und aktuelle Bedeutung," *Forstwissenschaftliches Centralblatt vereinigt mit Tharandter forstliches Jahrbuch 120*, 2001, 318–30, doi:10.1007/BF02796103.

[8] Thüringer Ministerium für Infrastruktur und Landwirtschaft (TMIL), *Waldzustandsbericht 2019: Forstliches Umweltmonitoring in Thüringen*, tech. rep. (Erfurt, 2020).

[9] Both Norway spruce and Baltic pine are softwoods.
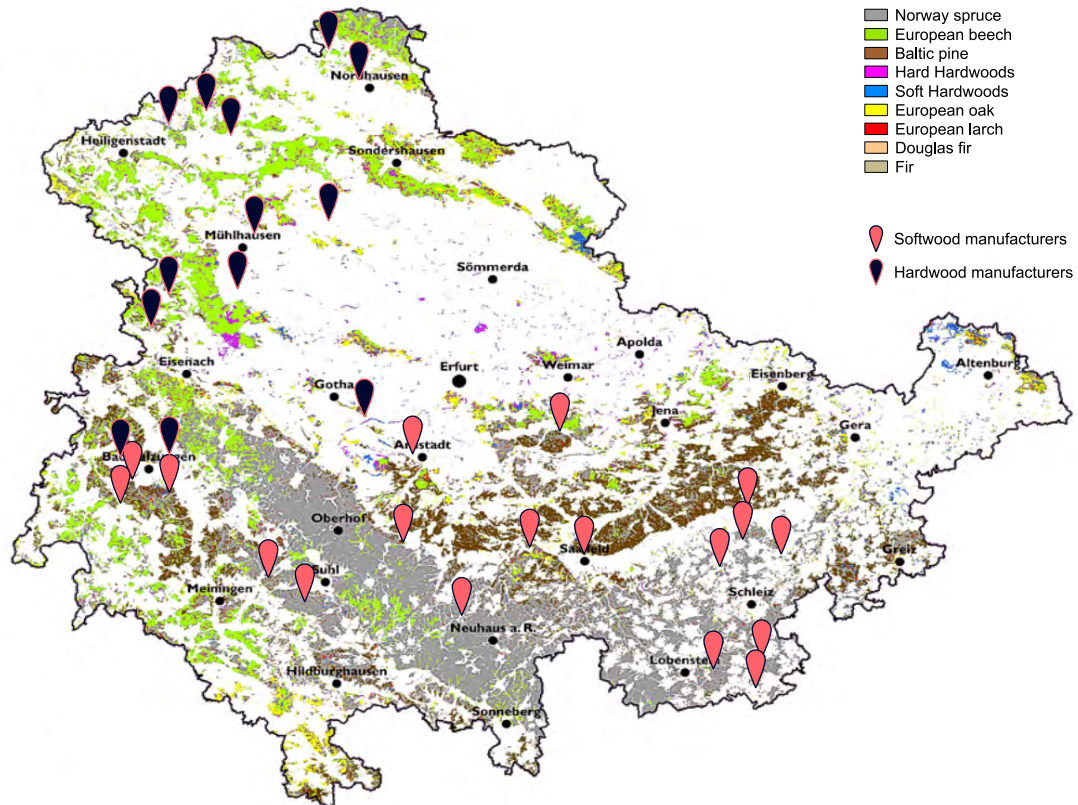
Figure 1.1: *Distribution of tree species in Thuringia and the relation to timber manufacturing companies.* Illustration by Ingolf Profft, December 2, 2020. Lecture at the Bauhaus-Universität Weimar. Edited by the author.

The process of creating offcuts was particularly interesting. Structural timber products must be inspected for any defects prior to shipment. Problematic areas are cut off from the piece of wood. Scraps are either re-glued or sold, while the so-called offcuts are disregarded as waste. There are several reasons for this procedure, such as blue mold, the number and size of knots, cracks, defect gluings, and bark residues (see Figure 1.4). These can be weak spots in an integral structural product.[10] However, with careful selection, these offcuts are still applicable for structural purposes, and, as such, for architectural applications beyond downcycling.

---

[10] There are also aesthetic reasons for cutting the pieces. For example, blue mold develops when a tree is cut and stored too long in a humid environment, e.g., in the forest. After the wood dries, blue mold is not a health hazard, nor does it affect the statics of the wood. However, it disrupts the clean surface aesthetic of the timber product and significantly reduces its selling price. Therefore, it is cut off.
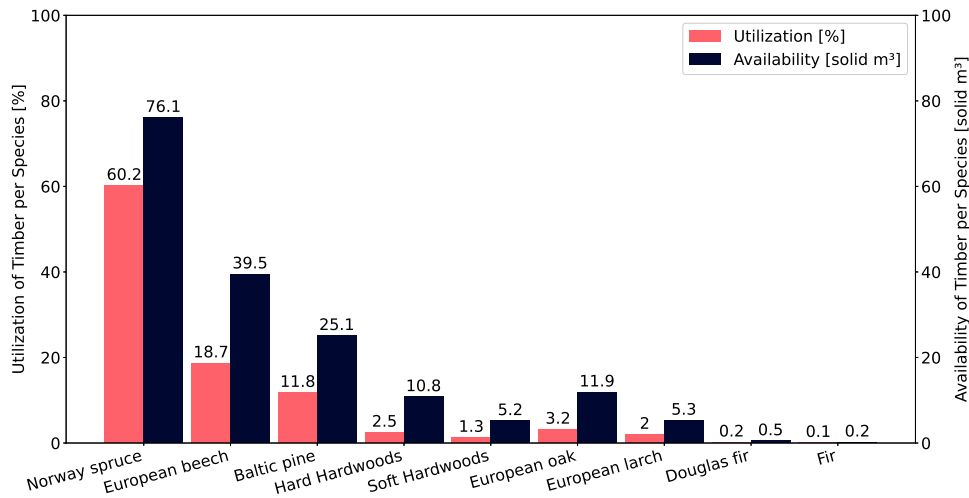
Figure 1.2: *Utilization and availability of timber per tree species in Thuringia.* Data retrieved from Wenzel et al.

1.1.3 Material and Offcut Properties

Working with offcuts requires an understanding of the material's characteristics. Multiple publications extensively described the properties of wood, most notably Dinwoodie[11] and Zwerger.[12] However, the ones most relevant for this work are covered in the following. The cellular structure of wood consists of cellulose fibers bonded together and protected by lignin, making it a natural composite material.[13] Since the majority of these cells are aligned vertically, i.e., in one direction, wood is considered an anisotropic material.[14] Accordingly, it possesses different properties depending on the orientation: Parallel to its fibers, it demonstrates the best structural performance and, thus, the weakest perpendicular to them. That is true for both tension and compression strengths.[15] Also, timber has significantly greater tension than compression strengths if the grains are relatively straight and only a few knots are present.[16] However, the resistance to compression forces is also dependent on the moisture content.[17]

The specific offcuts covered in the scope of this work are made of Norway spruce. It is softwood with typical characteristics. Compared to other species, its density is in a range of medium to high.[18] These variations are due to several factors, i.e., elevation, climate, and soil fertility, but also tree age and silvi-

---

[11] J. M. Dinwoodie, *Timber: Its Nature and Behaviour* (London: E & FN SPON Online Taylor & Francis, 2000).

[12] Klaus Zwerger, *Wood and Wood Joints: Building Traditions of Europe, Japan, and China* (Basel: Birkhäuser, 2011).

[13] Dinwoodie, *Timber*, 23–29.

[14] Dinwoodie, *Timber*, 5.

[15] Dinwoodie, *Timber*, 161.

[16] Knots distort and interrupt the grains of the timber, reducing its structural capabilities. The amount of impairment depends on their size and distribution. (Dinwoodie, *Timber*, 163).

[17] Dinwoodie, *Timber*, 161.

[18] Dinwoodie, *Timber*, 155.

Figure 1.3: *Waste products identified in the Thuringian timber industry: a) Branches and needles in a forest, b) Bark, c) Woodchips, d) Sawdust, e) Timber planks that were discarded due to deformations or splits, f) Offcuts.*

cultural practices.[19] In general, though, the density of timber correlates with its structural capabilities.

---

[19] Geir Vestøl et al., "Bending Properties and Strength Grading of Norway Spruce: Variation within and between Stands," *Canadian Journal of Forest Research* 44 (February 2014): 128–35, doi:10.1139/cjfr-2013-0187.

Figure 1.4: *Offcut with cracks and blue mold.*

Since Norway spruce wood is in the medium to high range, it also has a good strength to weight ratio.[20] Paired with the fast growth rate of the trees, their popularity in timber construction becomes obvious.[21] Therefore, from a material perspective, the offcuts are still suitable for the use in architecture.

1.2 Problem Statement

In the context of increasing demand for timber products, this thesis identifies three challenges: first, the upcycling of waste from wood production, second, the architectural and structural use of offcuts, and third, the integration into a unified design-to-fabrication workflow that streamlines all challenges to a common goal.

1.2.1 Upcycling of Timber

The recycling of timber is imperative from an environmental point of view. As mentioned above, the use of wood in the EU will steadily increase due to the advancing automation in timber manufacturing, awareness of the threat posed by the climate crisis, and recent policies. That could improve the environmental footprint of the construction sector, as buildings could become significant carbon sinks through

---

[20] Dinwoodie, *Timber*, 164.

[21] The maximum rate of height growth per anno for Norway spruce is among the highest of the examined tree species. (I. Colin Prentice and Harry Helmisaari, "Silvics of north European trees: Compilation, comparisons and implications for forest succession modelling," Modelling Forest Succession in Europe, *Forest Ecology and Management* 42.1 [1991]: 79–93, doi:https://doi.org/10.1016/0378-1127(91)90066-5).

the structural use of wood.[22] While this is a reasonable development, it assumes that the production cycle is also sustainable.

The timber industry is already very effective in the utilization of its waste. However, current processes for downcycling wood involve burning the majority of waste wood for energy. These practices have been industrially established over a long period of time and, simultaneously, are too efficacious to develop new strategies for wood reuse and upcycling. However, life cycle assessments (LCA) show that reused and upcycled wood reduces CO_2 emissions by 44–82% compared to new wood.[23] In this regard, reuse—rather than recycling—also appears to significantly reduce emissions.[24] Further LCA calculations showed that waste wood reuse improves all other environmental impact factors as well.[25] The data support the extension of the lifespan of timber products, and, therefore, the reuse of waste timber.[26]

From the previously identified timber waste products, the offcuts appeared to have the most potential. They are regularly produced in large enough quantities that upcycling for architectural and structural applications is justified. Also, their geometric constitution enables a range of possible implementations. However, designing with offcuts presents significant challenges.

Conventional design processes take place in an iterative manner, where material properties and details are considered as the project progresses. In the early stages, spatial and functional qualities claim most of the attention. However, there are exceptions, for instance, if a specific structural material is already part of the conceptual design because of sustainability or availability reasons. In particular, best practices in timber architecture demand that the material properties are already considered from the very beginning of the design and planning phase.[27] Designing with offcuts requires a partially similar, but rather unconventional and more restricted approach. There are added constraints since the material, i.e., the offcut, is already present with its dimensions and properties. Even though the discrete-like offcuts seem to be perfect cuboids, they have non-standard geometries.[28] Additionally, there are minor but relevant differences in their sizes.[29] Thus, the challenge is to adapt the design concept to what is achievable with the available material.[30] Furthermore, the selection process of the material is vital. Offcuts with cracks should be avoided because their structural capabilities are questionable. Also, it is not advisable to select heavily deformed offcuts since they have to be pre-cut. This additional step is time and resource-consuming.

---

[22] Galina Churkina et al., "Buildings as a global carbon sink," *Nature Sustainability 3*, 2020, 269–76, doi:10.1038/s41893-019-0462-4.

[23] Lendager, *Solution*, 278–94.

[24] Jim Hart and Francesco Pomponi, "More Timber in Construction: Unanswered Questions and Future Challenges," *Sustainability* 12.8 (2021): 58–70, doi:10.3390/su12083473.

[25] Ilze Vamza et al., "Life Cycle Assessment of Reprocessed Cross Laminated Timber in Latvia," *Environmental and Climate Technologies* 25.1 (2021): 58–70, doi:10.2478/rtuect-2021-0005.

[26] The production phases of timber products are responsible for most of their footprint. That includes the sowing, harvesting, and processing of the trees. If that is avoided, the bulk of the emissions is never produced. (Lendager, *Solution*, 194).

[27] Hermann Kaufmann, *Manual of Multi-Storey Timber Construction* (Munich: DETAIL, 2018), 130.

[28] Christoph Schindler, "Ein architektonisches Periodisierungsmodell anhand fertigungstechnischer Kriterien, dargestellt am Beispiel des Holzbaus" (PhD diss., Zurich: Swiss Federal Institute of Technology Zurich (ETHZ), 2009).

[29] The small deviations stem from the manufacturing of the structural timber elements. These are planed down in millimeter steps depending on the quality, i.e., the surface aesthetics, and the size needed.

[30] Lendager, *Solution*, 110.

1.2.2 Architectural Applications for Offcuts

The architectural and structural use of offcuts provides a range of possibilities. Since their geometry is highly generic, they can be assembled into linear, curved, or planar building components. The preliminary evaluation of the different concepts led to the exclusion of linear and the planar concepts (see Appendix A), while the concept for curved building components appeared to have the most potential. Curved elements are the basis for a range of free-form structures.

Recent developments in academia and practice made the design and fabrication of free-form timber structures accessible (see Chapter 2.3). That includes the theoretical knowledge and design tools to conceive such structures. However, they still demand high planning and fabrication efforts and resources for their construction.[31] For this reason, worldwide, only a few timber manufacturers can realize projects with complex free-form timber structures.[32] To address this status and to find an appropriate use for offcuts, this thesis proposes an approach that conceptually follows de l'Orme's developments (see Chapter 2.3.1).

Designing free-form timber structures with offcuts achieves an analogous aesthetic expression as the same structure built with glued laminated timber (*glulam*).[33] However, the approach of creating curved components out of small offcuts yields some benefits. One principal challenge of curved glulams is to align the fibers of the wood in parallel to the loads. Even small angular deviations reduce their structural capabilities substantially.[34] In contrast to this, the orientation of the offcuts' fibers can easily follow the principal loads. That is achieved through the discretization of the curve. Thereby, the waste material can suddenly create a complex structure that otherwise would require advanced techniques to achieve. Furthermore, there is a substantial difference in the costs. Curved glulam structures have a price that is five to fifteen times that of straight glulams.[35] In comparison, offcuts are considered cheap waste materials. Moreover, the fabrication of the curved elements probably produces less waste if constructed with offcuts. Due to the complex nature of glulams, they require multiple steps of fabrication, resulting in more waste.[36]

On the contrary, building physical free-form structures with offcuts has its difficulties too. Since it is a waste material, its structural capabilities are most likely below that of intact structural timber. Furthermore, as the components are built out of multiple offcuts, they require joints. Every joint is a weak spot in the force chain that is the alignment. Even though they yield good performance, they are never as good as solid timber. Moreover, the ends of the offcuts are partially exposed since they all have slightly different dimensions. This results in non-modeled material effects and tolerances as well as in a faster decay of the material. As is done in current free-form glulam practice, the structure could receive a finish too by trimming all elements down to some size. That, however, leads to the same problems, i.e., increased fabrication times and more material waste.

---

[31] Daniel Gethmann, "Kai Strehlke (Blumer-Lehmann AG) in Conversation with Urs Hirschberg (GAM)," in *Wood: Rethinking Material* (Berlin: Jovis Verlag, 2021), 110–29.

[32] Gethmann, "Kai Strehlke (Blumer-Lehmann AG) in Conversation with Urs Hirschberg (GAM)," 112–15.

[33] Tom Svilans, "Integrated material practice in free-form timber structures" (PhD diss., Copenhagen: The Royal Danish Academy of Fine Arts, 2020), 232–33.

[34] Gethmann, "Kai Strehlke (Blumer-Lehmann AG) in Conversation with Urs Hirschberg (GAM)," 120–23.

[35] Kai Strehlke, "Aspekte der Geometrie in der Planung von Vor- und Bauprojekt," in *Architektur fertigen: Konstruktiver Holzelementbau*, ed. Mario Rinke and Martin Krammer (Zurich: Triest Verlag, 2020), 59–65.

[36] Gethmann, "Kai Strehlke (Blumer-Lehmann AG) in Conversation with Urs Hirschberg (GAM)," 122–25.

1.3 Research Motivation and Objective

This research investigates the potential for upcycling offcuts as structural elements for free-form timber structures. It uses integrative design strategies, coupling algorithmic design tools with digital fabrication processes to handle complex geometries, and, ultimately, to foster a transfer into 1:1 applications. The applied methods are based on an empirical-materialistic pursuit, including incremental and iterative sequences of physical-computational development and experimentation. That is gained through physical and digital prototyping following a research-by-design strategy. The objective is to develop and demonstrate a design-to-fabrication workflow for "free-form offcut structures." The proposed workflow features several steps (see Figure 1.5). In principal, these are:

1. the selection and collection of offcuts.
2. the creation of a database of the offcut stock.
3. the design and optimization of curved structures.
4. the alignment of the offcuts on these curves.
5. the creation of the joints.
6. the fabrication of the aligned offcuts.
7. the assembly of the free-form offcut structure.

Each of these steps requires a certain scale. A multi-scalar model approach reflects and considers these requirements. It consists of an architectural scale, a detailing scale, and a fabrication scale, each with corresponding models. (see Figure 1.6).

To make the workflow feasible, a multi-component plugin was developed (see Appendix B.2). It provides specific functionality for each step to make the design and fabrication of free-form offcut structures possible. Also, it is implemented in McNeel's Rhino3d software framework (see Appendix B.1).

In addition, the complexity of the material and structure justify the use of computer numerical controlled (CNC) machinery, including industrial robotic arms. The sheer volume of offcuts required and their spatial relationship present a challenge that would otherwise be impossible to overcome. Also, the fabrication is unique for each offcut and, therefore, emphasizes the use of CNC machinery further.[37]

1.4 Thesis Structure

Beyond this introduction, the thesis consists of four chapters: 2. State of the Art, 3. Methodology, 4. Case Studies, and 5. Conclusion. Chapter 2 covers the state of the art in the recycling of timber for architectural and structural applications, the digital fabrication techniques in the industry and academia—including manufacturing and assembly strategies—, and the history of free-form timber structures and their current developments. Chapter 3 presents the methodology and the design-to-fabrication workflow. It includes the development of a software extension, the digitization of the offcuts, the algorithms for aligning offcuts, and the physical and digital robotic environments. Chapter 4 demonstrates the application of the proposed workflow with several digital and physical case studies. Chapter 5 provides a summary of results, a reflection on the methods and limitations, and an outlook for future research opportunities. Finally, the appendices cover the conceptual explorations (see Appendix A) and software frameworks (see Appendix B).

---

[37] Jan Willmann, "Digitale Revolution im Holzbau: Roboter, Narration, Entwurf," in *Architektur fertigen: Konstruktiver Holzelementbau*, ed. Mario Rinke and Martin Krammer (Zurich: Triest Verlag, 2020), 137–42.
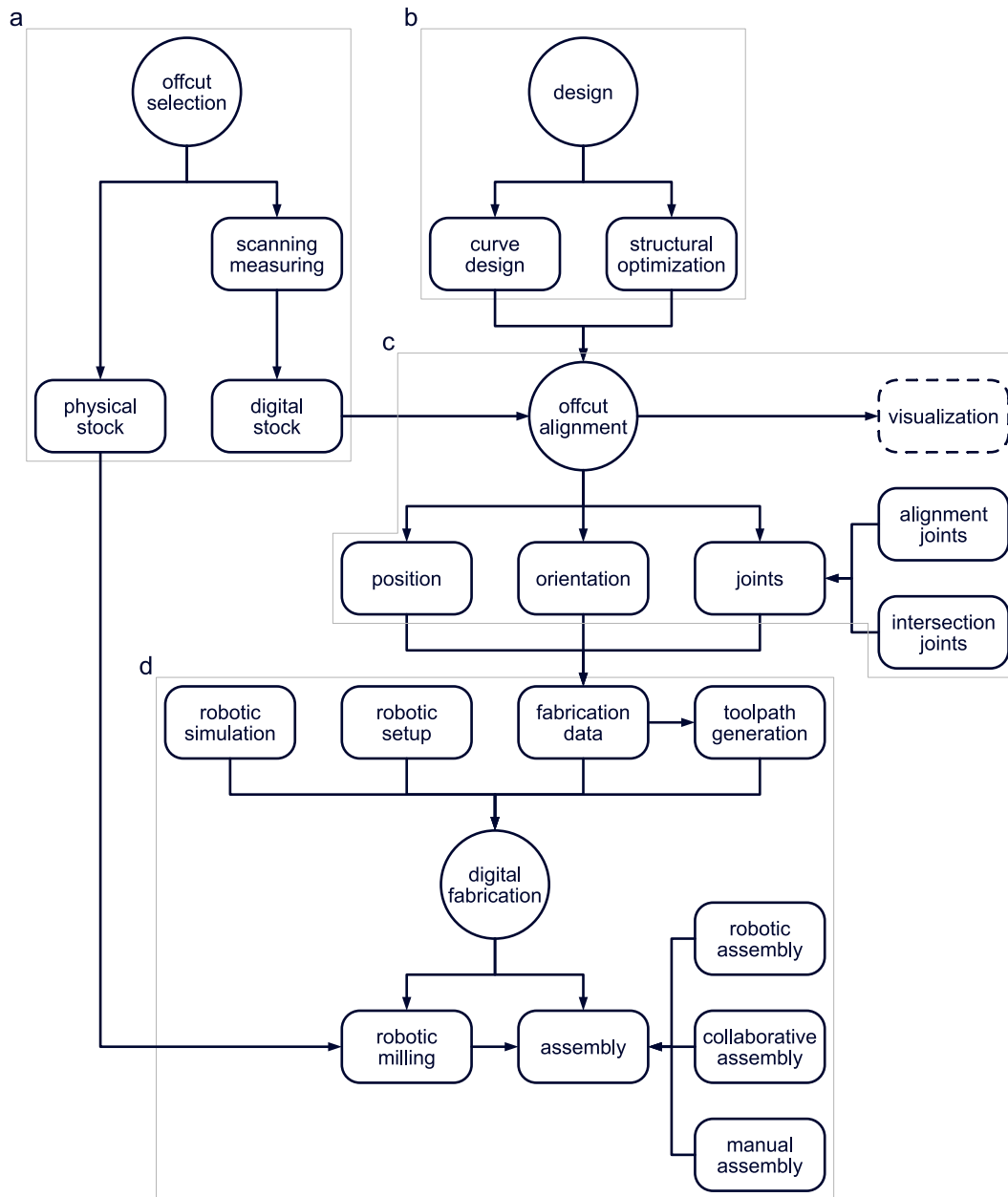
Figure 1.5: *The proposed design-to-fabrication workflow: a) Creation of an offcut database, b) Architectural design and structural optimization, c) Offcut alignment and the generation of joints and additional data, d) Digital fabrication including manufacturing and assembly.*
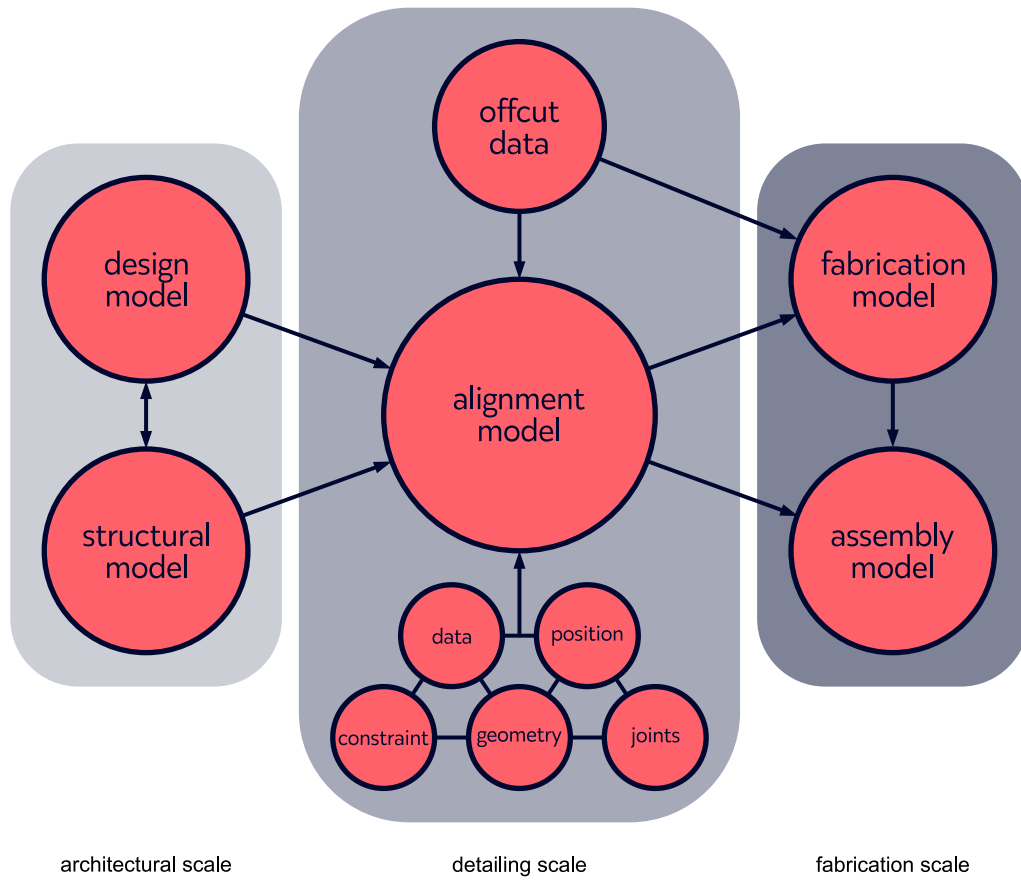
Figure 1.6: *The network of the multi-scalar model.*

Chapter 2
State of the Art

This chapter reviews the state-of-the-art of research and practice in timber construction. Thereby, it sets this thesis into the relevant context. For example, the chapter covers current reuse and upcycling strategies. Then, it illustrates the various digital design and fabrication techniques, including manufacturing and assembly. Finally, it provides an overview of the historical and recent developments of free-form timber structures.

2.1 Reuse and Recycling of Timber

Throughout history, timber was always considered a precious resource.[1] That was facilitated by the growing populations and their need for more and larger structures.[2] However, the practice of reusing timber emerged out of that scarcity. If a structure was not needed anymore, it was common practice to reuse its wood. The timber was then used to repair other structures or exchange their parts. Also, it was used to built new ones. Since the timber elements were already fabricated, they required a significantly reduced amount of work for their structural implementation. To that end, even the wood from old ships was reused for architectural purposes.[3]

A new interest in the reuse of timber emerged from various actors with business models based on the circular economy. Specifically, it is a trend in furniture design, with exponents like the Dutch designer Piet Hein Eek.[4] However, architectural practices are working with reclaimed timber as well. The Danish office Lendager Group demonstrated how they implemented waste wood in their projects. Even though they showed a great variety of use cases, they only used the material for interior and exterior finishes.[5] On the contrary, Roswag-Klinge presented a range of prototypical structural timber elements made out of reclaimed wood.[6]

In research, digital tools are more established in the process of recycling wood. With their "Sourced Wood" project, Salas et al. demonstrated a workflow of how to reuse reclaimed timber to create truss

---

[1] Zwerger, *Wood and Wood Joints*, 226–46.

[2] Zwerger, *Wood and Wood Joints*, 43.

[3] Zwerger, *Wood and Wood Joints*, 11.

[4] Piet Hein Eek, "pietheineek.nl," 2022, https://pietheineek.nl/en/product-category/collection/furniture/tabels-en.

[5] Lendager, *Solution*, 194–211.

[6] Eike Roswag-Klinge, "Designing Natural Buildings," in *Research Culture in Architecture: Cross-Disciplinary Collaboration*, ed. Cornelie Leopold (Basel: Birkhäuser, 2020), 236–46, doi:10.1515/9783035620238-023.

structures.[7] Additionally, Najari et al. presented a similar workflow for timber plate structures.[8] Both projects used scanning and robotic fabrication techniques to handle the complex geometries of the waste wood. Also, they implemented evolutionary algorithms that solved the alignment of the timber pieces. Furthermore, Sunshine demonstrated a novel workflow for designing with non-standard timber logs.[9] They utilized unique software that worked with digital twins of the logs. For that, they scanned the logs and created exact digital replicas. The software could simulate real-world physics as well. Coupled with its ability to generate dowel joints, it provides the means to design viable structures with the existing material (see Figure 2.1). Contrary to that, Poteschkin et al. recycled cutouts with standard sizes.[10] Cutouts are the remainders in the production of cross-laminated timber (CLT) components when openings for doors and windows are cut. From these cutouts, they developed a modular mass timber system for walls and ceilings. For that, a nesting algorithm sorted the cutouts. Then, loose tenon joints made of beech veneer plywood connected the aligned cutouts.[11] Furthermore, Robeller and von Haaren demonstrated how to construct timber shell structures out of CLT cutouts. To join the plates, they used form-fitting fasteners made of beech laminated veneer lumber.[12]

Figure 2.1: *A Medium Resolution beam.* Photograph by Gil Sunshine, 2021.
https://www.gilsunshine.com/projects/medium_resolution.html.

---

[7] Jasser Salas et al., "Sourced Wood," 2018, https://www.iaacblog.com/programs/sourced-wood/.

[8] Arman Najari et al., "Good Wood: Robotic Upcycling," 2018, https://www.iaacblog.com/programs/good-wood-robotic-upcycling/.

[9] Gil Sunshine, "Medium Resolution," 2021, https://marchthesis.mit.edu/Medium-Resolution.

[10] Viktor Poteschkin et al., "Recycling of Cross-Laminated Timber Production Waste," in *Research Culture in Architecture: Cross-Disciplinary Collaboration*, ed. Cornelie Leopold (Basel: Birkhäuser, 2020), 100–12, doi:10.1515/9783035620238-010.

[11] Poteschkin et al., "Recycling of Cross-Laminated Timber Production Waste," 103–6.

[12] Christopher Robeller and Niklas von Haaren, "Recycleshell: Wood-only Shell Structures Made From Cross-Laminated Timber (CLT) Production Waste," *Journal of the International Association for Shell and Spatial Structures* 61 (2020): 125–39, doi:10.20898/j.iass.2020.204.045.

2.2 Digital Fabrication in Timber Construction

From the mid-1980s onward, the timber industry started implementing digital fabrication technologies to boost their production. CNC machines transformed laborious manufacturing processes into highly efficient and flexible means of production.[13] Thereby, the high degree of automation led to an increase in standardization and serialization. However, it enhanced the quality of timber products and fostered innovation. Besides the industrialized manufacturing machines, the timber industry implements a range of scanning methods, e.g., "CT scanning, 3D analysis, LIDAR, and RADAR scanning," to optimize the production of straight timber.[14] However, these tools are only available at an industrial scale. Moreover, "the timber construction sector is still characterized by a high proportion of manual assembly tasks."[15]

In contrast, academic research tests and evaluates new tools and fabrication methods. That increasingly enables customization that is ever more efficient. In the following, the digital tools implemented are evaluated. In this thesis, they are divided into two categories: 1. manufacturing—and pre-fabrication—methods and 2. assembly methods.[16] Both methods exploit the possibilities of CNC milling machinery and industrial manipulators.

2.2.1 Manufacturing

Current manufacturing techniques are divided into two modes of operation. There are standardized and non-standardized tasks and routines. The first type enables mass production at an industrial scale. The tasks are defined once and executed countless times in automated processes. In contrast, the complexity increases significantly with non-standardized tasks. Here, a higher planning effort is required since the fabrication strategies must be adapted as necessary. However, it is also possible to automate these tasks with advanced algorithms.

Various subtractive manufacturing techniques are used for the manipulation of timber. That most commonly includes multi-axis milling. A CNC machine with three axes is the simplest form of that. With three degrees of freedom, the router can move in one plane in the x and y-axes and change its height on the z-axis. Thereby, the tool is always aligned in the same direction. Even though that is a simple manufacturing technique, it can achieve to fabricate complex structures. For instance, Wójcik and Strumiłło used three-axis milling to manufacture a wavy finger joint to connect raw wood elements. Through a ninety-degree rotation of the elements, they achieved to build a stiff mass-timber prototype.[17]

---

[13] Willmann, "Digitale Revolution im Holzbau," 137.

[14] Petras Vestartas, "Design-to-Fabrication Workflow for Raw-Sawn-Timber using Joinery Solver" (PhD diss., Swiss Federal Institute of Technology Lausanne (EPFL), 2021), 13.

[15] Jan Willmann, Fabio Gramazio, and Matthias Kohler, "New paradigms of the automatic: Robotic timber construction in architecture," in *Advancing Wood Architecture: A computational approach*, ed. Achim Menges, Tobias Schwinn, and Oliver David Krieg (New York: Routledge, 2017), 13–27.

[16] A combination of both strategies is also possible. In particular, the assembly methods usually entail some sort of manufacturing. However, this thesis divides the research to focus specifically on the manufacturing or the assembly methods.

[17] Marcin Wójcik and Jan Strumiłło, "Behaviour-based Wood Connection as a Base for New Tectonics," in *Proceedings of the 20th Annual International Sustainable Development Research Conference*, ed. Martina Keitsch, Resilience: the New Research Frontier (Trondheim: Norwegian University of Science; Technology, June 2014), 170–84, doi:https://doi.org/10.21427/D71R50.

Furthermore, Liu et al. used the same technique to mill multiple kerfs into timber slats. Thereby, the slats were bendable, making more complex structures possible.[18]

However, multi-axis fabrication is more widespread. In particular, the use of five-axis CNC machines and six-axis industrial robotic arms is common in both industry and academia. For a CNC machine, the additional two degrees of freedom are designed as either tilting and rotating the table or the tool, or a combination of both in various constellations. An industrial robotic arm is different from that. Its freedom of movement is generally defined by the number of joints it has. Accordingly, a typical robot with six joints has six degrees of freedom. Usually, these joints are named the base, shoulder, elbow, and wrists. At the end of wrist three is the tool flange where the end-effector, i.e., the tool, is attached (see Figure 2.2 left). Contemporary software tools provide the means to control these complex machines. There are two modes to control a robot: the Joint or Configuration Space and the Cartesian Space. Usually, the robot operating system works in the Configuration Space, where the exact rotation of each joint is defined. To reach a specific point, an algorithm calculates the position for each joint using "forward kinematics." In most manufacturing tasks, however, the robot must move to several coordinates in succession. The software defines these coordinates in the Cartesian Space. Then, an algorithm uses "inverse kinematics" to calculate the rotations of each joint and the position of the robot (see Figure 2.2 right).
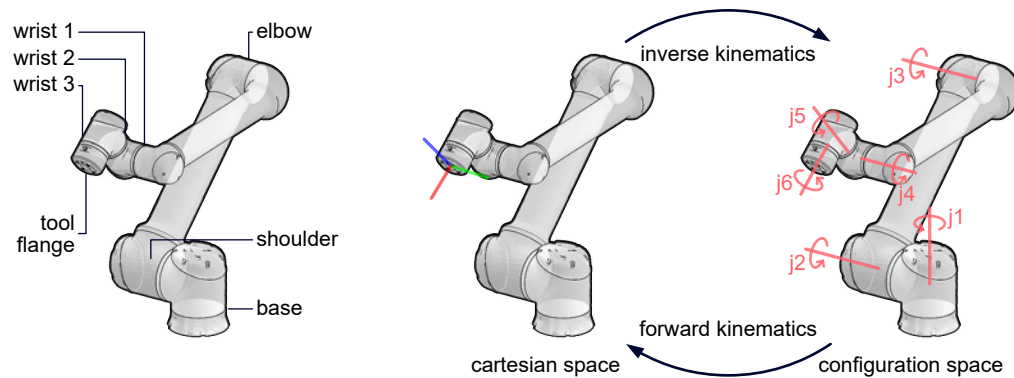
Figure 2.2: *The buildup of an industrial robotic arm (UR10e) and its modes of positioning.* Illustration adapted from Gonzalo Casas and Romana Rust, 2021. Robotic Fabrication with the COMPAS Framework workshop.

The use of these machines for multi-axis milling has already been demonstrated several times. For instance, Hua et al. used a six-axis industrial robot to mill the joints for a Voronoi shell consisting of thin timber slats.[19] Similarly, Schwinn et al. implemented a six-axis robot to fabricate the elements for a timber plate shell structure. For that, the robot milled the finger joints into the plates.[20] In addition,

---

[18] Yulun Liu, Yao Lu, and Masoud Akbarzadeh, "Kerf Bending and Zipper in Spatial Timber Tectonics: A Polyhedral Timber Space Frame System Manufacturable by 3-Axis CNC Milling Machine," in *ACADIA 21: Realignments: Toward Critical Computation*, Proceedings of the 41st Annual Conference of the Association for Computer Aided Design in Architecture (ACADIA) (2021).

[19] Hao Hua, Ludger Hovestadt, and Peng Tang, "Optimization and prefabrication of timber Voronoi shells," *Structural and Multidisciplinary Optimization* 61 (2020): 1897–911, doi:10.1007/s00158-019-02445-x.

[20] Tobias Schwinn, "Landesgartenschau Exhibition Hall," in *Advancing Wood Architecture: A computational approach*, ed. Achim Menges, Tobias Schwinn, and Oliver David Krieg (New York: Routledge, 2017), 111–24.

Robeller et al. have shown that more complex dovetail finger joints can also be milled using a five-axis CNC machine.[21] To this end, Vestartas has proven that both a five-axis CNC machine and a six-axis robotic arm can fabricate non-standard raw wood logs.[22] Specifically, they used the machines for milling, drilling, and saw blade cutting operations. Thereby, they achieved to manufacture the wood joints for a range of demonstrators.[23] In general, milling is specifically useful for precisely carving complex geometries out of wood. However, it is a comparably slow manufacturing method. Therefore, various research projects experimented with faster means of fabrication.

One of these manufacturing methods is saw blade cutting. Søndergaard et al. demonstrated how to use a table saw for the fabrication of a timber space-frame structure.[24] The structure's assembly required each timber beam to have specific angles at its ends. For this purpose, an industrial robotic arm cut the timber beams with a table saw. It had a custom parallel gripper capable of retaining the beams in place regardless of the cutting force.[25] Similarly, Thoma et al. used a three-axis CNC saw combined with industrial robotic arms to cut the timber beams for timber frame modules.[26] Moreover, there are saw blade end effectors with whom the movement of the object to be fabricated is avoided. Raith et al. demonstrated how cross-lap joints are fabricable with such a saw blade tool. They attached it to a five-axis CNC machine and precisely cut cross-lap joints into thin timber slats.[27] Hornung et al. proved that the same technique works for raw timber logs with a small diameter as well.[28] For that purpose, they attached the saw blade onto a six-axis industrial robot.

Additionally, Hornung et al. used a chainsaw end effector to cut joints at places that were hard to reach.[29] With its relatively long-range, the saw could cut areas that previously were unreachable with other tools due to branches. However, the resulting rough surface finish diminished the fitting of the wood joints. Similarly, Vercruysse et al. implemented a bigger chainsaw end effector for an industrial robot.[30] With that tool, the robot was able to cut wood joints into raw timber logs with a large diameter. They continuously monitored the manufacturing process and adjusted the cutting speed as needed (see Figure 2.3 f).

Vercruysse et al. developed an even more sophisticated end effector consisting of a customized bandsaw. Mounted on an industrial robot, it could create curved cuts in timber—a method that is related to

---

[21] Christopher Robeller and Yves Weinand, "Integral joints for timber folded plate structures," in *Advancing Wood Architecture: A computational approach*, ed. Achim Menges, Tobias Schwinn, and Oliver David Krieg (New York: Routledge, 2017), 73–83.

[22] Vestartas, "Design-to-Fabrication Workflow for Raw-Sawn-Timber using Joinery Solver," 156–77.

[23] Vestartas, "Design-to-Fabrication Workflow for Raw-Sawn-Timber using Joinery Solver," 181–218.

[24] Asbjørn Søndergaard et al., "Topology Optimization and Robotic Fabrication of Advanced Timber Space-Frame Structures," in *Robotic Fabrication in Architecture, Art and Design 2016*, ed. Dagmar Reinhardt, Rob Saunders, and Jane Burry (Zurich: Springer, 2016), 190–203, doi:10.1007/978-3-319-26378-6.

[25] Søndergaard et al., "Topology Optimization and Robotic Fabrication of Advanced Timber Space-Frame Structures," 197.

[26] Andreas Thoma et al., "Robotic Fabrication of Bespoke Timber Frame Modules," in *Robotic Fabrication in Architecture, Art and Design 2018*, ed. Jan Willmann et al. (Zurich: Springer, 2018), 448–59, doi:10.1007/978-3-319-92294-2.

[27] Karin Raith, "Wood Construction – On the Renewal of an Ancient Art," in *Conceptual Joining: Wood Structures from Detail to Utopia*, ed. Lukas Allner et al. (Basel: Birkhäuser, 2022), 96–107.

[28] Philipp Hornung, "Robotic Fabrication at the Angewandte Robotics Lab (ARL)," in *Conceptual Joining: Wood Structures from Detail to Utopia*, ed. Lukas Allner et al. (Basel: Birkhäuser, 2022), 180–89.

[29] Hornung, "Robotic Fabrication at the Angewandte Robotics Lab (ARL)," 184–85.

[30] Emmanuel Vercruysse, Zachary Mollica, and Pradeep Devadass, "Altered Behaviour: The Performative Nature of Manufacture: Chainsaw Choreographies + Bandsaw Manoeuvres," in *Robotic Fabrication in Architecture, Art and Design 2018*, ed. Jan Willmann et al. (Zurich: Springer, 2018), 309–19, doi:10.1007/978-3-319-92294-2.

robotic hot-wire cutting (see Figure 2.3 e).[31] Chai and Yuan presented a related bandsaw end effector that they attached to a gantry-mounted robot.[32] With that setup, they cut curved timber beams out of glulams. Then, they assembled these beams into a tree-like free-form structure. The first instance of robotic bandsaw cutting was demonstrated by Johns and Foley.[33] Their goal was to manufacture continuous curved elements out of material with a non-standard geometry. Also, they strove to reduce the fabrication waste as much as possible—what they achieved with the bandsaw cutting.

More recent research explored the possibility to implement traditional carpentry tools as robotic end effectors. For instance, Brugnaro and Hanna used chisels and gouges mounted on a robot to train a machine-learning algorithm. For that purpose, they first trained the algorithm with manual cutting operations.[34] Then, they attached the tool to the robot so that it could test the cutting itself. In the end, they presented that their trained network predicted the fabrication parameters quite precisely.[35] Furthermore, Takabayashi et al. translated traditional Japanese carpentry methods to robotic manufacturing.[36] They developed four end effectors for their concept (see Figure 2.3 a–d). These included a circular saw, a square chisel, a vibration chisel, and a router. With this setup, they manufactured a scale model of a corner of a traditional Japanese temple.

There are several strategies to generate toolpaths for the different manufacturing techniques. On the complex side of the spectrum is multi-axis milling. That is because the material is cleared in multiple steps. For that purpose, it requires an algorithm to calculate the most efficient movement pattern. Also, there is a range of different milling strategies, each with its specific use case. Specialized computer-aided manufacturing (CAM) software can calculate these paths.[37] In contrast, the toolpaths for the tools with a linear cutting motion, i.e., the saw blade and chainsaw, are relatively simple to generate. With both techniques, at least two curves are sufficient to generate the paths. Moreover, bandsaw cutting utilizes the medial curves extracted from 3D surfaces as paths.[38]

2.2.2 Assembly

As previously discussed, the timber industry implemented digital fabrication tools from the 1980s onward. However, the primary focus is on the manufacturing processes, excluding the assembly.[39] On

---

[31] Vercruysse, Mollica, and Devadass, "Altered Behaviour," 315.

[32] Hua Chai and Philip F. Yuan, "Investigations on Potentials of Robotic Band-Saw Cutting in Complex Wood Structures," in *Robotic Fabrication in Architecture, Art and Design 2018*, ed. Jan Willmann et al. (Zurich: Springer, 2018), 257–70, doi:10.1007/978-3-319-92294-2.

[33] Ryan Luke Johns and Nicholas Foley, "Bandsawn Bands: Feature-Based Design and Fabrication of Nested Freeform Sufaces in Wood," in *Robotic Fabrication in Architecture, Art and Design 2014*, ed. Wes McGee and Monica Ponce de Leon (Cham: Springer, 2014), 17–32, doi:10.1007/978-3-319-04663-1.

[34] Giulio Brugnaro and Sean Hanna, "Adaptive Robotic Training Methods for Subtractive Manufacturing," in *ACADIA 16: POSTHUMAN FRONTIERS: Data, Designers, and Cognitive Machines*, Proceedings of the 36th Annual Conference of the Association for Computer Aided Design in Architecture (ACADIA) (Ann Arbor, 2016), 164–69.

[35] Brugnaro and Hanna, "Adaptive Robotic Training Methods for Subtractive Manufacturing," 167–68.

[36] Hiroki Takabayashi, Kado Keita, and Gakuhito Hirasawa, "Versatile Robotic Wood Processing Based on Analysis of Parts Processing of Japanese Traditional Wooden Buildings," in *Robotic Fabrication in Architecture, Art and Design 2018*, ed. Jan Willmann et al. (Zurich: Springer, 2018), 222–32, doi:10.1007/978-3-319-92294-2.

[37] Hua, Hovestadt, and Tang, "Optimization and prefabrication of timber Voronoi shells," 1907–8.

[38] Vercruysse, Mollica, and Devadass, "Altered Behaviour," 317.

[39] Obviously, the timber industry assembles their prefabricated building components. Nevertheless, the transport and assembly of the components on the construction sites are performed manually.
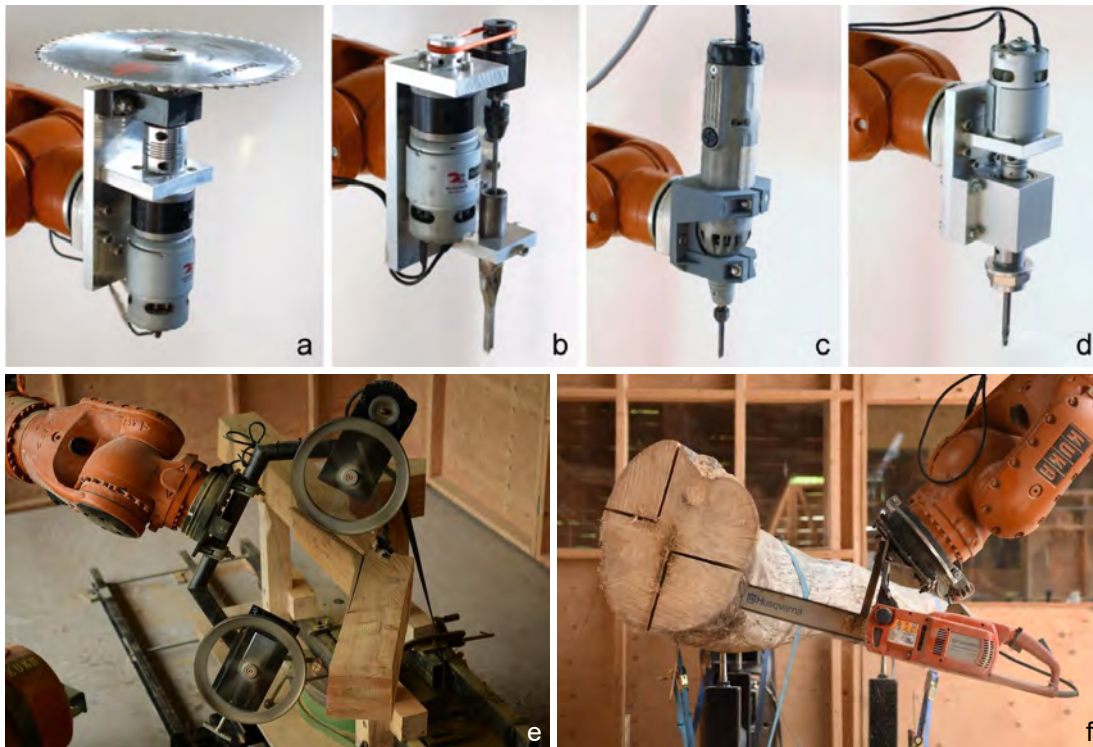
Figure 2.3: Top: *Developed tools and processing examples: a) circular saw, b) square chisel, c) vibration chisel, and d) router.* Photographs by Hiroki Takabayashi et al., 2018.
Bottom: *e) Bandsaw end effector used during "Bandsaw Manoeuvres," f) Chainsaw end effector used during "Chainsaw Choreographies."* Photographs by Emmanuel Vercruysse et al., 2018.

the contrary, the assembly process was a fundamental part of the first robotic applications in academic research.

In particular, the research of Gramazio Kohler Research at ETH Zurich is pioneering. Their early timber projects the "Sequential Wall,"[40] the "Stacked Pavilion,"[41] and the "Sequential Structure"[42] demonstrated how the simple technique of robotic layering erects complex structures. As part of these projects, they developed an advanced design-to-fabrication workflow. That culminated in the design and construction of the "Sequential Roof."[43] It is a truss-like structure consisting of numerous thin timber slats. These were cut, placed, and joined into multiple trusses according to a digital model of the non-repetitive geometry (see Figure 2.4).[44] For the fabrication of the structure to be feasible, a novel robotic setup was

---

[40] Fabio Gramazio et al., *The Robotic Touch: How Robots Change Architecture; Gramazio & Kohler Research ETH Zurich 2005–2013* (Zurich: Park Books, 2014), 144–57.

[41] Gramazio et al., *The Robotic Touch*, 196–207.

[42] Gramazio et al., *The Robotic Touch*, 238–49.

[43] Jan Willmann et al., "Robotic timber construction: Expanding additive fabrication to new dimensions," *Automation in Construction* 61 (2016): 16–23, doi:10.1016/j.autcon.2015.09.011.

[44] Aleksandra Anna Apolinarska, "Complex Timber Structures From Simple Elements: Computational design of novel bar structures for robotic fabrication and assembly" (PhD diss., Zurich: Swiss Federal Institute of Technology Zurich (ETHZ), 2018), 38–40, doi:10.3929/ethz-b-000266723.

developed. It consisted of a six-axis gantry robot with exchangeable end effectors. Thereby, the robotic cell could perform all fabrication steps fully automated.[45] Furthermore, Kunic et al. presented an approach for the design and assembly of a reversible timber beam. For that purpose, they used a predefined kit of short wooden slats only. Two collaborative robotic arms with multi-tool end effectors could then mill and place the slats as designated in layers. To fixate the elements, they screwed them together with industrial screwdrivers. The overall setup demonstrated a combination of serial production and agile manufacturing.[46]

Figure 2.4: *Fabrication of the "Sequential Roof". Left: Placement of a part at its destination position.* Right: *Installation of a pair of partially pre-fitted trusses on site.* Photographs by Aleksandra Anna Apolinarska, 2018.

The technique of layering timber can either be performed by stationary or gantry-mounted robotic cells—as demonstrated in the projects just covered—or by mobile robots. Helm et al. presented several use-cases of mobile robots for in-situ fabrication.[47] Among others, they assembled two distinct installations. The "Stratifications" installation investigated various strategies in response to construction and material tolerances. The mobile robot detected these with its scanner and adapted its stacking strategy accordingly.[48] The "Fragile Structure" installation was an eight-meter-long modular wall built by stacking simple timber elements.[49] For that, the robot repositioned itself several times, scanning its surroundings on the way. By interacting with its environment, e.g., local points or humans, the robot established novel modes of assembly.[50]

More recent research explores the possibilities of collaborative robot-human and robot-robot assemblies. The fabrication of the "Shifted Frames" pavilion is an early example of that.[51] There, an industrial robotic arm cut each timber element and positioned it spatially. Then, the element was fixated manually

[45] Apolinarska, "Complex Timber Structures From Simple Elements," 68–70.

[46] Anja Kunic et al., "Design and assembly automation of the Robotic Reversible Timber Beam," *Automation in Construction* 123 (2021): 103531, doi:10.1016/j.autcon.2020.103531.

[47] Volker Helm et al., "Mobile Robotic Fabrication on Construction Sites: dimRob*," in *2012 IEEE/RSJ International Conference on Intelligent Robots and Systems* (Vilamoura, 2012), 4335–41, doi:10.1109/IROS.2012.6385617.

[48] Gramazio et al., *The Robotic Touch*, 266–67.

[49] Gramazio et al., *The Robotic Touch*, 268–71.

[50] Helm et al., "Mobile Robotic Fabrication on Construction Sites," 4339–41.

[51] Gramazio et al., *The Robotic Touch*, 352–63.

by screwing. The assembly method was further improved in the "Complex Timber Structures" research project. Its goal was to explore the possibilities of novel joining techniques and constructive typologies.[52] The demonstrator was conceived as a reciprocal frame structure made of simple timber slats. The slats' fabrication only required two angled cuts at the ends. A mobile robot could then place each slat at its final position. Due to its reciprocal nature, the segments were connected at the ends of two slats only. That proved to be advantageous for the assembly sequence since the slats could be placed one at a time. Finally, they were fixated manually with a specific gluing technique and nails.[53] Eversmann et al. implemented a similar assembly approach. They demonstrated a continuous digital workflow for the additive fabrication of complex timber structures. For that, they developed a customized robotic cell that consisted of two industrial robotic arms mounted on a double carriage linear axis. These could fabricate wooden slats of up to five meters with various tools. During the assembly, the robot positioned each wooden slat as intended in the 3D model. Then, after manual fixation, the robot released the slat and proceeded with the next iteration.[54]

Thoma et al. expanded the possibilities of collaborative assemblies further.[55] Using three case studies, they demonstrated how two robotic arms mounted on a gantry can work together to fabricate dowel-laminated timber structures. The first robot positioned the timber slats, while the second drilled the holes for the dowels and cut them to size. However, the insertion of the dowels was done manually.[56] Moreover, they presented how timber frame modules can be robotically prefabricated.[57] Their workflow began with the computational design of the frame structures. The digital model consisted of instances of a customized "Beam" class. That stored all the relevant data for the fabrication of the corresponding physical timber element. After the evaluation and optimization of the design, two gantry-mounted robotic arms performed the fabrication and assembly (see Figure 2.5). For that purpose, both robots were equipped with automatic tool changers and a range of tools. The assembly of a frame structure had a predefined sequence. At first, the robots assembled the floor, followed by the corners. These had to be fixated collaboratively by them. Then, the walls and, finally, the ceiling followed. The whole process demanded the implementation of advanced planning software. Gandía et al. developed a sophisticated tool that could calculate the best path for each step of the robots.[58] It combined algorithms for robot path planning and collision detection and implemented them in a common software framework. The tool proved to be effective for the complex assembly of the long timber beams. However, due to their lengths, there was a build-up of tolerances. Therefore, human intervention was still necessary to fixate and adjust the timber elements.[59] Another concept of collaborative robotic fabrication was presented by Wagner et al.[60] They developed a transportable robotic cell that consisted of a turntable and two

---

[52] Gramazio et al., *The Robotic Touch*, 364–77.

[53] Willmann et al., "Robotic timber construction," 18–19.

[54] Philipp Eversmann, Fabio Gramazio, and Matthias Kohler, "Robotic prefabrication of timber structures: towards automated large-scale spatial assembly," in *Construction Robotics 1* (2017), 49–60, doi:10.1007/s41693-017-0006-2.

[55] Andreas Thoma et al., "Cooperative Robotic Fabrication of Timber Dowel Assemblies," in *Research Culture in Architecture: Cross-Disciplinary Collaboration*, ed. Cornelie Leopold (Basel: Birkhäuser, 2020), 77–87, doi:10.1515/9783035620238-008.

[56] Thoma et al., "Cooperative Robotic Fabrication of Timber Dowel Assemblies," 83–84.

[57] Thoma et al., "Robotic Fabrication of Bespoke Timber Frame Modules."

[58] Augusto Gandía et al., "Towards Automatic Path Planning for Robotically Assembled Spatial Structures," in *Robotic Fabrication in Architecture, Art and Design 2018*, ed. Jan Willmann et al. (Zurich: Springer, 2018), 60–74, doi:10.1007/978-3-319-92294-2.

[59] Thoma et al., "Robotic Fabrication of Bespoke Timber Frame Modules," 453–57.

[60] Hans Jakob Wagner et al., "Flexible and transportable robotic timber construction platform – TIM," *Automation in Construction* 120 (2020): 16–23, doi:10.1016/j.autcon.2020.103400.

industrial robots with multiple tools. Thereby, the machines could fabricate wooden cassettes out of multiple timber elements.

Figure 2.5: *Collaborative Fabrication of a timber frame module. a) CNC-saw cutting a beam in cooperation with a robotic arm, b) Pre-drilling a screw hole, c) Robotic arm carrying a beam to its final position, d) Robotic assembly of the bridge technique, e) Cooperative robotic assembly of the corner technique.* Photographs by NCCR Digital Fabrication / Roman Keller, 2018.

Other recent developments explored the robotic assembly of timber structures with wood joints. Robeller et al. used a robotic cell mounted on a double carriage linear axis for the assembly of timber plate structures.[61] The plates had integral through-tenon joints. For their assembly, a custom end effector was developed. It could hold a plate and measure the force applied at the assembly. Also, it could vibrate, making the simultaneous insertion of multiple tenon joints possible.[62] Moreover, Leung et al. developed custom-built and remote-controlled high-force robotic clamps for the assembly of wood joints.[63] These provided the possibility to apply a force large enough to overcome the joint friction. With a non-standard spatial structure, they demonstrated that their concept works with the simultaneous assembly of multiple cross-lap joints. Building on that, Apolinarska et al. applied the method of "Reinforcement Learning" to improve the assembly further.[64] They trained a machine-learning algorithm in numerous simulations. Then, they conducted multiple successful assembly tasks. In addition, Kramberger et al. used collaborative robotic arms (cobots) and their ability of "kinesthetic guiding" to teach an algorithm

---

[61] Christopher Robeller et al., "Robotic Integral Attachment," in *Fabricate 2017: rethinking design and construction*, ed. Achim Menges et al. (London: UCL Press, 2017), 92–97, doi:10.14324/111.9781787350014.

[62] Robeller et al., "Robotic Integral Attachment," 96–97.

[63] Pok Yin Victor Leung et al., "Automatic Assembly of Jointed Timber Structure using Distributed Robotic Clamps," in *PROJECTIONS*, Proceedings of the 26th International Conference of the Association for Computer-Aided Architectural Design Research in Asia (CAADRIA), ed. Anastasia Globa et al., vol. 1 (Hong Kong: The Chinese University of Hong Kong, 2021), 583–92.

[64] Aleksandra Anna Apolinarska et al., "Robotic assembly of timber joints using reinforcement learning," *Automation in Construction* 125 (2021): 103569, doi:10.1016/j.autcon.2021.103569.

the assembly process.[65] The concept proved effective even if the wooden studs posed manufacturing imperfections.

2.3 Free-form Timber Structures

This section presents concurrent advances in free-form timber structures. It covers shell structures, bent structures, and glulam structures. However, beforehand, it gives an overview of the relevant historical developments.

2.3.1 Historical Practice

In Europe, the process of bending timber has a long tradition. Archaeological excavations found that people used a variety of hardwoods as a construction material in the Neolithic Age. If it had a small diameter, it was especially suitable for braiding.[66] The Romans started using bent timber for structures that needed larger spans (see Figure 2.6).[67] They did so by layering beams and fastening them together. Thereby, the structural capabilities of the material increased significantly. Also, the resulting arch forms were structurally more optimized than unconnected straight sections. That system was relevant for bridges.[68] However, it expanded to other use cases where wide spans were necessary. Especially in the construction of pitched roofs, it proved to be viable. Oftentimes, these structures used naturally-grown curved timber and exploited its shape for optimized stability.[69] Since timber elements rarely had the desired shape and were often crooked, a process of discretization began. The increased scarcity of wood reinforced that development. That led to the deployment of roof trusses consisting of shorter timber pieces. In combination, they formed coherent structures.[70] The more complex the structures became, the more they facilitated the use and development of wood joinery.

A range of developments stand out: The hammer-beam roof elevated the use of short timber pieces to an artistic endeavor. It is a truss structure developed in England during the 14th century.[71] Furthermore, in the early 16th century in France, Philibert de l'Orme presented an invention that broke with traditional carpentry. His proposed form of construction consisted of short wooden boards. They were aligned upright in two layers and fastened with tenon joints and keys. Thereby, it was possible to construct curved structures with straight elements (see Figure 2.7 top).[72] Additionally, the inventor highlighted the benefits of the structure, i.e., "the much cheaper form of construction (lower material and labour

---

[65] Aljaz Kramberger et al., "Robotic Assembly of Timber Structures in a Human-Robot Collaborative Setup," *Frontiers in Robotics and AI* 8 (2022), doi:10.3389/frobt.2021.768038.

[66] Zwerger, *Wood and Wood Joints*, 36.

[67] Wolfram Graubner, *Holzverbindungen Gegenüberstellungen japanischer und europäischer Lösungen* (Munich: Deutsche Verlags-Anstalt, 2015), 94.

[68] Zwerger, *Wood and Wood Joints*, 42.

[69] Zwerger, *Wood and Wood Joints*, 44–45.

[70] Zwerger, *Wood and Wood Joints*, 52.

[71] Zwerger, *Wood and Wood Joints*, 240.

[72] Joram F. Tutsch, "Weitgespannte Lamellendächer der frühen Moderne: Konstruktionsgeschichte, Geometrie und Tragverhalten" (PhD diss., Munich: Technical University of Munich, 2020), 24–25.
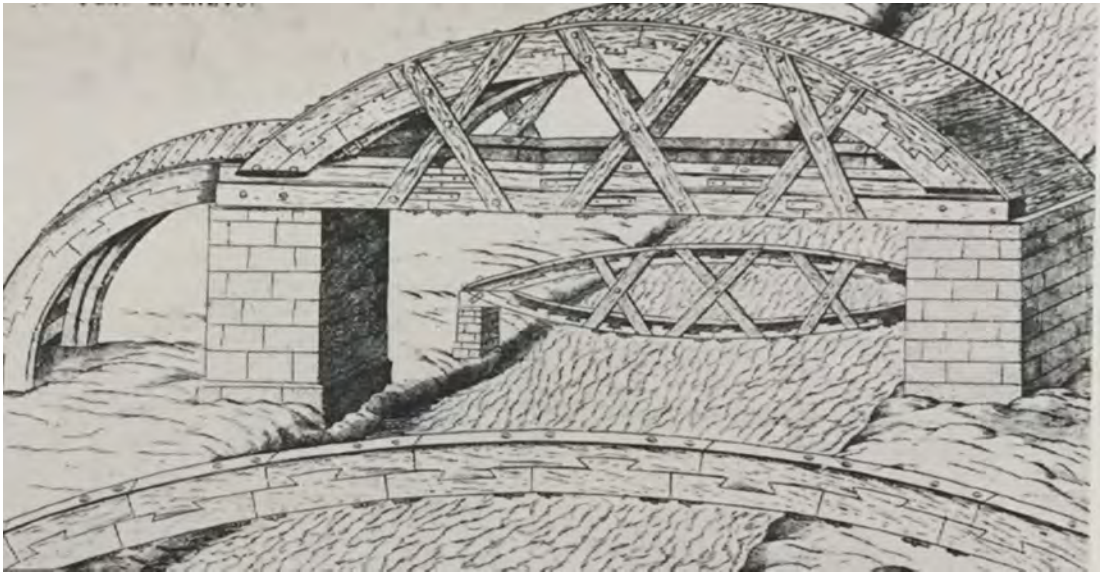
Figure 2.6: *Depiction of a Roman bridge.* Illustration taken from Wolfram Graubner, 2015.

costs), the easy replacement of defective pieces and, […] the relative independence from other trades."[73] In the 19th century, David Gilly analyzed and propagated that system.[74] It is thanks to his contribution that a large number of vaulted roof structures were built during this period.[75] In the 1920s, this inspired Friedrich Zollinger and led to the development of his "Zollinger Roof" system.[76] It consists of wooden lamellae aligned in a diamond shape. The orientation of every element alternates, while they connect only at their centers.[77] Thereby, the system is able to span distances of up to fifty meters at least.[78]

In parallel, the development of similar systems with horizontally layered timber elements took place. Hans Ulrich Grubenmann constructed a bridge with interlocking pinned beams in that way.[79] It lends its logic from earlier structures that layered timber but improved them. In the 19th century, Amand-Rose Emy presented an advancement of that system. He layered and bent the flat planks to avoid any time-consuming cutting processes. To connect these layers, he used clamping bolts and collars (see Figure 2.7 bottom).[80] Thereby, the Emy composite system can be considered a mechanical glulam.

The de l'Orme and Emy structural systems suffered from deflections and displacements due to low stiffness and flexural strength. The connections between the layers are not interlocking ideally and, thereby, cause these effects.[81] Therefore, it was proposed to glue the layers of the beams together. The

---

[73] Zwerger, *Wood and Wood Joints*, 240.

[74] David Gilly, *Ueber Erfindung, Construction und Vortheile der Bohlen-Dächer: mit besonderer Rücksicht auf die Urschrift ihres Erfinders* (Berlin: Friedrich Vieweg dem Aelteren, 1797).

[75] Tutsch, "Weitgespannte Lamellendächer der frühen Moderne," 25.

[76] Tutsch, "Weitgespannte Lamellendächer der frühen Moderne," 26.

[77] Tutsch, "Weitgespannte Lamellendächer der frühen Moderne," 32–33.

[78] Tutsch, "Weitgespannte Lamellendächer der frühen Moderne," 35.

[79] Christian Müller, *Holzleimbau = Laminated Timber Construction* (Basel, Berlin, Boston: Birkhauser, 2000), 14.

[80] Müller, *Holzleimbau = Laminated Timber Construction*, 15.

[81] Müller, *Holzleimbau = Laminated Timber Construction*, 15.

first structure to use glued glulams is the assembly hall of the King Edward College from 1860.[82] However, the system expanded only with the developments of Otto Hetzer. He achieved to glue two or more laminations together, joining them permanently. Even if the glulams were subjected to moisture, their connections remained. With his patented invention, he could build curved timber structures with large spans that matched the ideal line of forces. They had the maximum obtainable bending strength and did not need intermediate columns.[83]
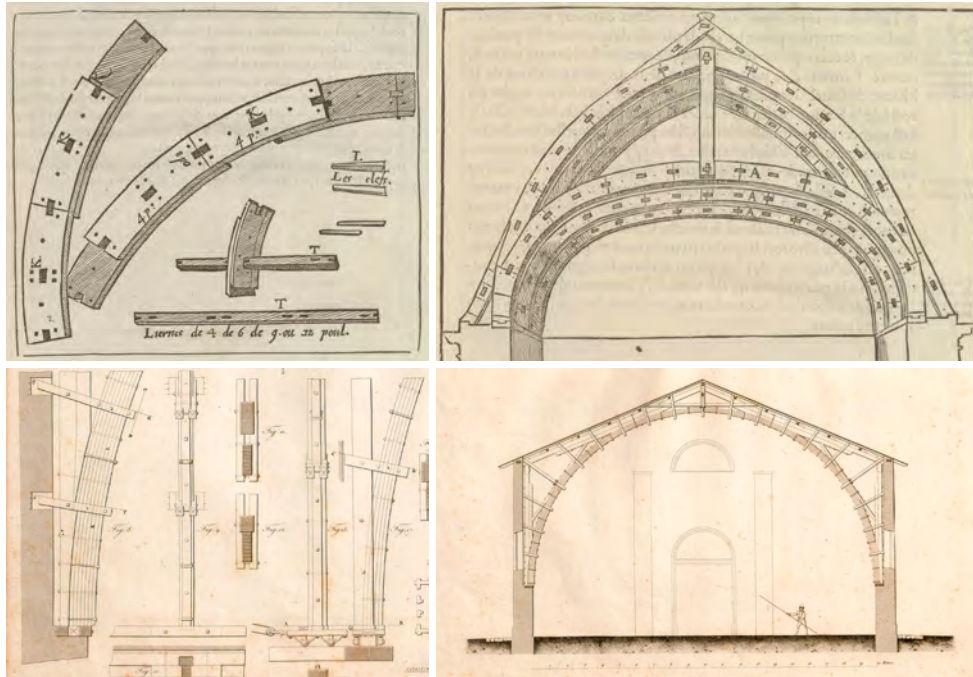
Figure 2.7: Top: *Structural system of de l'Orme.* Illustration by Philibert de l'Orme, 1561. Bottom: *Structural system of Emy.* Illustration by Amand-Rose Emy, 1828.

Frei Otto expanded the repertoire of timber structures further. In the 1960−70s, he developed and designed a variety of timber gridshells and lattice domes.[84] Contrary to previous timber structures, they consisted of long thin wooden laths instead of an aggregation of shorter pieces or laminated components. These laths were easily bendable and could take on any desired form. Because of that, the forms avoided any discretization. Inspired by the works of Antoni Gaudí, Otto applied a similar catenary-based form-finding approach.[85] For that, he used models with hanging chains to get an optimized form.[86] Then, he deducted the corresponding compression shells from these models. The *Multihalle* for the German Federal Garden Exhibition in Mannheim in 1975 is the primary example of that concept (see Figure 2.8).

[82] Müller, *Holzleimbau = Laminated Timber Construction*, 18.

[83] Müller, *Holzleimbau = Laminated Timber Construction*, 25.

[84] Irene Meissner, *Frei Otto: forschen, bauen, inspirieren = a life of research, construction and inspiration* (Munich: DETAIL, 2015), 80−87.

[85] Meissner, *Frei Otto*, 81.

[86] Meissner, *Frei Otto*, 82.

Its delicate structure consists of a grid of thin timber laths with flexible joints at the intersection points. It was laid out and assembled on the ground. Then, it was gradually lifted and shaped into its final form.[87] With his unprecedented works, Otto also inspired and influenced more recent developments.[88]

Figure 2.8: *Multihalle Mannheim, Gridshell.* Photograph by Eberhard Möller, 2015.

2.3.2 Recent Developments

2.3.2.1 Shell Structures

Building on that past, current research explores the possibilities of timber grid shells and segmented timber plate shells. Most notably are the research pavilions of the Institute of Computational Design and Construction (ICD) and the Institute of Building Structures and Structural Design (ITKE) of the University of Stuttgart. Over ten years, they developed and built a range of timber shell demonstrators.[89] That experience lead to their most recent structure, the "BUGA Wood Pavilion" (see Figure 2.9).[90] It consists of segmented planar timber plates. These plates discretize the shell to achieve the organic

---

[87] Meissner, *Frei Otto*, 83.

[88] Meissner, *Frei Otto*, 84–87.

[89] Achim Menges and Jan Knippers, *Architecture Research Building: ICD/ITKE 2010-2020* (Basel: Birkhäuser, 2020), 28–29.

[90] Martín Alvarez et al., "The BUGA Wood Pavilion: Integrative Interdisciplinary Advancements of Digital Timber Architecture," in *ACADIA 19: UBIQUITY AND AUTONOMY*, Proceedings of the 39th Annual Conference of the Association for Computer Aided Design in Architecture (ACADIA) (Austin: The University of Texas at Austin School of Architecture, 2019), 490–99.

form. With a span of 30 meters, the structure covers an area of 500 square meters. A hollow-cassette system that reduced the material and weight enabled that. Also, the early-stage structural optimization of the shell's form played a vital role.[91]

Figure 2.9: *View of the BUGA Wood pavilion with illuminated hollow chambers of the structural cassette segments.* Photograph by ICD/ITKE University of Stuttgart, 2020.

Furthermore, a range of publications demonstrated how the discretization of curved forms is possible with straight timber elements. In the "Hila Pavilion," Österlund and Wikar abstracted a vault-like form with wooden laths that they connected orthogonally.[92] On the contrary, their "Sotkanmuna Pavilion" consists of short timber pieces that form an egg-like shell. Thereby, it makes use of the Zollinger system.[93] Furthermore, Eversmann et al. demonstrated a complete design-to-fabrication workflow for a multi-story timber grid shell.[94] They only used short timber pieces between 400 and 1500 mm in length to construct the spatial trusses. That enabled a discretization of the desired form and created a smooth shape (see Figure 2.10).[95]

The development of computational design and simulation tools facilitates that research trend. Specifically, a range of open-source software led to a liberalization of various form-finding solutions. These

---

[91] Alvarez et al., "The BUGA Wood Pavilion," 494–96.

[92] Toni Österlund and Markus Wikar, "Freeform Timber Structures: Digital Design and Fabrication," in *Rethinking Wood: Future Dimensions of Timber Assembly*, ed. Markus Hudert (Basel: Birkhäuser, 2019), 132–49.

[93] Österlund and Wikar, "Freeform Timber Structures," 141–43.

[94] Eversmann, Gramazio, and Kohler, "Robotic prefabrication of timber structures."

[95] Eversmann, Gramazio, and Kohler, "Robotic prefabrication of timber structures," 57–59.

Figure 2.10: *Exterior image showing the shingle pattern and opening sequence of the structure.* Photograph by Philipp Eversmann et al., 2017.

include physics engines like Kangaroo 2,[96] approaches based on graphic statics like COMPAS CEM[97] and COMPAS 3GS,[98] and tools based on the "Thrust Network Analysis"[99] like RhinoVault 2.[100]

2.3.2.2 Bent Structures

In recent years, research on structural applications for bent thin wood laths has expanded. Heikkinen et al. demonstrated with their "Säie Pavilion" how curvilinear forms are achievable through active bending.[101] Besides the challenge of finding a balanced form, the connections of the bent laths were problematic. They solved that by fabricating unique joints from birch plywood and layered the elements to connect.[102] Similarly, Schleicher et al. implemented an active bending approach for thin tim-

---

[96] Daniel Piker, "Kangaroo: Form Finding with Computational Physics," in *Computation Works: The Building of Algorithmic Thought*, ed. Brady Peters (London: John Wiley & Sons, 2013), 136–37.

[97] Rafael Pastrana et al., *COMPAS CEM: The Combinatorial Equilibrium Modeling framework for COMPAS* (2021), doi:10.5281/zenodo.5705740.

[98] Juney Lee and Tom Van Mele, *compas 3gs: 3D graphic statics package for the COMPAS framework* (2019), https://github.com/compas-dev/compas_3gs.

[99] Matthias Rippmann and Philippe Block, "Funicular Shell Design Exploration," in *ACADIA 13: Adaptive Architecture*, Proceedings of the 33rd Annual Conference of the Association for Computer Aided Design in Architecture (ACADIA) (Cambridge, 2013), 337–46.

[100] Block Research Group, *rhinoVault 2: Funicular Form Finding for Rhinoceros 6+* (2020), https://github.com/BlockResearchGroup/compas-RV2.

[101] Pekka Heikkinen and Philip Tidwell, "Designing Through Experimentation: Timber Joints at the Aalto University Wood Program," in *Rethinking Wood: Future Dimensions of Timber Assembly*, ed. Markus Hudert (Basel: Birkhäuser, 2019), 60–87.

[102] Heikkinen and Tidwell, "Designing Through Experimentation," 75.

ber plates.[103] They achieved the multi-directional bending through the strategic removal of material. Thereby, the plywood lost its stiffening constraints. Two case studies built out of three-millimeter thick plywood served as proof of their concept.[104] The inspiration for their work was the 2010 ICD/ITKE research pavilion.[105] That pavilion consisted of eighty single-bent plywood strips with a thickness of 6.5 millimeters.[106] Through their interconnectedness, they formed a self-stabilizing structure.[107] These projects partially build upon the fundamental research of Weinand et al.[108] They tested the limits of actively bent wood by conducting several load tests and structural analyses on timber rib shells.[109] Their findings led them to the design and fabrication of a "three-directional timberfabric" structure. That is a complex structure consisting of multi-directional bent timber plates that are interwoven like a fabric.[110] Alvarez et al. further explored the integration of weaving patterns to fabricate thin wooden shells.[111] For that purpose, they developed a workflow that included the bending and fastening of the thin plywood segments. To fixate the elements, an industrial robotic arm sewed the segments together.

Satterfield et al. demonstrated how a similar structure is achievable through "kerf-bending."[112] The "kerf-bending" describes the process of multiple parallel cuts through solid timber, after which that is bendable. For their demonstrators, they milled the kerfs in two laths per beam. Then, they zipped the laths together and bent them to the desired shape (see Figure 2.11).[113] Baseta further developed that system by conducting several strength tests to gain a better understanding of its structural behavior.[114] These tests included computational simulations and physical prototypes.[115] Also, they investigated two different kerf geometries.[116] Furthermore, Liu et al. applied the technique of kerf-bending to develop nodes for timber space frames. Their proposed system is easy to fabricate and extends the design possibilities of bent timber.[117]

[103] Simon Schleicher, Riccardo La Magna, and Jan Knippers, "Bending-Active Plates: Planning and Construction," in *Fabricate 2017: rethinking design and construction*, ed. Achim Menges et al. (London: UCL Press, 2017), 242–49, doi:10.14324/111.9781787350014.

[104] Schleicher, La Magna, and Knippers, "Bending-Active Plates," 247–48.

[105] Menges and Knippers, *Architecture Research Building*, 46–55.

[106] Menges and Knippers, *Architecture Research Building*, 52.

[107] Menges and Knippers, *Architecture Research Building*, 48.

[108] Yves Weinand, *Advanced Timber Structures: Architectural Design and Digital Dimensioning* (Basel: Birkhäuser, 2017), 91–124.

[109] Weinand, *Advanced Timber Structures*, 102–7.

[110] Weinand, *Advanced Timber Structures*, 108–17.

[111] Martín E. Alvarez et al., "Tailored Structures, Robotic Sewing of Wooden Shells," in *Robotic Fabrication in Architecture, Art and Design 2018*, ed. Jan Willmann et al. (Zurich: Springer, 2018), 406–21, doi:10.1007/978-3-319-92294-2.

[112] Blair Satterfield et al., "Bending the Line: Zippered wood creating non-orthogonal architectural assemblies using the most common linear building component (THE 2x4)," in *Fabricate 2020: making resilient architecture*, ed. Jane Burry et al. (London: UCL Press, 2020), 58–65, doi:10.14324/111.9781787358119.

[113] Satterfield et al., "Bending the Line," 62–63.

[114] Efilena Baseta, "BEND & BLOCK: a shape-adaptable system for the rapid stiffening of active-bending structures" (PhD diss., Vienna: University of Applied Arts Vienna, 2019).

[115] Baseta, "BEND & BLOCK," 22–27.

[116] Baseta, "BEND & BLOCK," 74–75.

[117] Liu, Lu, and Akbarzadeh, "Kerf Bending and Zipper in Spatial Timber Tectonics."

Figure 2.11: Left: *Team members demonstrate the bending of a two-by-four prepared for use in the pavilion prototype. No steaming or soaking was required to bend the member. Members are glued and vacuum-bagged.* Right: *One Bay Prototype.* Photographs by Blair Satterfield et al., 2020.

The mechanical approach to bending timber poses a variety of challenges. Specifically, that is the process of bending the timber elements into the desired shape without breaking the material. Even if that succeeds, the timber tries to deform itself back into its original shape.[118]

A different approach to bending timber makes use of its material-inherent properties. This is its hygroscopic nature, i.e., its behavior related to the moisture content. Krieg et al. demonstrated with their "HygroSkin Pavilion" how that behavior can influence an architecture that responds to its environment.[119] The pavilion consisted of bent plywood sheets with small circular openings.[120] Attached to these openings were hygroscopic apertures made out of polyurethane and wood. These apertures opened and closed depending on the relative humidity.[121] Wood et al. demonstrated how that concept applies to large-scale structures.[122] For the design of a 14.2 meters tall tower, they used timber boards with a thickness of forty millimeters (see Figure 2.12). These boards were kiln-dried to a wood moisture content of 12%. Then, they were shaped to the target curvature. Together, two elastic wooden bilayers and an elastically bent locking layer achieved form stability through being glued together. The curvature of the tower's twelve components increased the bending stiffness of the overall structure. Also, their primary fiber orientation aligned to the vertical load-bearing direction. Thereby, the tower had a coherent and efficient structure.[123]

---

[118] Gethmann, "Kai Strehlke (Blumer-Lehmann AG) in Conversation with Urs Hirschberg (GAM)," 122.

[119] Oliver David Krieg et al., "Hygroskin: Meteorosensitive Pavilion," in *Fabricate 2014: negotiating design and making*, ed. Fabio Gramazio, Matthias Kohler, and Silke Langenberg (London: UCL Press, 2017), 272–79, doi:10.14324/111.9781787352148.

[120] Krieg et al., "Hygroskin," 274.

[121] Krieg et al., "Hygroskin," 278.

[122] Dylan Wood et al., "From Machine Control to Material Programming: Self-Shaping Wood Manufacturing of a High Performance Curved CLT Structure – Urbach Tower," in *Fabricate 2020: making resilient architecture*, ed. Jane Burry et al. (London: UCL Press, 2020), 50–57, doi:10.14324/111.9781787358119.

[123] Wood et al., "From Machine Control to Material Programming," 54.

Figure 2.12: *The Urbach Tower, a high performance timber structure utilising self-shaping wood manufacturing for curved CLT.* Photograph by Rolland Halbe, 2020.

Furthermore, Jahn et al. demonstrated the possibilities of steam-bending timber into forms with high curvature.[124] For their prototypes, they dried the timber strips for 30–45 minutes. Afterward, they had 90 seconds to bend and fixate the strips. For the assembly, they implemented augmented reality (AR) tools. Due to the short drying duration, their prototypes suffered from a significant amount of spring back.[125] However, these prototypes led to the construction of the "Steampunk Pavilion" for the 2019 Tallinn Architecture Biennale (see Figure 2.13).

2.3.2.3 Glulam Structures

Since its invention by Otto Hetzer, glulams were mainly used to construct arch and shell structures.[126] However, the roof structure of the brine baths in Bad Dürrheim, Germany, from 1987 marks a relevant shift. There, five tree-like columns support the lattice shell that forms the roof structure.[127] The lattice

---

[124] Gwyllim Jahn, Andrew John Wit, and James Pazzi, "[BENT]," in *ACADIA 19: UBIQUITY AND AUTONOMY*, Proceedings of the 39th Annual Conference of the Association for Computer Aided Design in Architecture (ACADIA) (Austin: The University of Texas at Austin School of Architecture, 2019), 438–47.

[125] Jahn, Wit, and Pazzi, "[BENT]," 441–42.

[126] Müller, *Holzleimbau = Laminated Timber Construction*, 42–165.

[127] Müller, *Holzleimbau = Laminated Timber Construction*, 166.

Figure 2.13: Left: *STEAMPUNK Pavilion.* Right: *AR-assisted assembly.* Photographs by Peter Bennets, Hanjun Kim, and Cameron Newnham, 2019.
https://soomeenhahm.com/portfolio-item/steampunk-pavilion/.

shell consists of numerous, partially double-curved glulam ribs. At their intersections, cross-lap joints make a transition in one layer possible. Additionally, the tree-like columns portray the possibilities of glulams. Just before each main branch reaches the top, it splits into two separate branches. This happens exactly between two layers of lamination. Here, the glulam is simply bent in two directions so that no cutting operations are required (see Figure 2.14). The structure as a whole was well optimized and material efficient. However, it was accompanied by an extensive planning and assembly process—a scheme that further free-form structures inherit as well.[128]

Figure 2.14: *Tree columns at the Bad Dürrheim brine baths.* Photograph by Kur- und Bäder GmbH Bad Dürrheim, 2016.
https://www.db-bauzeitung.de/therapiezentrum-solemar-in-bad-duerrheim/.

---

[128] Müller, *Holzleimbau = Laminated Timber Construction*, 168.

In the past decade, a range of built projects demonstrated the advancements of free-form glulam structures. The development began with two buildings designed by architecture practice Shigeru Ban Architects: the Centre Pompidou in Metz, France, and the Haesley Nine Bridges Golf Club in Yeoju, South Korea (see Figure 2.15). In both projects, the design and consulting firm Design-to-Production acted as an intermediary between the design and the production. For that purpose, they developed generic workflows and corresponding tools to make these projects feasible.[129] The workflows start with the detailing of the 3D model in computer-aided design (CAD) software. Then, the data is passed on to the computer-aided manufacturing (CAM) software that generates the machine code for fabrication.[130] Stehling et al. improved that workflow further, as they demonstrated with the fabrication and assembly of the Seine Musicale.[131] The bending of the double-curved elements and their assembly presented the greatest challenges. Most of the glulam blanks consisted of thin stick lamellae, allowing the blanks to be bent in two directions. For others, they applied a conventional two-step approach. Thereby, they first laminated straight planks into single-curved blanks. These are then cut crosswise into strips again. The resulting lamellae are laminated again, resulting in a double-curved glulam blank.[132] Furthermore, Stehling et al. demonstrated that their workflow applies to complex large-scale structures as well.[133] Similarly, Yuan et al. presented a related workflow for the fabrication of a large-scale non-uniform timber gridshell.[134] They implemented multi-objective optimization algorithms to generate a structurally optimized form. Additionally, they investigated the stiffness of the joints. That informed the digital fabrication of the necessary parts as well.[135]

Most of the recent developments of free-form timber structures happened within an industry and practice-related context. However, there is significant research that further extends the possibilities of curved glulam blanks. Svilans presented range of tools and concepts for a complete design-to-fabrication workflow.[136] Starting at the design stage, they developed a software extension that facilitates the design of glulam blanks based on curves.[137] It provides the ability to analyze the generated glulam blanks, in particular, the curvature and bending within a component.[138] Additionally, they implemented the functionality to create a range of intersection joints, including cross-lap joints and splice joints (see Figure 2.16). The glulams could then be fabricated.[139]

---

[129] Hanno Stehling, Fabian Scheurer, and Jean Roulier, "Bridging the Gap from CAD to CAM: Concepts, Caveats and a new Grasshopper Plug-In," in *Fabricate 2014: negotiating design and making*, ed. Fabio Gramazio, Matthias Kohler, and Silke Langenberg (London: UCL Press, 2017), 52–60, doi:10.14324/111.9781787352148.

[130] Stehling, Scheurer, and Roulier, "Bridging the Gap from CAD to CAM," 54–56.

[131] Hanno Stehling et al., "From Lamination to Assembly: Modelling the Seine Musicale," in *Fabricate 2017: rethinking design and construction*, ed. Achim Menges et al. (London: UCL Press, 2017), 258–63, doi:10.14324/111.9781787350014.

[132] Stehling et al., "From Lamination to Assembly," 261–62.

[133] Hanno Stehling, Fabian Scheurer, and Sylvain Usai, "Large-Scale Free-From Timber Grid Shell: Digital Planning of the new Swatch Headquarters in Biel, Switzerland," in *Fabricate 2020: making resilient architecture*, ed. Jane Burry et al. (London: UCL Press, 2020), 210–17, doi:10.14324/111.9781787358119.

[134] Philip F. Yuan et al., "Robotic Fabrication of Structural Performance-based Timber Gridshell in Large-Scale Building Scenario," in *ACADIA 16: POSTHUMAN FRONTIERS: Data, Designers, and Cognitive Machines*, Proceedings of the 36th Annual Conference of the Association for Computer Aided Design in Architecture (ACADIA) (Ann Arbor, 2016), 196–205.

[135] Yuan et al., "Robotic Fabrication of Structural Performance-based Timber Gridshell in Large-Scale Building Scenario," 199–203.

[136] Svilans, "Integrated material practice in free-form timber structures."

[137] Svilans, "Integrated material practice in free-form timber structures," 161–202.

[138] Svilans, "Integrated material practice in free-form timber structures," 203–13.

[139] Svilans, "Integrated material practice in free-form timber structures," 196–98.

Figure 2.15: Left: *Centre Pompidou-Metz.* Right: *Haesley Nine Bridges Golf Club House.* Photographs by Shigeru Ban Architects, 2010.
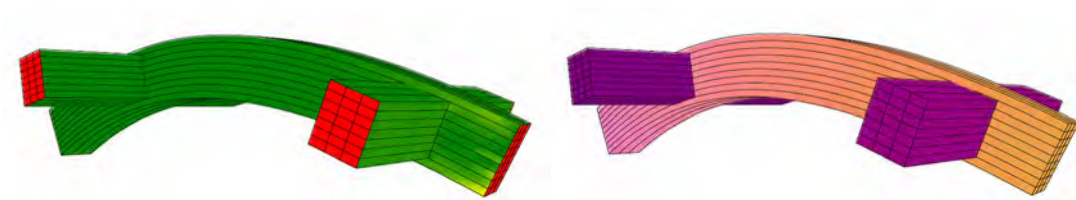https://www.shigerubanarchitects.com/.

Figure 2.16: *The fibre analysis of the Cross-laminated Joint Blank.* Illustration by Tom Svilans, 2020.

Svilans further demonstrated how to achieve a direct material feedback loop at the fabrication stage. That is especially relevant for complex geometries fabricated with multi-axis machines to achieve the desired results.[140] That culminated in a range of prototypes, specifically of bridge structures and art installations (see Figure 2.17).[141]

In general, the reviewed research portrays that the bending and simultaneous gluing of timber planks is a major challenge of curved glulams.[142] To that end, Bahar et al. presented a process to bend glulams without the need for external clamping.[143] They constrained a stack of wooden lamellae at their ends and bent them to the desired form. The embedded forces pressed the planks together, enabling a glue-

---

[140] Svilans, "Integrated material practice in free-form timber structures," 256–78.

[141] Svilans, "Integrated material practice in free-form timber structures," 281–356.

[142] Svilans, "Integrated material practice in free-form timber structures," 218–19.

[143] Bahar Al Bahar et al., "Bending-Active Lamination of Robotically Fabricated Timber Elements," in *Research Culture in Architecture: Cross-Disciplinary Collaboration*, ed. Cornelie Leopold (Basel: Birkhäuser, 2020), 89–97, doi:10.1515 / 9783035620238-009.

Figure 2.17: *Grove.* Image by Tom Svilans and Leonardo Castaman, 2017.
https://tomsvilans.com/#grove.

based lamination.[144] They developed a tool to simulate that behavior. Finally, a robotic arm could bend the prototypical glulams to the desired shape as calculated.[145]

The state-of-the-art review revealed several insights. The digital fabrication practices in timber construction are very advanced in both the industry and academia. While industrial processes cultivate mechanisms of serialization, standardization, and mass production, academic research develops methods to expand the bespoke, non-serial and performative possibilities of timber construction. However, both sectors implement cutting-edge tools, e.g., multi-axis CNC-machines, industrial robots, and 3D scanners. These developments coincide with new structural expressions. Specifically, free-form timber structures benefited immensely from the advancements of algorithmic design tools and digital fabrication methods. Their historical evolution supports that notion. However, they still require significant expertise and resources for their construction. Also, the review revealed a research gap in the recycling of timber both regarding the design and fabrication, and the implementation of a digital toolchain and integrated workflow. Even though there are conceptual developments, only a few research projects seriously propose scalable solutions.

---

[144] Al Bahar et al., "Bending-Active Lamination of Robotically Fabricated Timber Elements," 91–93.

[145] Al Bahar et al., "Bending-Active Lamination of Robotically Fabricated Timber Elements," 94.

Chapter 3
Methodology

In this chapter, the design-to-fabrication workflow is explained in detail. It is divided into four sections. The first part covers the digitization of the offcuts and the creation of digital twins. Then, the alignment of elements along given curves builds up on that. The third part deals with the required wood joints to create integral structures. Finally, the fourth section explains the digital fabrication setup, i.e., the tools and methods used to fabricate and assemble the offcuts.

3.1 Offcut Data

This section covers the process from collecting the offcuts to creating a digital twin for each one of them. That includes the measuring and scanning as well as the creation of a unique Class with multiple properties to store and work with the generated data. Figure 3.1 highlights this step within the design-to-fabrication workflow.

3.1.1 Digitizing Offcuts

The process of digitizing the offcuts is the principal step in working with the material. Its goal is to register the relevant data of each object and store it in a database. Primarily, the main dimensions are measured. There, the z dimension corresponds to the length in the fiber direction of an offcut. The x and y dimensions define the object's cross-section, where x is always the bigger of the two values (see Figure 3.2). Also, every offcut receives a numerical ID, so that the digital and the physical objects correspond. All data is stored within an XLS (Microsoft Excel Spreadsheet) or CSV (Comma Separated Values) file. It would also be possible to use the JSON (JavaScript Object Notation) or XML (Extensible Markup Language) file formats, though that has not been implemented yet.

In the scope of this thesis, a millimeter ruler and a spirit level were used for manual measuring. This method has its advantages and disadvantages. The manual measuring process is fast and relatively precise. Within one minute, two to three offcuts can be measured and tagged. However, the method lacks precision if the offcut is not a perfect cuboid, which in very few cases is true. Oftentimes, there are differences in a range of 0.1–2.0 millimeters. Therefore, while working with this method, it is necessary to pick a reasonable value for the dimension and accept that there are tolerances.

On the contrary, a digital measuring process would be very precise but take more time. Not only would it measure the dimensions precisely, but it would also detect any irregularities on the surface.
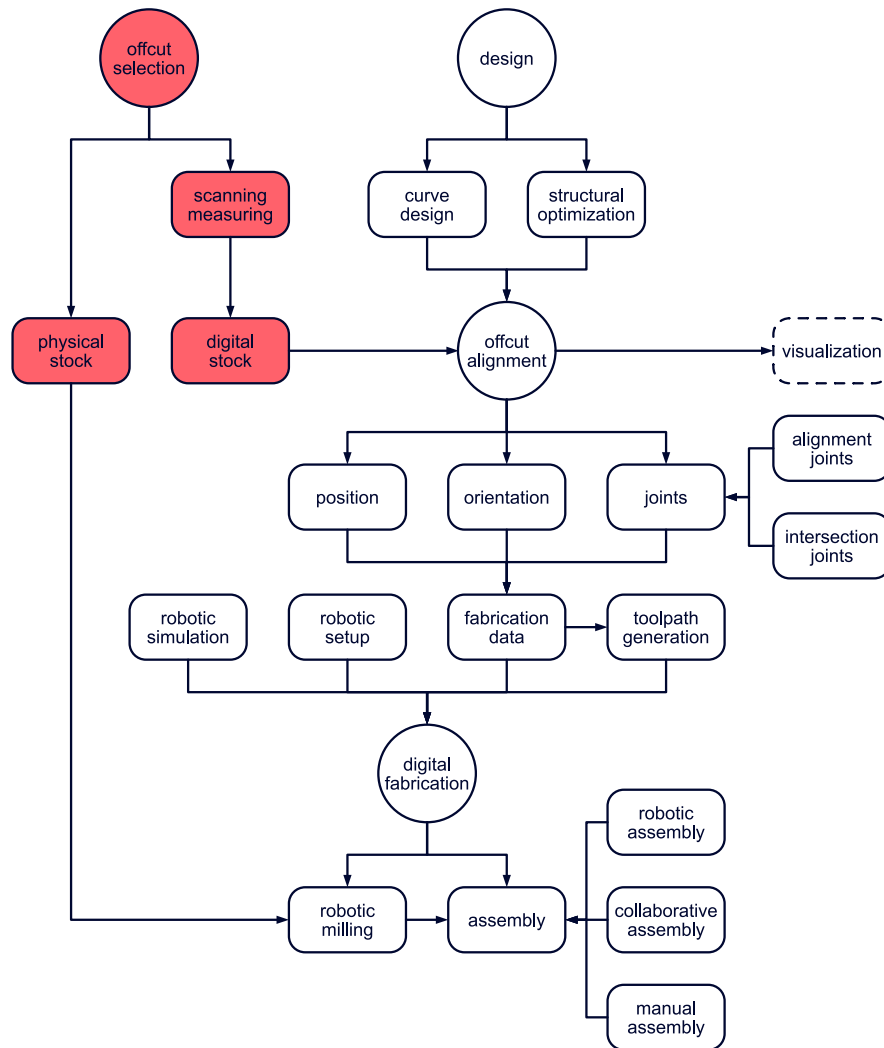
Figure 3.1: *Offcut database within the workflow.*

That accuracy is relevant for further digital fabrication processes that are very precise as well. However, measuring the offcuts with a 3D scanner attached to a robotic arm, for instance, takes its time. For each object, the robot would move to specific positions to collect data. Then, the software in the background constructs a point cloud that would have to be post-processed again.

In general, the process of digitizing the offcuts has the potential of being scaled up to an industrial process. Already, 3D scanning is a vital part of the timber industry (see Chapter 2.2). In combination with conveyor belts, that process could be sped up immensely. However, that technology was not available for this work.

Figure 3.2: *Dimensions of an offcut.*
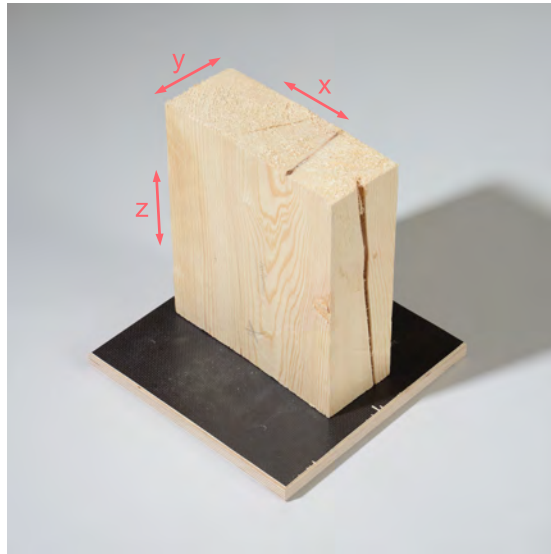
3.1.2 Digital Twin

After the measuring process is complete, the data for each offcut is stored within a file. The plugin provides the means to access this data in Rhino3d and Grasshopper. Since the process of working with the material will generate more information, the plugin uses a custom Class called *Offcut*. In its most primitive form, every instance of that Class contains the ID, the *x*, *y*, and *z* dimensions, and the volume of the corresponding offcut. The components "XLS to Offcut" and "CSV to Offcut" use the data in the respective files and convert it to the basic Offcut instances (see Listing 3.1). Furthermore, there is the component "Construct Offcut" that enables the creation of Offcut instances within the software environment. For that, it simply needs three numerical values.

```
1   // read CSV file and add string data to list
2   ReadCSV readCSV = new ReadCSV(filePath);
3   List<string> coordinatesTxt = readCSV.GetCSVData();
4
5   // initialise new list of Offcuts
6   List<Offcut> offcutList = new List<Offcut>();
7
8   // iterate over strings from csv file, convert to Offcut and add to list
9   for (int i = 0; i < coordinatesTxt.Count; i++)
10  {
11      // split string into coordinate strings
12      string[] coordinates = coordinatesTxt[i].Split(';');
13
14      // convert strings to doubles
15      double index = Convert.ToDouble(coordinates[0]);
16      double x = Convert.ToDouble(coordinates[1]);
17      double y = Convert.ToDouble(coordinates[2]);
18      double z = Convert.ToDouble(coordinates[3]);
19
```

```
20        // initialise new Offcut instance
21        Offcut offcutInstance = new Offcut(index, x, y, z);
22
23        // add Offcut to list
24        offcutList.Add(offcutInstance);
```

Listing 3.1: Convert CSV data to Offcut instances.

The Offcut class is able to store additional information (see Listing 3.2). Depending on the process, the various components available will generate more data and update every instance accordingly. Most notably, it stores the geometry of the Offcut as a Boundary Representation (BRep).[1] That is the basis for further Boolean operations and for generating the fabrication data. The Class also stores the initial volume that the components covered above. In every subsequent process that changes the Offcut, the volume is calculated again but stored in another property called "FabVol" (Fabricated Volume). Furthermore, the Offcut can store a range of planes that any of the alignment components covered in Section 3.2 generate. Also, it sets an index for the position on the alignment. The component "Deconstruct Offcut" can deconstruct Offcut instances and make available all properties. Then, this data can be manipulated and, finally, assembled back into an Offcut instance with the "Assemble Offcut" component.

```
1     public Brep OffcutGeometry { get; set; }
2     public double Index { get; set; }
3     public double X { get; set; }
4     public double Y { get; set; }
5     public double Z { get; set; }
6     public double Vol { get; set; }
7     public double FabVol { get; set; }
8     public Plane FirstPlane { get; set; }
9     public Plane SecondPlane { get; set; }
10    public Plane AveragePlane { get; set; }
11    public Plane MovedAveragePlane { get; set; }
12    public Plane BasePlane { get; set; }
13    public int PositionIndex { get; set; }
```

Listing 3.2: Offcut data.

All data is collected because it is necessary for subsequent steps. That includes the design and the fabrication processes. It also provides relevant information about how much material would be lost during fabrication. That informs a more efficient planning process with less waste and reduced fabrication times.

To this end, additional data would be storable in the Offcut class. Most notably, that includes specific material properties, e.g., the wood species, the age, the time of harvesting, the date and the reason an offcut was cut, and its storage time. Furthermore, it could store the geometrical information as a mesh geometry, potentially resulting in faster computation times and more robust results.

---

[1] Vadim Shapiro, "Chapter 20 - Solid Modeling," in *Handbook of Computer Aided Geometric Design*, ed. Gerald Farin, Josef Hoschek, and Myung-Soo Kim (Amsterdam: North-Holland, 2002), 473–518, doi:https://doi.org/10.1016/B978-044451104 -1/50021-6.

3.2 Offcut Alignment

In this section, the alignment of the offcuts along given curves is covered. As a prerequisite, the dimensions of the offcuts should be available. As covered in section 3.1.1, that data is stored in an XLS or CSV file. The components "XLS to Offcut" and "CSV to Offcut" convert that data into Offcut instances.

In the scope of this thesis, an alignment is defined as the positioning of Offcut instances on a line-like or curved curve. Thereby, the grain direction of the offcuts—which is defined by their z dimensions—always follows the orientation of the curve. Because of that, the transfer of forces is as optimal as possible. However, the offcuts have to be cut at their ends to enable a smooth alignment. Figure 3.3 highlights this step within the design-to-fabrication workflow.
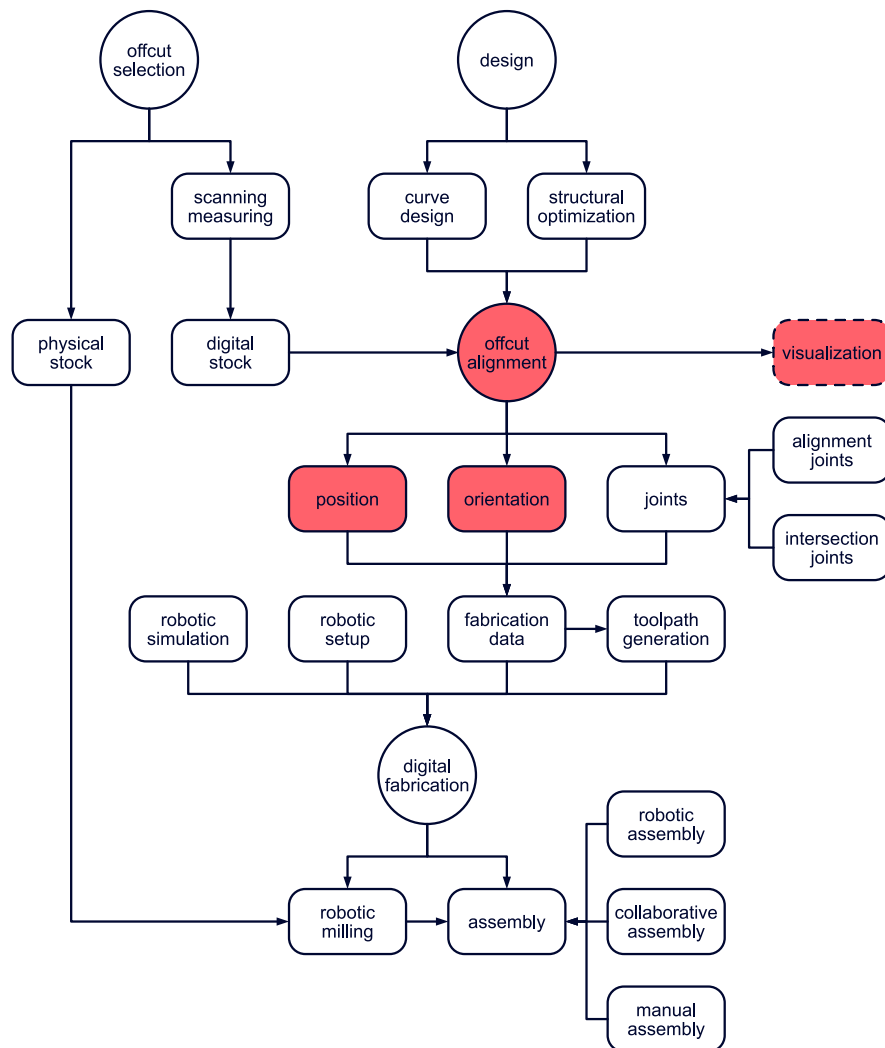

Figure 3.3: *Offcut alignment within the workflow.*

3.2.1 Basic Alignment

There are three components available for aligning offcuts on a curve. These are "Curve Alignment", "Optimized Alignment", and "Direct Alignment". Each of them has specific functionality. However, they all share the same basic principles. The algorithm iteratively places each offcut, deciding after each iteration which element to place next. Thereby, it follows the steps depicted in figure 3.4.
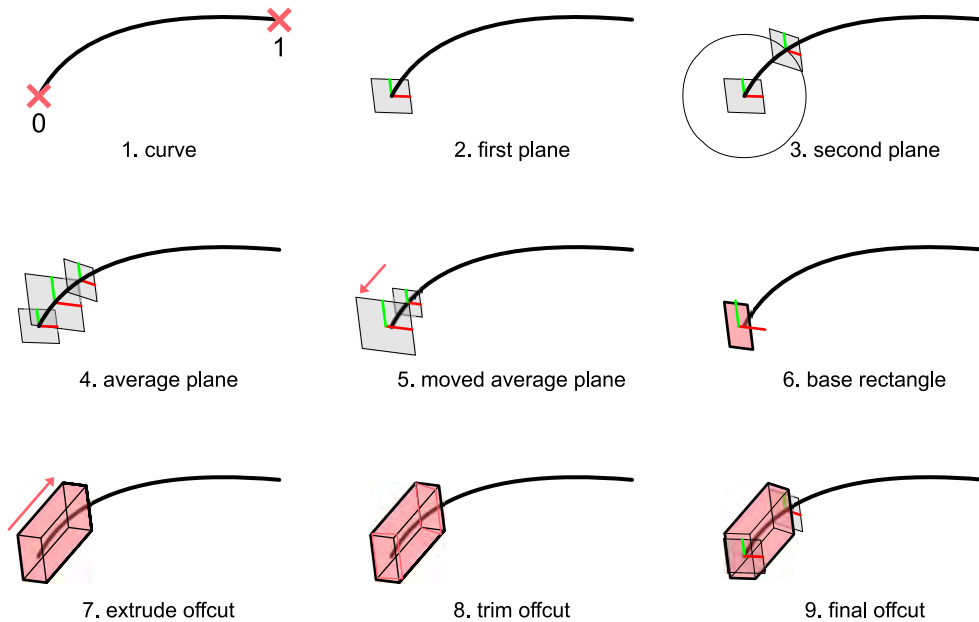

Figure 3.4: *The sequential steps of the alignment: 1. Set curve domain, 2. Compute first plane, 3. Compute second plane, 4. Compute average plane, 5. Move average plane, 6. Generate base rectangle, 7. Extrude rectangle to cuboid, 8. Trim cuboid, 9. Final cuboid, i.e., offcut.*

For the components to solve the instances it is necessary to provide a curve and Offcut data. At first, the curve is reparameterized. That means that its domain is set to a boundary between 0 at its start and 1 at its end. To generate the Offcut geometry, three planes are necessary. For the first one, the algorithm computes a plane in the form of a perpendicular frame at the start of the curve instance. Then, a sphere is created with the first plane's origin as the center point. Its radius is determined by the z-value of the Offcut to be placed. At the intersection of the sphere and the curve, the algorithm computes another perpendicular frame, which is the second plane. If the center point of the sphere is not close to the start or the end of the curve, there will be two intersection points. In that case, only the second one is considered. Otherwise, the alignment would go backward and the geometry would overlap. Now, to generate the Offcut geometry, an average plane is computed from the first and second planes (see Listing 3.3).

```
1    // get average origin point
2    Point3d originPt = new Point3d(
3        (firstPlane.Origin + secondPlane.Origin) / 2);
4
5    // get average plane
6    Plane averagePlane = new Plane(originPt,
7        (firstPlane.XAxis + secondPlane.XAxis) / 2,
8        (firstPlane.YAxis + secondPlane.YAxis) / 2);
```

Listing 3.3: Compute average plane.

The average plane is the base plane of the Offcut geometry. Its x, y, and z-axis correspond to the x, y, and z dimensions of the Offcut. Also, it determines the geometry's orientation. Next, the average plane is moved along its z-axis in the negative direction by half the current z dimension. Then, a rectangle is created with various positioning options. It is always generated from its lower-left corner. To get different positions, the x and y dimensions must be used accordingly. The nine main positions are predefined and implemented within the code (see Figure 3.5).[2] Each position has an index that is stored as data within each Offcut instance for further operations.

Finally, the rectangle is extruded along the z-axis with the amount of the z dimension. Now, the Offcut is at its correct position. However, it has to be cut to ensure a perfect fit between all Offcuts on the alignment. Therefore, the first and second planes trim the cuboid (see Listing 3.4). For that, the first plane has to be flipped, since the geometry in its z direction is deleted. Afterward, the open faces of the cuboid are closed and a clean-up is performed.

```
1    // trim Offcut for optimal alignment
2    firstPlane.Flip();
3
4    Brep firstTrim = unionOffcuts.Trim(firstPlane, 0.0001)[0];
5    Brep firstCap = firstTrim.CapPlanarHoles(0.0001);
6    Brep secondTrim = firstCap.Trim(secondPlane, 0.0001)[0];
7
8    firstPlane.Flip();
9
10   // cap holes and split kinky faces
11   Brep outputOffcut = secondTrim.CapPlanarHoles(0.0001);
12   outputOffcut.Faces.SplitKinkyFaces(0.0001);
```

Listing 3.4: Trim Offcut.

The function returns the geometry in the form of a BRep and a list of planes. The BRep data is stored in the correct Offcut instance, while the planes are necessary for further computations. Specifically, in the next iteration, the second plane becomes the new first plane, and the cycle repeats.

As the algorithm is now, it would fail when it reaches the end of the curve. There, it would take the first—and only—intersection point of the curve and the sphere, and go backward with the computation. However, trimming the geometry with the planes that way would produce a *null*, resulting in the subsequent code failing. To ensure that does not happen, the algorithm checks at every iteration the distance between the origin of the second plane and the endpoint of the curve. If that distance is smaller than

---

[2] Of course, further parametrization is possible, where the exact position of the rectangle could be set by x and y domains between 0 and 1. However, the defined positions are all that is necessary for this work, and, therefore, this has not been implemented.
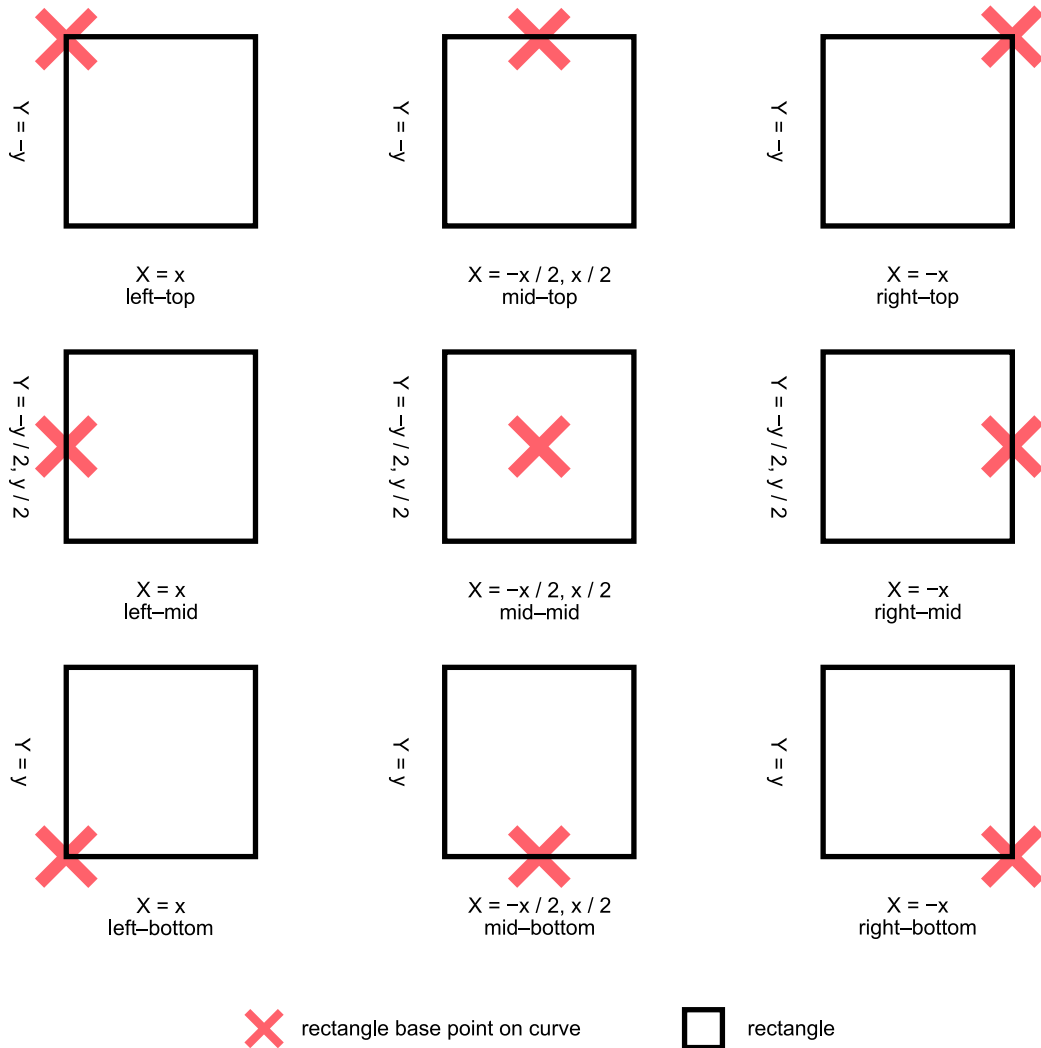
Figure 3.5: *Rectangle positioning on the Curve.*

the largest *z* dimension still available in the list of Offcuts, the code knows that the end of the curve is reached. It then takes the longest Offcut and places it as the last item of the alignment. The geometry of that item is cut with the plane at the curve's endpoint, completing the computation.

All of the alignment components have the added functionality of torsion, i.e., the alignment can be twisted. For that, a start and an end angle must be provided. By default, they are set to 0 degrees[3], letting the alignment behave normally. However, changing the values will result in a gradual rotation of the Offcuts. To achieve that, the algorithm creates an interval between the start and the end angle

---

[3] By default, the rotation transformation works with radians. However, the algorithm translates all values provided in degrees into radians.

and remaps that onto an interval between 0 and 1. Now, for each point on the curve's domain between 0 and 1, an exact angle is defined. Then, every plane that is computed for the alignment is rotated by a specific angle that is determined by its location. Thus, it also influences the computation of each average plane, and, therefore, the placement and orientation of the Offcut geometry. The benefit of that functionality lies within the possibility of orienting the alignments as necessary, regardless of the curve's shape. For instance, if each the start and the end of an alignment need a specific orientation, only the required angles would have to be provided. Furthermore, the alignment can be rotated as a whole without changing the relation between the Offcuts by providing the same start and end angles (see Figure 3.6).
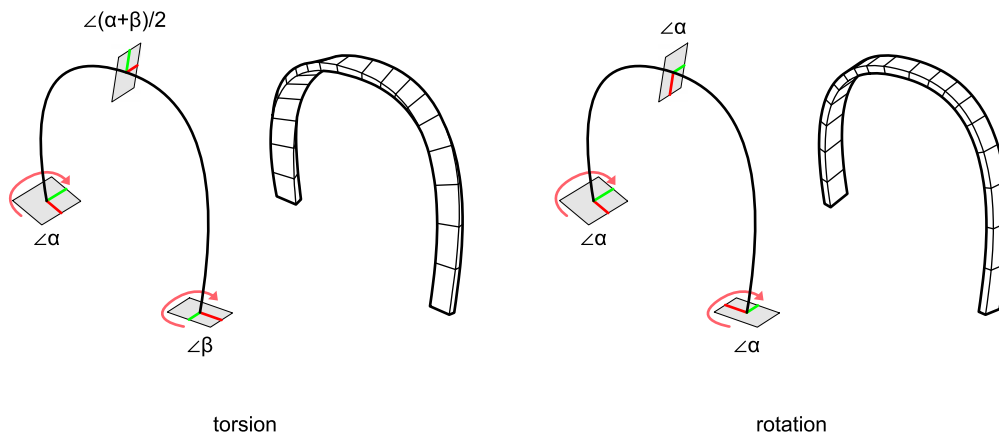

torsion   rotation

Figure 3.6: Left: *Torsion of an alignment with different start (α) and end (β) angles.* Right: *Rotation of an alignment with the same start and end angles.*

Finally, the alignment components return the aligned Offcuts on the curve and a list of all unused Offcuts still available in the list. Then, another alignment can be computed with the updated data. Additionally, the components return a centered curve.

3.2.2 Alignment Optimization

As mentioned in Section 3.2.1, the different types of alignment components have specific functionality. The most relevant differentiation is the selection of which Offcut instance to place next. The component "Curve Alignment" takes the items from the list as is. Thereby, the alignment is determined by how this list is organized. However, that might result in the placement of longer Offcuts at points with high curvature. As a result, more of the geometry has to be cut to follow the curve, leading to increased material waste. Additionally, the alignment might be coarse, leading to decreased structural and aesthetic qualities (see Figure 3.7).

Contrary to that, the other two alignment components use an optimization algorithm. Its logic consists of matching the z dimensions of the Offcuts to the curvature of the curve. For that process, it is necessary to compute the curve's curvature at multiple points. Within the components, a value of 400 points is predefined. A higher number would result in higher accuracy, though it would also slow down
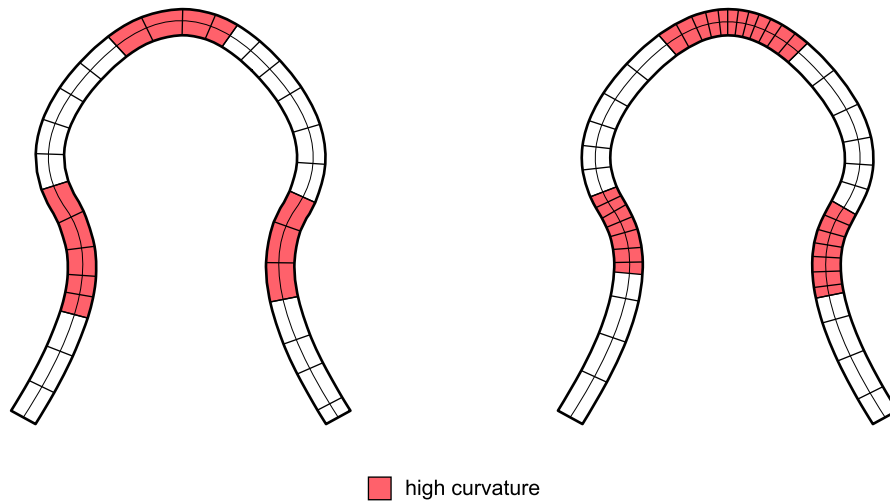
high curvature

Figure 3.7: Left: *Alignment of offcuts regardless of the curvature.* Right: *Optimized alignment with shorter offcuts at places with high curvature.*

the computation. From the resulting values, the minimum and maximum ones are extracted. These determine the domain of the curvature (see Listing 3.5). Simultaneously, the algorithm checks if the radius of the curvature is below a certain threshold, in this case, 0.25 meters. Below that value, any alignment is neither structurally nor material-wise feasible.[4] Then, the domain consisting of the minimum and maximum values of the Offcut's z dimensions is matched to the domain of the curvature. Any point on the curve now corresponds to a certain z dimension. The code is executed on every placement iteration, beginning with the start point of the curve. Already here, it is determined which Offcut to place. As mentioned in Section 3.2.1, the origin of the second plane will become the first point of the next iteration, where, again, it is determined on which Offcut to place.

```
1    // list to store curvature values
2    List<double> lengthList = new List<double>();
3
4    // predefine accuracy value
5    double accuracy = 400;
6
7    for (int i = 0; i <= accuracy; i++)
8    {
9        var curvature = crv.CurvatureAt(i * (1 / accuracy));
10       lengthList.Add(curvature.Length);
11   }
12
13   // define interval of the curvature
```

[4] The relation between the bending of a beam and its size is defined in Eurocode 5. However, since the alignments are rather experimental structures of single elements than industrial glulam beams, the norm has not been considered. (European Committee for Standardization (CEN), *Eurocode 5: Design of timber structures – Part 1–1: Common rules and rules for buildings*, tech. rep. EN 1995-1-1 [Brussels, 2004])

```
14     var curvatureMax = lengthList.Max();
15     var curvatureMin = lengthList.Min();
16
17     // check if curvature is too high
18     if (CurvatureRadius(crv, curvatureMax) < 0.25)
19         throw new Exception("Curvature is too high!");
20     else if (CurvatureRadius(crv, curvatureMin) < 0.25)
21         throw new Exception("Curvature is too high!");
22
23     // create interval
24     Interval curveBounds = new Interval(curvatureMin, curvatureMax);
25
26      private static double CurvatureRadius(Curve crv, double t)
27         {
28             Vector3d curvature = crv.CurvatureAt(t);
29             double curvatureRadius = 1.0 / curvature.Length;
30
31             return curvatureRadius;
32         }
```

Listing 3.5: Curve Curvature.

3.2.3 Linear Alignment

Up to now, the alignment only dealt with curves with a curvature, i.e., single or double-curved curves. However, if the Offcuts are to be aligned on a linear curve, i.e., a line, the algorithm will perform a slightly different logic to avoid errors. Primarily, the issue lies within the trimming of the Offcuts. This step is redundant if the curve is linear since the Offcuts are perfectly aligned and oriented. Also, it most likely will cause the operation to fail because the plane and the face of the BRep geometry are coinciding. In that case, the mathematical tolerances are impossible to solve for the software resulting in the calculation being stopped and an error thrown.

To overcome that issue, the cutting part is completely dismissed. Only the Offcut placed last on the alignment has to be cut because of its distinct way of being placed. For the "Curve Alignment" component, there are not too many changes. Most notably, it checks if the provided curve is linear and executes the relevant code according to that. However, the optimization logic of the other two alignment components is different if the curve is linear. Calculating the curvature on a line will yield no usable results, specifically since there is no interval to map the z dimensions onto. Therefore, the Offcut with the highest z dimension left on the list is taken on every iteration. In that way, the number of elements and joints is reduced as much as possible, resulting in reduced fabrication and assembly times.

In general, the logic of the algorithm is not only from a computational perspective legit but also from a material and fabrication perspective. In both cases, it is unnecessary to cut away any geometry since the Offcuts are aligned in parallel to the curve. However, in reality, it might be good practice to treat the end-faces of every Offcut, depending on their quality. Sometimes, the cut was performed roughly, meaning the surface is coarse as well. In that case, the strength of the connection between the elements could suffer, leading to problems in the structure as a whole.

3.3 Wood Joints

Having the Offcuts aligned on one or multiple curves of a design is fine within the digital realm of the software. However, in physical reality, joints are necessary to connect all elements to form coherent structures. Therefore, a crucial step is to design the joints and implement them in the correct position so that they can be fabricated. The components "Tenon Joints", "Spline Joints", and "Intersection Joints" provide that functionality. Figure 3.8 highlights this step within the design-to-fabrication workflow.
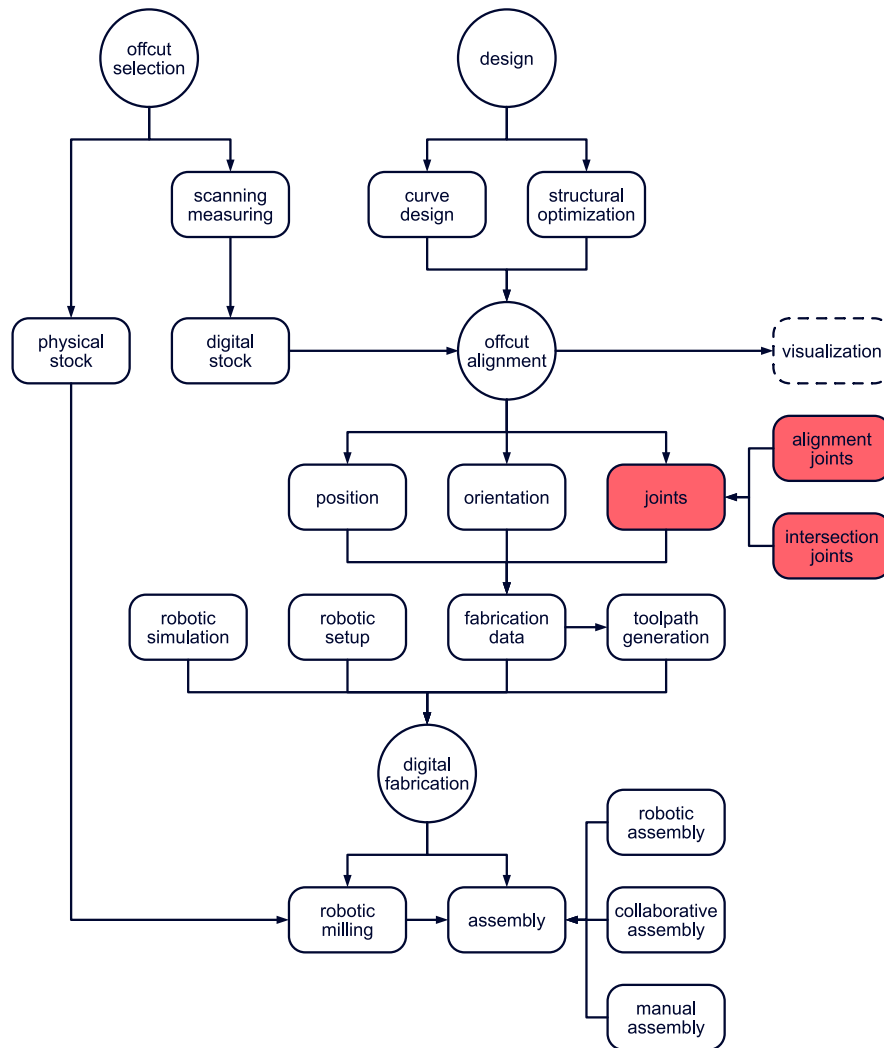
Figure 3.8: *Wood joinery within the workflow.*

Beforehand, it is necessary to clarify why wood joints are implemented instead of other joinery types, e.g., metal fasteners or adhesives. On the one hand, because of ecological, economical, and physical

issues, both glued connections and metal fasteners have not been considered.[5] On the other hand, wood joints have the added benefit that structures can be disassembled or even recycled waste-free. Also, their fabrication and assembly are comparably simple with digital tools. Of course, other joinery types have their benefits as well, while wood joints also pose some weaknesses. However, the arguments provided here are reason enough for that decision.

3.3.1 Tenon Joints

Tenon joints are geometrically simple joints that can transfer compression and shear forces in multiple directions. Their geometry consists of a base shape that is extruded, with a usual length of 40 mm per side of insertion.[6] They are either used as external connectors or in the more conventional method of a negative and a positive joint. In the scope of this thesis, only the first variation is used. There, merely the negative shapes of the offcuts to connect have to be cut. Thereby, as much of their length is preserved as possible. However, tenon joints are not able to transfer any significant tensile forces. Figure 3.9 shows the assembly sequence of a tenon joint.
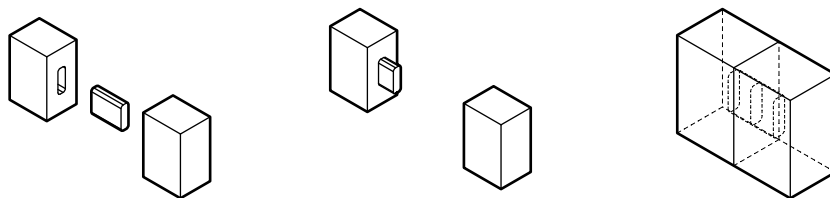

Figure 3.9: *Assembly sequence of a tenon joint.*

The component "Tenon Joints" generates that type of joint between the Offcuts of an alignment. To do this, it needs the list of Offcuts from an alignment component. All other options of parametrization are predefined with the possibility to change them. For instance, the size of the tenon joint is changeable by providing different x, y, or z values. Additionally, there can be multiple tenons between every two offcuts. They are generated along the x-axis of the relevant plane (see Listing 3.6). For fabrication purposes, the diameter of the milling tool must be provided. The value determines the radius by which the corners of the tenon joints are filleted. Thereby, the positive and negative joints fit perfectly after being milled.

The process of generating the tenon joints occurs iteratively, starting at the first Offcut of the alignment and ending at the last. For each Offcut, the start and the end plane are the basis to generate the tenon joints. There, the relevant plane is first moved along its z-axis in the negative direction by half the z dimension of the joint. Then, the number of joints to be computed is determined. The algorithm computes the base points depending on that number and the size of the x dimension of the current Offcut. Following that, it creates a centered rectangle at each point. Then, their corners are filleted according to the radius of the milling tool. Finally, the shape is extruded and a clean-up is performed.

---

[5] Wójcik and Strumiłło lay out the issues with metal fasteners, specifically. (Wójcik and Strumiłło, "Behaviour-based Wood Connection as a Base for New Tectonics," 177)

[6] Graubner, *Holzverbindungen Gegenüberstellungen japanischer und europäischer Lösungen*, 106.

```
1    // create lines
2    Line firstLine = new Line(basePlane.Origin, basePlane.XAxis, length/2);
3    Line secondLine = new Line(basePlane.Origin, basePlane.XAxis, -length/2);
4
5    // add lines to list and convert to curve
6    List<Curve> lineList = new List<Curve>
7    {
8    firstLine.ToNurbsCurve(),
9    secondLine.ToNurbsCurve()
10   };
11
12   // join curves
13   Curve centerLine = Curve.JoinCurves(lineList, 0.001)[0];
14
15   // divide curve by joint count and return points
16   centerLine.DivideByCount(count + 1, false, out Point3d[] points);
```

Listing 3.6: Computing the base Points for the Tenon Joints.

Now, that the tenon joints have been created as BReps at the correct position, the intersection between them and the Offcut must be solved. To generate the negative shape of the joint, the algorithm performs a "Boolean Difference" operation (see Listing 3.7). The method can perform that on lists and arrays of BReps, meaning it has to be called only once per Offcut. That reduces computation times immensely since Boolean operations on NURBS geometries are quite resource-demanding. Additionally, to increase the speed of computation even further, every iteration is performed within a multithreaded loop, specifically in a data-parallel operation. That means that the algorithm performs multiple operations, i.e. iterations, concurrently. However, the performance boost is heavily dependent on the number of cores available by the machine and their capacities. Also, that method poses problems if it is used on iterations that depend on being solved linearly. Therefore, the alignment components are not using it. After the Boolean operation succeeded, a clean-up is performed. The faces of the BRep are merged, split, and, after checking its orientation, returned. As a final step, the data for each Offcut is updated. That includes its geometry and volume after fabrication. Additionally, the component returns the geometry and the volume of each tenon joint.

```
1    public static Brep CutOffcut(Brep[] cuttingGeometry, Brep offcutInstance)
2    {
3        // store Offcut geometry in an array
4        Brep[] offcutBrep = new Brep[] { offcutInstance };
5
6        // boolean difference
7        Brep[] finOffcut = Brep.CreateBooleanDifference(
8            offcutBrep, cuttingGeometry, 0.0001);
9
10       // brep clean-up
11       finOffcut[0].Faces.SplitKinkyFaces(0.0001);
12       finOffcut[0].MergeCoplanarFaces(0.0001);
13       finOffcut[0].Faces.SplitKinkyFaces(0.0001);
14
15       // check solid orientation and return
16       if (BrepSolidOrientation.Inward == finOffcut[0].SolidOrientation)
17       {
18           finOffcut[0].Flip();
```

```
19        return finOffcut[0];
20     }
21   else
22        return finOffcut[0];
23 }
```

Listing 3.7: Cutting the Offcut with a Boolean Difference.

The "Tenon Joints" component provides further functionality. For instance, it is possible to change the shape of the tenon. There are two geometries predefined, i.e., a rectangular and a cross-shaped one. However, it is also possible to provide a custom shape in the form of a planar curve. That is scaled to fit the defined x and y dimensions to avoid any issues.

Furthermore, the algorithm determines at which position the Offcut is and executes different streams of the same logic. If the current element is the first or the last, the side where there is no neighboring Offcut is excluded from the calculation. Besides that, the logic stays the same.

Also, it is necessary to check the positioning of the alignment, as covered in Section 3.2.1. If it is not centered, i.e., mid-mid, the position of the joints has to be changed as well. For that purpose, the algorithm uses the same method to generate a rectangle at every plane based on the position index provided by the Offcuts. The x and y dimensions of that rectangle are calculated by a specific method. It compares the x- and y-values of each Offcut to those of its neighbors. Thereby, the minimum values are identified and used as the rectangle's dimensions. Then, its center point is assigned as the new origin of the tenon joints' base plane. Finally, the computation continues as described above.

3.3.2 Spline Joints

Spline joints are external connectors that are inserted in the timber pieces to join. They come in various shapes and sizes.[7] The joints are especially beneficial if the length of the timber to interlock is to be preserved since only the negative shape is cut. They will perform the best if they are made out of hardwood and inserted into softer wood species since the hygroscopic changes differ significantly.[8] Figure 3.10 shows the assembly sequence of a spline joint.
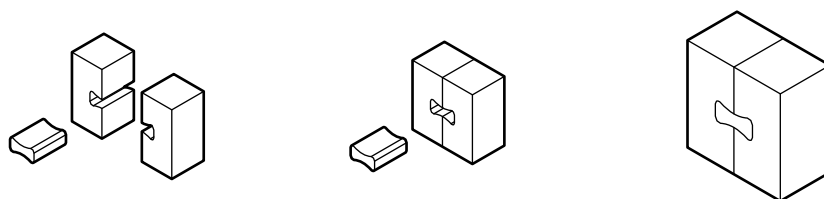

Figure 3.10: *Assembly sequence of a spline joint.*

[7] Koichi Nii, *The Complete Japanese Joinery* (Point Roberts, WA: Hartley & Marks, 1995), 193.

[8] Graubner, *Holzverbindungen Gegenüberstellungen japanischer und europäischer Lösungen*, 68.

The "Spline Joints" component generates that type of joint between the Offcuts on an alignment. It provides similar functionality as the "Tenon Joints" (see Section 3.3.1), i.e., controlling the x and y dimensions of the joint, the number of joints, and the tool diameter. Also, the algorithmic logic is the same. However, the main difference is the generation of the joint and its shape.

Since the spline joints are not parallel to the curve—as the tenon joints—but perpendicular to it, their base plane has to be rotated. That operation is performed around its x-axis with an angle of 90 degrees. Furthermore, the plane is moved along its z-axis in the negative direction by double the y dimension of the current Offcut. That is to ensure that the joint will cut through the geometry, regardless of how strong the torsion and the curvature are. Then, depending on the joint count, for each point, there are two BReps generated. The first one is the cutter with excessive length, ensuring that the negative shape is cut completely. The second one is for displaying and fabrication purposes. It has the length of the minimal y dimension of the two adjacent Offcuts.

The shape of the spline joints is derived from a simple rectangle with controllable dimensions (see Figure 3.11). For that, the four corner points and the center point are needed. In the x direction, the two points on each side are connected by a line, forming the top and the bottom of the joint. Then, a Control Point Curve connects the two corners points in the y direction. Having the center as a control point gives the curve and, therefore, the joint its distinct shape. Then, the two lines and the two curves are joined into one single curve. As a final step, the sharp angles are filleted by the tool radius. Then, that geometry is extruded into a BRep and the logic continues as described above.
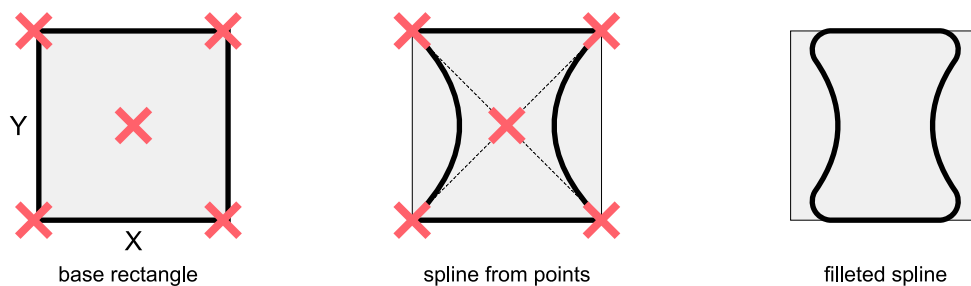

base rectangle   spline from points   filleted spline

Figure 3.11: *Creating the shape of a spline joint.*

3.3.3 Intersection Joints

When designing free-form timber structures with multiple curves, most of the time it is necessary to define the relations, i.e., the connections, between those curves. These connections are collectively called intersection joints in this work. There are various possibilities to solve these in wood joinery. However, in the scope of this thesis, two types are used (see Figure 3.12).

The first type is a cross-lap joint for structures with compression as principal stress. It allows for an almost ideal overlap, with both alignments in the same plane. Thereby, it protects the end grains of the timber pieces. However, that type of joint weakens the cross-section of the timber by halving it.[9]

---

[9] Graubner, *Holzverbindungen Gegenüberstellungen japanischer und europäischer Lösungen*, 123.

lap joint   split joint
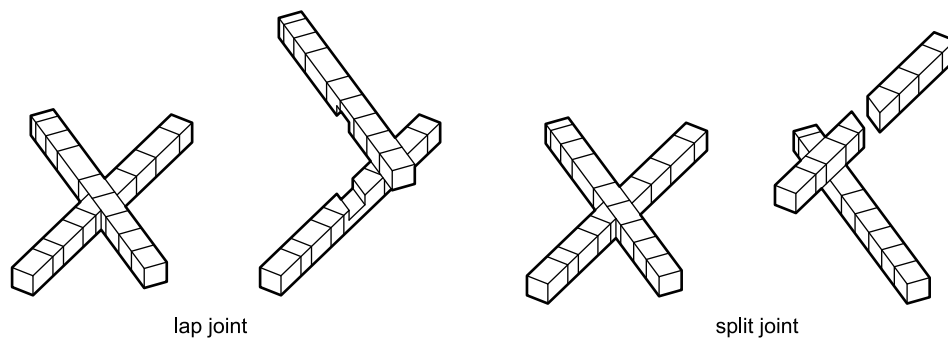
Figure 3.12: *Intersection joints.*

Therefore, it is less capable to resist all forces other than compression. In that case, the shape is filled and able to withstand it. Also, since the dimensions are decreased, there are fewer options to place the joints to connect the offcuts of the alignment. That diminishes its structural capabilities even further. Additionally, a lot of material is removed in the fabrication of the joint.

The second type is a split that enables manual editing. There, one of the alignments splits the other at the intersection point. Thereby, the first one stays mostly intact. The benefit of that connection is its simplicity and versatility. Sometimes, the intersections are too complex for the algorithm to compute reasonable joints. In these instances, it is better to intervene manually.

The two components "Intersection Joints" and "Find Intersections" solve the intersection instances. At first, it is necessary to detect if there are any intersections between the curves designed. For that, the algorithm uses the RhinoCommon class "CurveIntersections". It returns the intersection instances that provide further information about the position they occur at the curves. Also, the algorithm computes the type of intersection, i.e., end-to-end, crossover, or T-intersection. To get the best results, it is also possible to define the tolerances, increasing the chance of detecting intersections. Finally, the component returns the relevant points on the curves that are necessary for further computations as well.

Provided with two alignments and an intersection point, the "Intersection Joints" component is now able to solve the joint instance. It does so by first identifying the Offcut per alignment that is the closest to the intersection. For that, the algorithm computes the distances between the intersection point and the origin points of each Offcut's average plane. The minimum distance determines the closest Offcut instance. Also, it takes the second two closest Offcuts and returns them separately. The next steps differ depending on the joint type.

For the cross-lap joint, the algorithm computes an average plane from the moved average planes of both Offcuts to construct the cutters. Before that, one of the planes has to be rotated 180 degrees around its *z*-axis. Then, the intersection point is set as the new origin of the average plane. The algorithm can generate the cutters at the correct position, now. Finally, the three closest Offcuts of each alignment are intersected with the cutters in a "Boolean Difference" operation. Depending on how the alignments intersect, the result might yield more than three BReps per operation. Since every Offcut instance can only hold one BRep, that outcome poses difficulties. To deal with that, the algorithm computes the volumes of each geometric element that the operation returned. It stores these values in a list, sorts it, and takes the three biggest values. Then, it references the volumes back to the geometry list and, thereby, solely returns the three largest pieces left of the Offcuts. Finally, the algorithm assigns the geometry to the correct Offcut instance and returns the data.

For the split, the algorithm duplicates the Offcut geometry closest to the intersection point and scales it to create the cutter. The cutter has an excessive size so that it can cut the alignment completely. Then, the algorithm uses the same method as with the cross-lap joint to cut one of the alignments with the cutter.

In general, to get the best results from the intersection, it is advisable to first optimize the position of the curves. That already starts in the design process, where the relationship of the curves to each other and their intersections are defined. It is also considerable how the Offcuts are placed on these curves and how their orientation is. Finally, all components provide the necessary functionality to rotate, twist and reposition the alignments without altering the curves to get the best results.

3.4 Digital Fabrication

This section covers the process from generating the data to the fabrication. As of now, the workflow covered all steps from the design to the joint creation. The last steps include the robotic setup, the fabrication, and the assembly. Figure 3.13 highlights this step within the design-to-fabrication workflow.

3.4.1 Robotic Setup

The central part of the robotic setup was the robotic arm itself. This project used a Universal Robots UR10e. Since it is a collaborative robot (Cobot), it is suitable for a range of tasks. Specifically, assembly operations benefited greatly from its human-friendly nature. However, the robot was also able to mill the offcuts.

The setup was configured in a square modular system. It was constructed with strut profiles with a cross-section of 40 mm × 40 mm. The footprint of every element—from the robot mount to the fabrication tables—had a size of 800 mm × 800 mm. The base point of the robotic arm was elevated one meter off the ground and defined the origin of the coordinate system. To enable an array of possible use cases, the fabrication tables had a total height of 810 mm. A wooden plate with a height of 18 mm can be added to the tables to have a flat surface.

A major issue in digital fabrication—specifically with milling operations—is how to fixate the work objects. There are machine-vises available, though they do not always fit the needs of a project. Thus, fabrication mounts are oftentimes designed and made as needed.[10] Two setups were tested: (1) a custom fixture, and (2) a machine-vise mounted on a wooden plate (see Figure 3.14). For the custom fixture, two extra strut profiles were added to the fabrication table. These act as adjustable rails to accommodate the varying sizes of the workpieces. On top of them, a clamp made out of MDF with a thickness of 16 mm is mounted. The larger pieces clamp the offcut, while the smaller pieces increase the stiffness of the structure. Also, they act as a support for the workpieces. Now, a clamp is inserted between the two strut profiles. It presses the MDF clamping jaws together and, thus, fixates the object. However, that setup proved to be not stiff enough. Therefore, the machine-vise mounted on the wooden plate was used for all milling operations.

To effectively carry out its procedures, the robot needs the right end effectors, i.e., tools. For the assembly process, a commercial gripper was available. It had a stroke span of 85 mm and could carry offcuts with a width less than that. Since the gripper was explicitly designed for the UR10e, no testing was necessary.

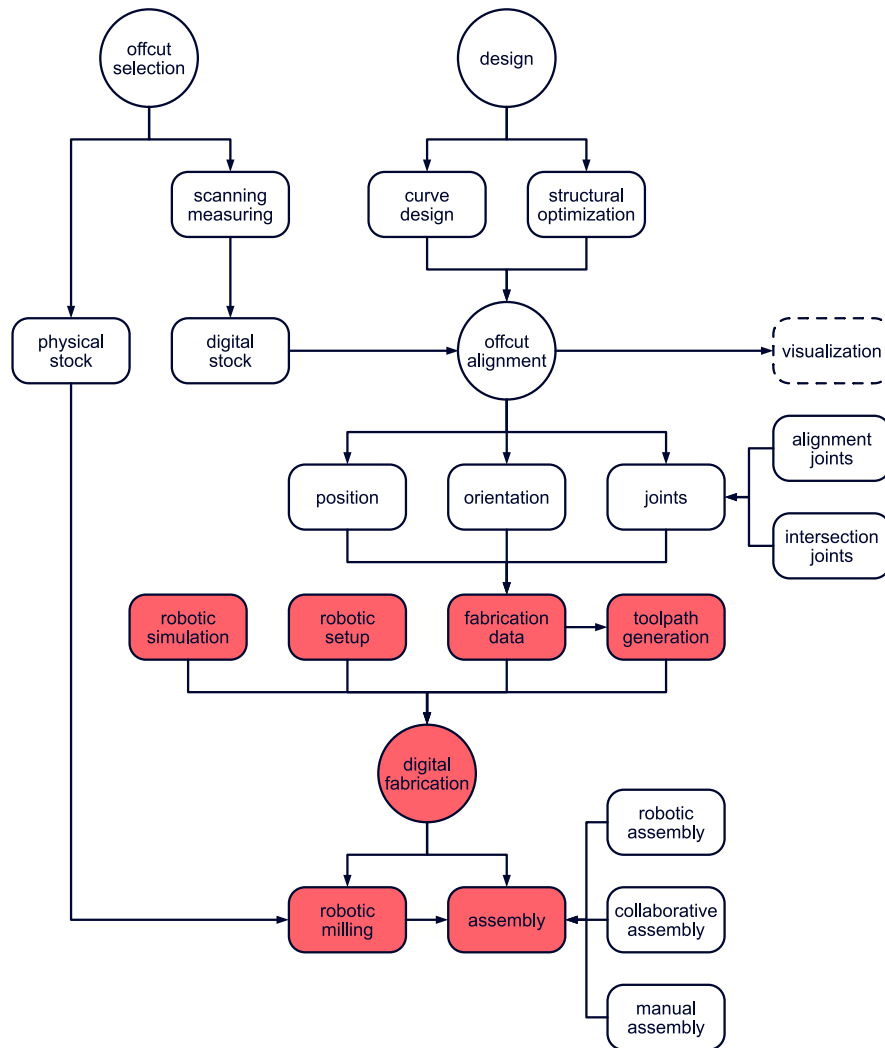[10] Vestartas, "Design-to-Fabrication Workflow for Raw-Sawn-Timber using Joinery Solver," 156–63.

Figure 3.13: *Digital fabrication within the workflow.*

On the contrary, the milling operations used a custom setup. To keep the weight low, a relatively small but still capable milling spindle was chosen. For that, the robot distributor manufactured a tailored aluminum mount. Additionally, a control unit and a power adaptor were necessary. The milling spindle gets the electricity from its control unit, which is connected to the power adaptor and the control unit of the robot. Via a digital output signal, the robot can now control the spindle. It sets the rotations per minute (RPM) and the rotation direction by the amount of voltage supplied through an analog output signal. All of that is controllable with the teach pendant or through specific software (see Section 3.4.3). Furthermore, two solid carbide end mills with a diameter of six millimeters and two flutes were used for all milling operations. They had cutting lengths of 45 millimeters and 65 millimeters.
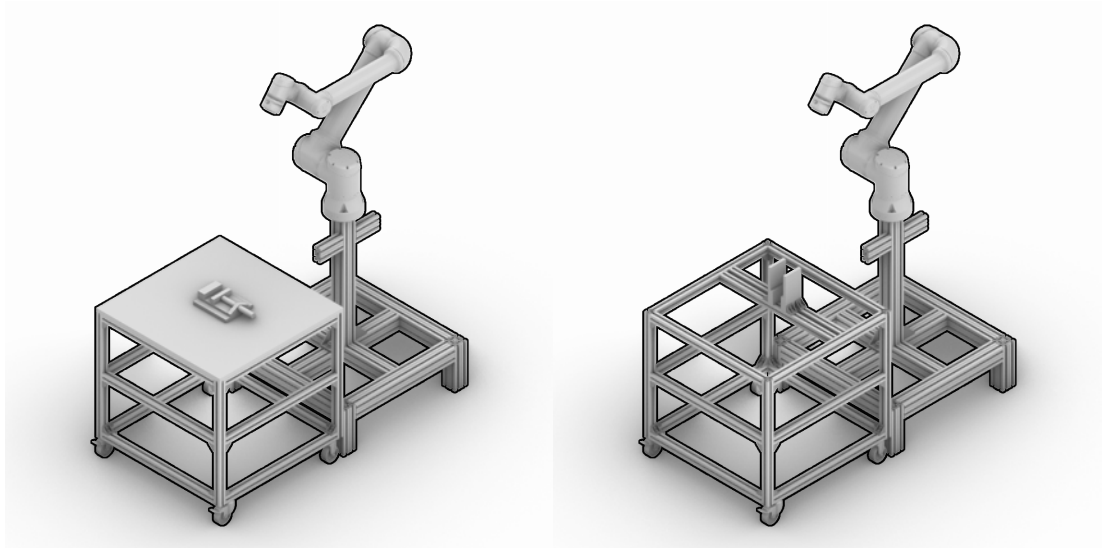
Figure 3.14: *Robotic setup variations.* Left: *Machine-vise.* Right: *Custom fixture.*

3.4.2 Toolpath Generation

As covered in Chapter 2.2.1, the milling of wood with CNC machines or robots has been shown multiple times and is also a standard in the timber industry. There are various well-documented strategies available to generate the toolpaths paths.[11] However, there are three options available: (1) free open-source software, (2) commercial software, and (3) programming the software. The first option was ruled out quickly since most of the free software can only generate 2D milling paths. However, the designs generated require complex 3D toolpaths executable by a machine with five or more axes. To that end, option three was ruled out as well, since programming software for these operations is quite complex and time-consuming. Therefore, option three was chosen. Specifically, the software Autodesk Fusion 360 was selected, since it provides the required functionality and free access for educational purposes (see Section B.3).

Introducing another software environment brings the challenge of data exchange. Specifically, the geometrical data has to be passed from Rhino3d to Fusion 360, and numerical data, i.e., coordinates, have to be passed back from Fusion 360 to Rhino3d. That step is necessary since the robotic arm is controlled within Rhino3d/Grasshopper. However, Fusion 360 is able to read Rhino3d-native documents, i.e., 3DM files. Also, it exports the coordinates as a CSV file that is readable in Rhino3d with a custom component.

Before the data exchange, the geometry has to be prepared in Rhino3d. For that, the Offcuts aligned in space on a curve have to be moved to the fabrication table. The component "Orient on Plane" provides that functionality. It takes an alignment as input and moves the Offcut instances to a specified target plane. Ideally, that plane is the point where the Offcut will sit on the fabrication table. Additionally, it is possible to choose which of the Offcut's planes is the initial plane, i.e., the plane that is oriented on the target plane. Furthermore, the component computes the stock model, i.e., the offcut in its original form, enclosing the fabricated shape (see Listing 3.8). An individual Offcut can now be selected and generated as Rhino3d geometry, i.e., baked into a closed polysurface.

---

[11] Hua, Hovestadt, and Tang, "Optimization and prefabrication of timber Voronoi shells."

```
1    // call CreateOffcutBrep method
2    offcutStock = Offcut.CreateOffcutBrep(offcut, offcut.AveragePlane,
     offcut.PositionIndex);
3
4    // duplicate Offcut data to avoid any problems
5    Offcut localOffcut = new Offcut(offcut);
6
7    Brep localBrep = localOffcut.OffcutGeometry.DuplicateBrep();
8    Plane fP = new Plane(localOffcut.FirstPlane);
9    Plane sP = new Plane(localOffcut.SecondPlane);
10   Plane aP = new Plane(localOffcut.AveragePlane);
11   Plane maP = new Plane(localOffcut.MovedAveragePlane);
12   Plane bp = new Plane(localOffcut.BasePlane);
13
14   // select a specific Offcut plane
15   Plane initialPlane = new Plane();
16
17   switch(planeIndex)
18   {
19       case 0:
20           {
21               initialPlane = new Plane(offcut.BasePlane);
22           }
23           break;
24       case 1:
25           {
26               initialPlane = new Plane(offcut.FirstPlane);
27           }
28           break;
29       case 2:
30           {
31               initialPlane = new Plane(offcut.SecondPlane);
32           }
33           break;
34       case 3:
35           {
36               initialPlane = new Plane(offcut.AveragePlane);
37           }
38           break;
39       default:
40           {
41               initialPlane = new Plane(offcut.BasePlane);
42           }
43           break;
44   }
45
46   // orient Offcuts
47   Transform orientation = Transform.PlaneToPlane(initialPlane, targetPlane);
48
49   // transform stock model
50   offcutStock.Transform(orientation);
51
52   // transform geometrical Offcut data
53   localBrep.Transform(orientation);
54   fP.Transform(orientation);
55   sP.Transform(orientation);
56   aP.Transform(orientation);
```

```
57    maP.Transform(orientation);
58    bp.Transform(orientation);
59
60    orientedOffcut = new Offcut(localOffcut)
61    {
62        OffcutGeometry = localBrep,
63        FirstPlane = fP,
64        SecondPlane = sP,
65        AveragePlane = aP,
66        MovedAveragePlane = maP,
67        BasePlane = bp
68    };
```

Listing 3.8: Orient Offcut for fabrication.

Now, the Rhino3d file can be imported in Fusion 360. The software recognizes the position of the geometrical elements and the origin point. With that, it can generate the toolpaths for the milling operations as necessary. For that purpose, the offcut's original geometry is selected as the stock model, while the final offcut geometry serves as the model. The work coordinate system is set to the world coordinate system. Thereby, the output coordinates will match the digital model in Rhino3d. After the definition of the setup, the milling strategies can be defined. In total, three were used for specific purposes. First, a 3D Adaptive Clearing strategy created the paths for the angled surfaces. Second, a 3D Pocket strategy created the paths for the milling of the joint shapes. Third, a 2D Contour created the paths for the fabrication of the spline and tenon joints. There, it was possible to mill an extra 0.05–0.1 mm off so that the joints fit into the offcuts. Besides that, the milling values were similar. The optimal step size proved to be between 1.0 and 1.5 mm, whereas the optimal feed rate was 600–800 mm/min. A tool engagement of 3.5–4.0 mm proved to be fine as well. The RPM and speed were set in the simulation software (see Chapter 3.4.3). Furthermore, it was necessary to set to correct tool orientation for each milling operation. With these values set, the software exports the toolpaths as a CSV file. For this operation, it uses the post-processor "XYZ.cps" provided by Autodesk. However, it was necessary to edit the file to allow different tool orientations (see Listing 3.9).

```
1    function onSection() {
2      { // pure 3D
3        var remaining = currentSection.workPlane;
4
5        // commented out to allow multiple tool orientations
6        /*
7        if (!isSameDirection(remaining.forward, new Vector(0, 0, 1))) {
8          error(localize("Tool orientation is not supported."));
9          return;
10        }
11        */
12
13        setRotation(remaining);
14      }
15
16      // writeln("");
17    }
```

Listing 3.9: Edits made to the post-processor file.

After the export of the milling toolpaths succeeded, the component "Get Coordinates" can access the CSV file in Rhino3d. It reads the data and converts the strings into doubles, i.e., from text to numerical data. Then, it uses that information to generate points and outputs them (see Listing 3.10). For that operation, it is necessary to specify the correct delimiter, which is a semicolon. Furthermore, if there are multiple tool orientations involved in the process, these have to be exported as separate CSV files. For each of them, the correct plane, i.e., tool orientation, has to be set in Grasshopper. That process would be complicated if there is only one file. To make this workaround as efficient as possible, the component "Get CSV Files" provides the paths to all CSV files in a folder given the path they are in.

```
1    // read CSV file and add string data to list
2    ReadCSV readCSV = new ReadCSV(filePath);
3    List<string> coordinatesTxt = readCSV.GetCSVData();
4
5    // initialise list of points
6    List<Point3d> ptList = new List<Point3d>();
7
8    for (int i = 0; i < coordinatesTxt.Count; i++)
9    {
10       // split string into coordinate strings
11       string[] coordinates = coordinatesTxt[i].Split(
12       delimiter.ToCharArray()[0]);
13
14       // convert strings to doubles
15       double x = Convert.ToDouble(coordinates[0]);
16       double y = Convert.ToDouble(coordinates[1]);
17       double z = Convert.ToDouble(coordinates[2]);
18
19       // create new point and add to list
20       ptList.Add(new Point3d(x, y, z));
21    }
```

Listing 3.10: CSV data to Points.

There are different strategies to get the correct planes for each milling path. A manual way would be to construct each plane as was done in Fusion 360. However, it is also possible to use the planes stored within the Offcut instances. In both cases, their origin would have to be set to the coordinates provided by the CSV file. From that, the robotic arm knows exactly where to move along and in what orientation.

3.4.3 Robotic Control

This section covers the robotic control from within the Rhino3d software environment for fabrication. For that, a plugin is necessary. Out of several available options, HAL Robotics was chosen (see Appendix B.3).

To control the robot with HAL Robotics, it was first necessary to define the physical environment in the software. Conveniently, it provides a library of robots that also included a UR10e. Its location was set to the origin of the document. Thereby, the physical and the digital setups had the same base point

as a reference. Also, it was good practice to change the position of each of the robot's joints to avoid any singularities.[12] This position is set as the "home" position.

The next step included defining the end effector with the "Tool" component. For that purpose, a base frame was necessary that determines how the tool is attached to the robot. Also, a tool frame must be provided that is the tool center point (TCP). The TCP can be set through modeling the tool and placing a point at its tip in Rhino3d. A more precise way was to calibrate the TCP with the teach pendant. For that, the tip of the tool where the TCP should be located must be placed at one point from four different directions (see Figure 3.15). Then, the software calculates the coordinates of the TCP. To have the same values in the simulation software, it is first necessary to place the base frame of the tool, i.e., the point where it attaches to the tool flange of the robot, at the origin of the world coordinate system. Then, the coordinates from the teach pendant can be put into a "Quaternion Frame" component. The resulting frame is set as the tool frame. Additionally, the end effector required an alias and a tool body in the form of a mesh to calculate collisions. Thereby, it was crucial to have the tool frame and the base frame correctly oriented. Finally, the tool was attached to the robot with the "Attach" component. It provides a visualization of the current setup, helping to figure out if a correction is required.
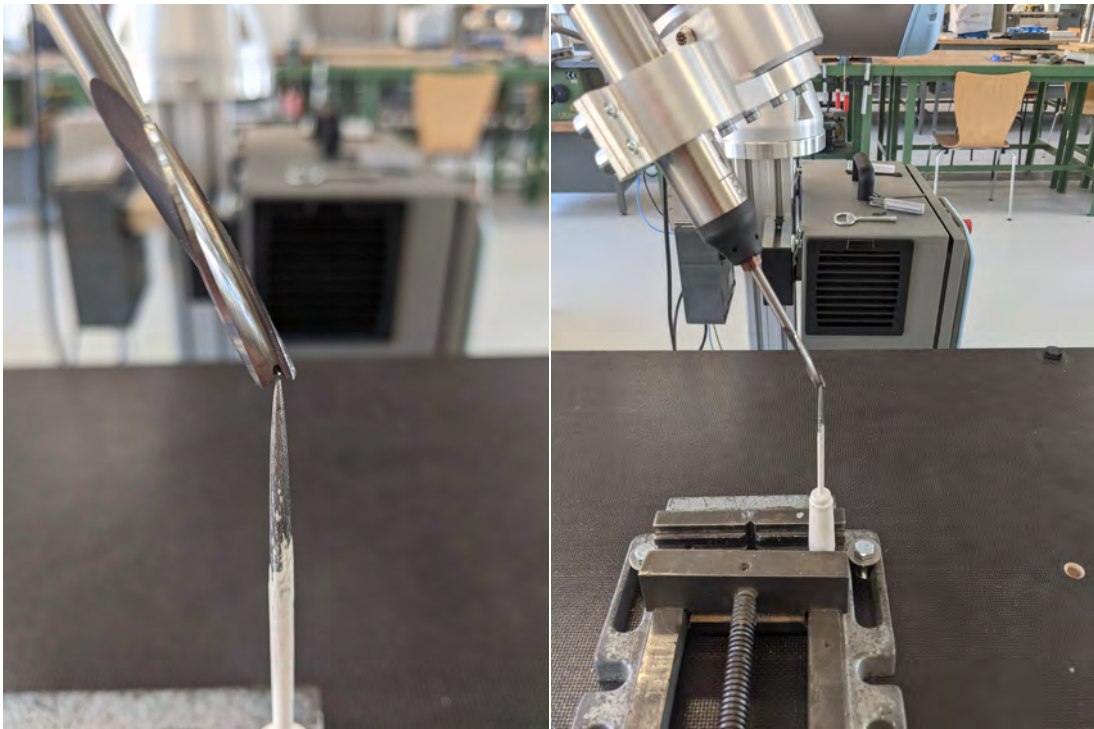

Figure 3.15: *Calibration of the TCP.*

The next step entailed the definition of the rest of the environment, i.e., the "Cells", including the robotic mount, the fabrication tables, the vise, and the offcut to be fabricated. For this purpose, the geometric components were imported from Rhino3d into Grasshopper. Then, for each group, the algorithm

---

[12] Singularities do occur when too many joints are set to zero degrees. In such a case, the algorithm controlling the robot fails to calculate the inverse kinematics. However, that is a requirement since the targets are set in Cartesian space. Therefore, it is good practice to change its initial position to avoid any divisions by zero or infinite angular velocities.

computes a bounding box. That is the basis for the subsequent meshing operation. The component "Mechanical Part" takes that information, and, provided with a base frame and an alias, generates "Parts".

All of that is vital for collision detection. The component "Diagnosis" can perform this analysis. It requires two parts to be checked and an alias for later reference. For this work, the algorithm carried out the following collision checks: Between (1) the robot and the robotic mount, (2) the robot and the fabrication table, (3) the robot and the vise, (4) the robot and the offcut, (5) the robot and the spindle, (6) the spindle and the robotic mount, (7) the spindle and the fabrication table, and (8) the spindle and the vise. Then, the software passes that information to the solver. As the environment is defined now, the robot is ready to carry out any procedure. For every action, it requires targets to move to. However, every action needs a specific strategy.

For the milling operations, the coordinates for the targets are generated as described in section 3.4.2. After their import, the component "Target Filter" decreases their amount to reduce the computation and fabrication times. Then, the first frame is copied and moved 10 mm on its z-axis. That is the first point the robot moves to. It performs that motion in the Configuration (or Joint) space to move efficiently and, thereby, avoiding any collisions with other cells. Furthermore, the speed, acceleration, and blend radius of the motion are controllable. After the robot arrives at the starting position, it waits for one second and turns on the spindle. Then, it starts the milling operation by following the specified path. The robot always performs this action in the Cartesian space. That means that it follows the coordinates, i.e., the target frames, directly depending on their order. For that, it is vital to assign appropriate speed, acceleration, and blend settings. As soon as the robot is done with the milling operation, it moves away from the offcut. Then, it waits for one second and turns off the spindle. Finally, it performs a motion in Configuration space to its designated home position.

Finally, all actions were combined and put into a "Controller" component. To output the robotic instructions in the correct format, the Universal Robots e-Series controller had to be selected. It passes the data on to a solver that computes the instructions. Also, it provides additional information, e.g., collisions between parts. Now, the component "Execute" simulated the motion of the robot. That simulation is vital to verify that all targets and frames are set correctly. As a final step, the instructions, i.e., the machine code in the URScript language (see Appendix B.5), were exported to the robot. That is possible via a USB flash drive or a direct link between the computer and the teach pendant. In general, though, it is only possible to achieve offline control with the plugin.[13] After importing the instructions in the teach pendant, the robot can execute the program.

---

[13] Offline control means that the data is transmitted unidirectionally only. This is exacerbated further since the robotic procedure is always recalculated and converted into URScript. By definition, that method cannot achieve true online control.
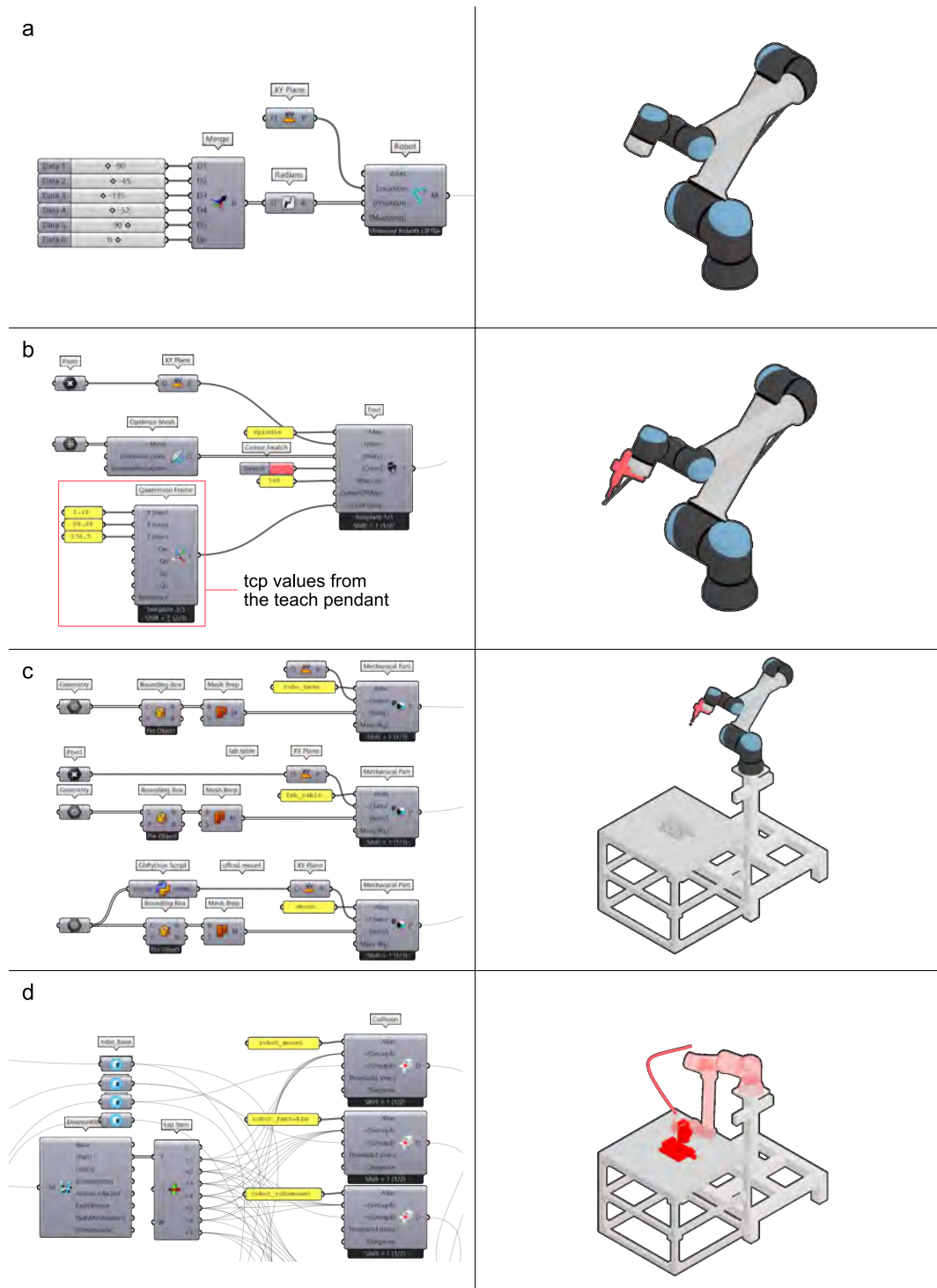
Figure 3.16: *Robotic control with HAL Robotics in Grasshopper: a) Selecting a UR10e, b) Defining the tool, i.e., the milling spindle, c) Defining the environment, d) Collision detection.*
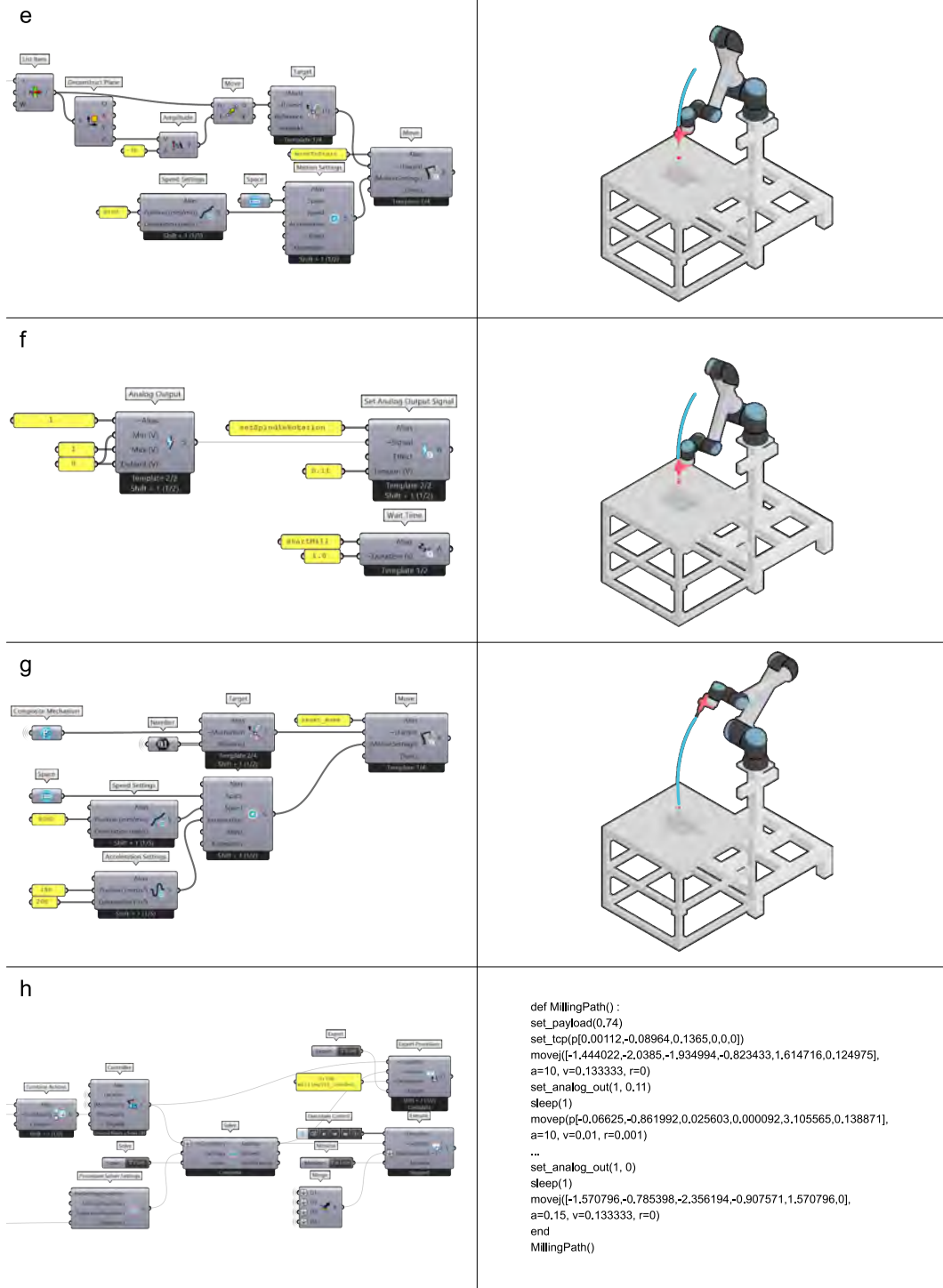
```
def MillingPath() :
set_payload(0.74)
set_tcp(p[0.00112,-0.08964,0.1365,0,0,0])
movej([-1.444022,-2.0385,-1.934994,-0.823433,1.614716,0.124975],
a=10, v=0.133333, r=0)
set_analog_out(1, 0.11)
sleep(1)
movep(p[-0.06625,-0.861992,0.025603,0.000092,3.105565,0.138871],
a=10, v=0.01, r=0.001)
...
set_analog_out(1, 0)
sleep(1)
movej([-1.570796,-0.785398,-2.356194,-0.907571,1.570796,0],
a=0.15, v=0.133333, r=0)
end
MillingPath()
```

Figure 3.17: *Robotic control with HAL Robotics in Grasshopper: e) Initial move to a target, f) Milling move, g) Ending move to the defined home position, h) Output of the URScript machine code.*

Chapter 4
Case Studies

This chapter presents the implementation of the methods proposed previously. At first, the design space exploration examines the possibilities with the developed software tool. Then, the following section presents a variety of physical case studies. These include handcrafted and robotically fabricated prototypes and strength tests. For all of these studies, a database consisting of 190 offcuts has been created as described in Chapter 3.1.

4.1 Design Space Exploration

The goal of the design space exploration was to examine the potentials and limitations of the developed software extension (see Appendix B.2). It is divided into two groups. The first group exclusively covers 2D typologies. That gives an understanding of fundamental structural forms. Specifically, the curvature, transitions, and connections are of interest. The second group covers 3D typologies. It provides insights into spatial structures and the connections of their elements.

4.1.1 2D Typologies

The 2D explorations covered a variety of typologies. These include conventional structures with flat floor slabs (see Figure 4.1 a and b), archs and arch-like structures (see Figure 4.1 c–f and 4.2 g), unconventional structures (see Figure 4.2 h and i), and bridge-like structures (see Figure 4.2 j–l). For each typology, the figures portray the base curves, the offcuts aligned on these curves, and a detail highlighting a specific area of interest.

The software tool can deal with a wide range of curve typologies. However, straight sections appear to be the most challenging. Although the algorithm can place the offcuts on a line correctly, it fails if the angle is too sharp. Specifically, orthogonal transitions are unsolvable. Therefore, the lines of typology *a* are separate. That means that it consists of three alignments. Thereby, the correct positioning of the offcuts ensures the orthogonal transition. If the sharp corners are filleted—as in typology *b*—a continuous alignment with a single curve is possible. Since the curvature is the highest at the circular transition, the algorithm places a range of shorter offcuts there. The typologies *c* and *d* display a similar phenomenon. Even if it is possible to align the offcuts on the curve despite a sharp angle, the transition will be coarse. Therefore, the structural viability of that connection is questionable. This is exacerbated

by the fact that in the corners of frame structures, the forces are the highest. Again, a simple solution is the filleting of the sharp corner—as in typology *d*.

If the typology is continuous (see Figure 4.1 e), the curvature is the same everywhere and optimization is not effective. Therefore, improving the overall form would yield better results. That is true both from a structural as well as a material perspective. Typology *f* shows that kind of typology in the form of a steep arch. At its crown, it has a range of smaller offcuts for a smooth transition. On the contrary, a Gothic arch (see Figure 4.2 g) yields a corner too sharp for a continuous alignment at its crown. Therefore, its structure consists of two curves. Now, the challenge is to connect both alignments. For that, the plugin provides the means to solve intersection instances by cutting one alignment with the other (see Chapter 3.3.3). However, the results are not ideal and might necessitate manual edits.

Typology *h* reveals a major deficit in the software tool. The curve is designated to be a complete circle. However, the algorithm is not able to align offcuts on closed curves. That would contradict its internal logic. Additionally, the endpoints of a curve should have an adequate distance from each other. If they are too close, the algorithm could perform the sphere intersection backward (see Chapter 3.2.1). Thereby, its logic gets distorted, resulting in an error.

The typologies *j*–*l* present typical compression-tension bridge structures. Due to their designs, they consist of multiple curves. Specifically, the intersection instances were of interest. For the typologies *j* and *l*, the results are promising. In particular, the intersections between the lower chords and the pillars are fitting. For the top chord, it was difficult to find the ideal length of the curve. It determines the position of the offcuts, and, therefore, the cutting positions. If the curve is too long or too short, the resulting intersection would yield overlapping geometries. Furthermore, the joints between the alignments need to be specified as well. For now, that is best done manually, since the ideal joint position is heavily dependent on the offcuts' orientation. Furthermore, the typology *l* reveals another issue. While the typology *i* solves the intersection instances through the alignments' positioning, that is sometimes too complex. Specifically, the creation of multiple joints in 2D space poses challenges. It requires the curves' positions to be adjusted depending on the offcuts. Otherwise, the geometries would overlap or have no connections at all. However, solving these intersection instances in 3D space could prevent the issues.
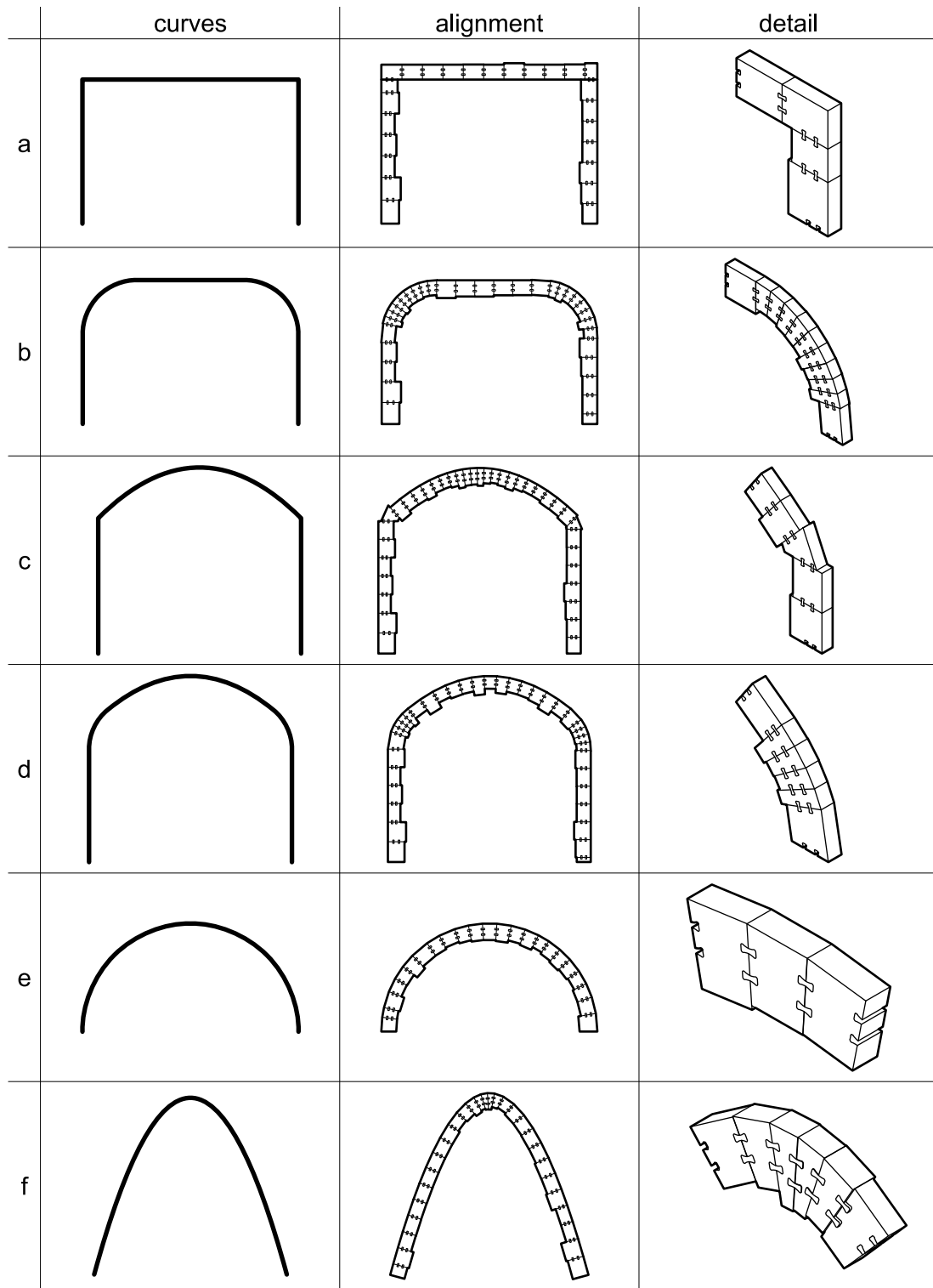
	curves	alignment	detail
a			
b			
c			
d			
e			
f			

Figure 4.1: *2D typologies a–f.*

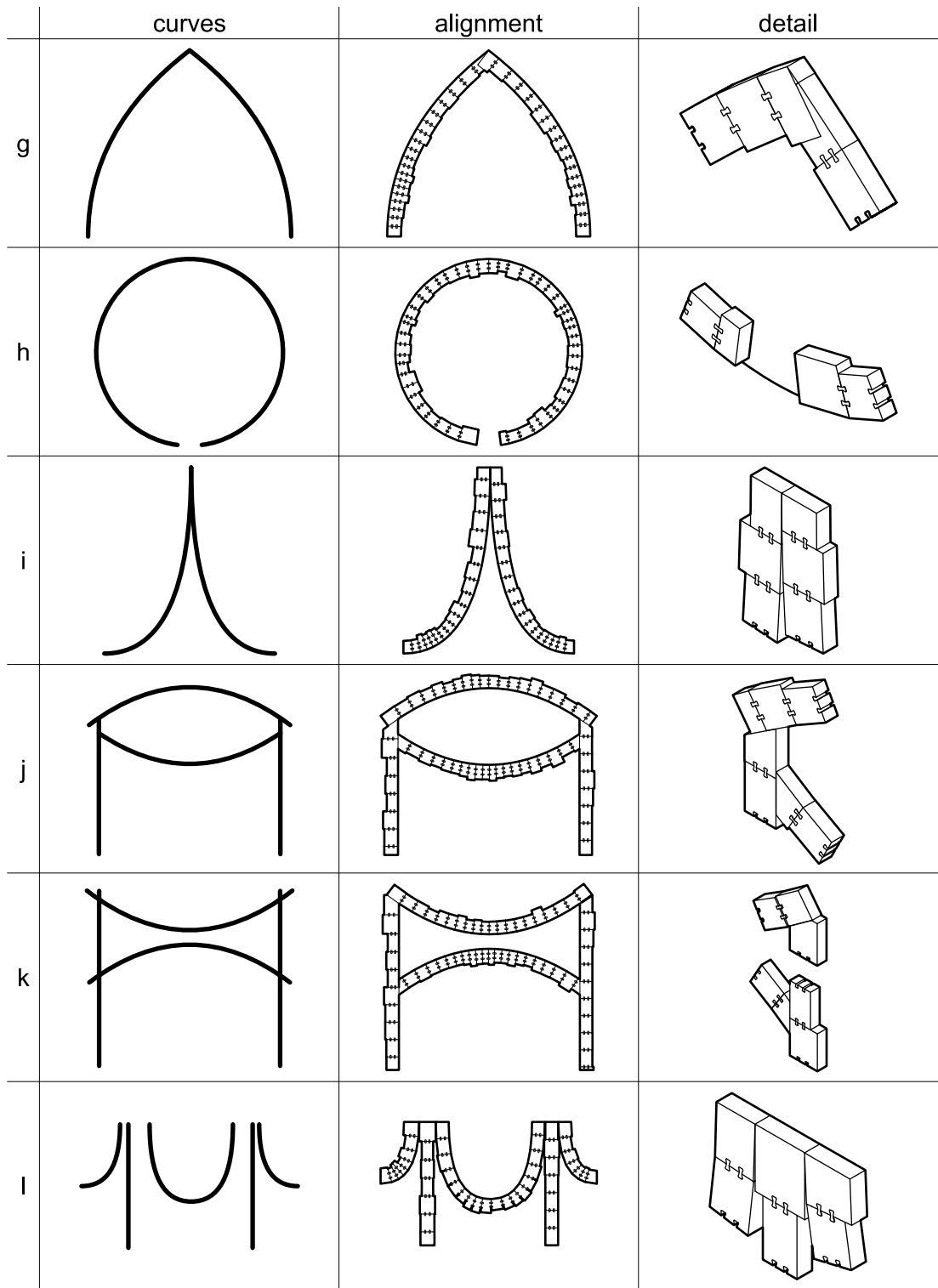| curves	alignment	detail
g		
h		
i		
j		
k		
l		

Figure 4.2: *2D typologies g–l.*

4.1.2 3D Typologies

The 3D explorations covered a variety of spatial typologies and their connections. These are portrayed in the figures 4.3, 4.4, and 4.5. The software tool can create vault structures easily. *A* and *b* show two simple examples of this typology. They consist of three and four curves, respectively. The special feature is the intersection of the arcs. The targeted positioning avoids overlaps and achieves an ideal result. The method is also used for typology *c*. There, the juxtaposition of several arc-like curves forms a massive structure. Once again, the positioning of the objects is essential to achieve an ideal result.

Typologies *d* and *e* represent structures with mixed tension and compression forces. Their static logic is based on a balance that is optimized by the software. However, the connections between the alignments are problematic. In particular, the corner intersections of typology *d* represent a major challenge. There, four objects meet at one point. In contrast, the algorithm can easily solve the cross intersections at *d* and *e*.

The typology *f* represents a tent structure. The connections between the column-like alignments and the upper ring are made possible by the positioning. However, again there is the problem that the ring can not be closed. Furthermore, typology *g* is an example of a mushroom-like column. The individual alignments are again connected by a continuous ring. In this case, however, this consists of individual curves and allows relatively good connections.

In addition, the algorithm can create alignments in the form of barrel vaults. The typologies *h*, *i*, and *j* serve as examples for this. For all three, the intersection points are solved with the intersection components. The alignments of typology *h* were also unified, i.e., trimmed to one size. It was also important that the basic shape of the vaults was optimized so that the results of the intersections could be solved well.

The typologies *k—o* represent a set of rather unrealistic structures (see Figure 4.5). However, with these partly extreme forms, further possibilities and obstacles of the tool can be recognized. For example, the spiral *k* depicts that too strong a curvature leads to poor connections between the offcuts. Typology *l* shows that the rotation at the beginning and end of the curve can be well controlled. However, there are large rotational differences in the alignments, which are not always desired. Furthermore, typology *m* demonstrates that the algorithm can generate a large number of spline joints. At the same time, the sometimes extremely short offcuts are questionable from a static perspective. In this context, typology *n* shows that the algorithm can compute a large number of connections perfectly despite an exaggerated torsion. Finally, typology *o* shows how a connection of three objects from different directions could work.

In summary, the design space exploration gave a good overview of the capabilities and limitations of the software. This resulted in insights that are relevant for the design with the offcuts. In particular, structures based on an optimized basic shape were easy to generate in all parts. In contrast, free-form structures were complex, especially the intersections of the individual alignments. This insight could be used as a basis for the further development of the software tool.
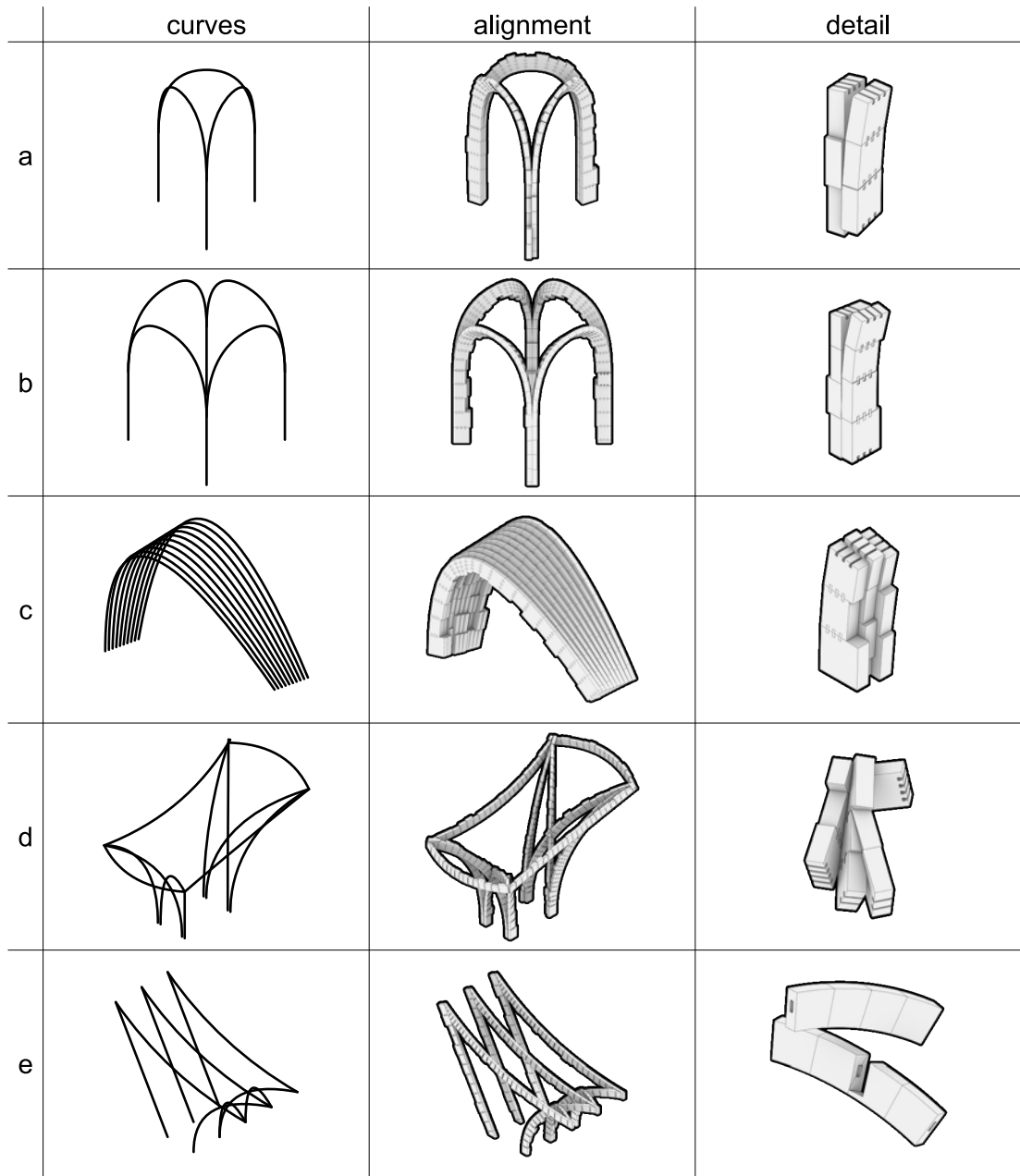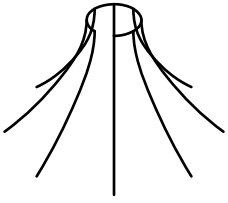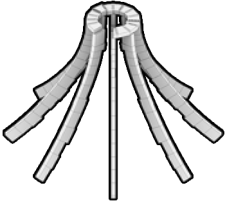
	curves	alignment	detail
a			
b			
c			
d			
e			

Figure 4.3: *3D typologies a–e.*
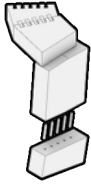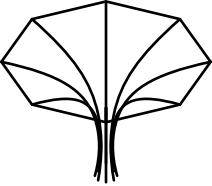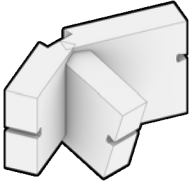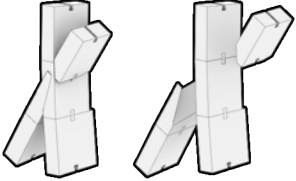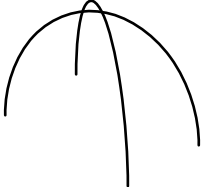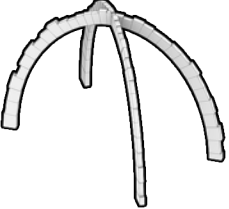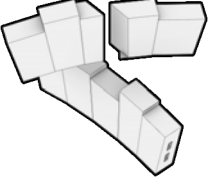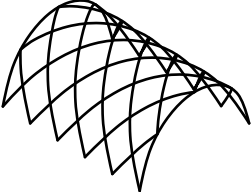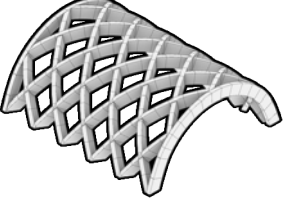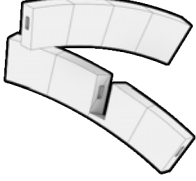
	curves	alignment	detail
f			
g			
h			
i			
j			

Figure 4.4: *3D typologies f–j.*
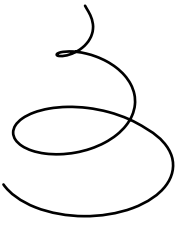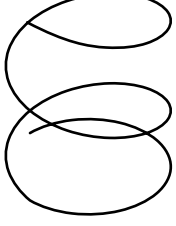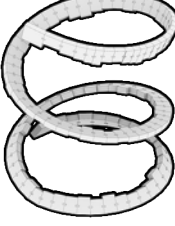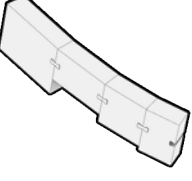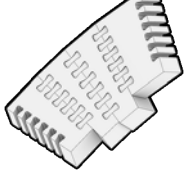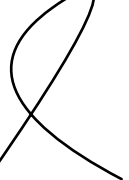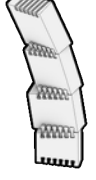
	curves	alignment	detail
k			
l			
m			
n			
o			

Figure 4.5: *3D typologies k–o.*

4.2 Physical Case Studies

While working with a specific material, it is beneficial to expand the digital research, e.g., simulations, with physical experiments. It provides the possibility to verify that what was true in the digital realm is also true in the physical. For that, prototypes have been handcrafted and robotically fabricated. They serve as proof of the concept for the design-to-fabrication workflow. Also, strength tests have been conducted to examine the capabilities of the waste wood and the joints.

4.2.1 Handcrafted Prototypes

To test the concept of the double-curved timber structures built with offcuts, the first prototypes were handcrafted in the wood workshop. For this purpose, different tools were used, including a double-edged Japanese saw, a wooden hammer, chisels, clamps, a table saw, and a sanding machine for finishes.

The first challenge consisted of cutting the end of the offcut at an angle. Within one axis, that would be possible with a handsaw. However, the aspiration was to fabricate a double-curved prototype. Therefore, a cut with an angle in two axes was necessary. A table saw with an adjustable blade provided that possibility. It was rotated by ten degrees to get the first angle. Through a rotation of the stop by ten degrees, the second angle resulted. Then, the end of the offcut was cut to the specified angles.

The second challenge consisted of cutting the negative joint shapes into the angled surface. For that, multiple clamps held the offcut in place. Also, it proved to be good practice to draw the shape of the joint onto the offcut. Depending on the joint, there are different strategies required to handcraft them. The tenon joint must be chiseled out completely, while it is possible to partially saw the spline joint. In both cases, it is beneficial to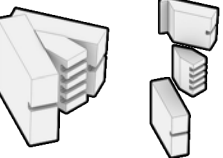 use the angled piece that was cut off before as a template. It helps to work at the correct angle, that is perpendicular to the sloped surface. With the chisel, layer by layer is removed in one-millimeter steps until the desired depth is reached.

The handcrafting of the external joints depends on the type. The tenon joints are simple cuboids that can be quickly cut with a table saw. The basic shape of the spline joints can be fabricated that way as well. Then, with a hand saw, its specific shape can be cut. Finally, a sanding machine was used to clean up all the faces so that they have a tight fit.

The prototypes are handcrafted in a way that their grain direction always aligns with the forces. That is not true for the external joints, though. It would have been better if the tenon and spline joints' grain direction would also align with the forces. For that, the wood they are made of would have had to be rotated by 90 degrees. Due to size constraints of the available material, that is not always possible. Though in further physical case studies, it will be considered.

The finished handcrafted prototypes are depicted in the figures 4.6 and 4.7. The handcrafting of the prototypes proved to be labor-intensive and thus time-consuming. Furthermore, it was very difficult to cut the right angle at the ends of the offcuts. This lack of precision also affected the joints, which did not fit tightly enough. These challenges can be overcome with the implementation of digital fabrication methods.

Figure 4.6: *Images of the handcrafted prototype with spline joints.*

Figure 4.7: *Images of the handcrafted prototype with tenon joints.*

4.2.2 Strength Tests

The utilization of waste timber as a structural material bears a certain risk since, mostly, its background is not documented. Also, there is no certification available to guarantee the capabilities of the waste wood. Thus, only strength tests may provide the needed clarity. The objective of the tests is to find out if the wood is still structurally viable. It is relevant since the material was deemed unfit for structural purposes. Some elements endured rain, sun, fungi, etc. Also, the strength of the spline joint connection in comparison to solid timber was of interest.
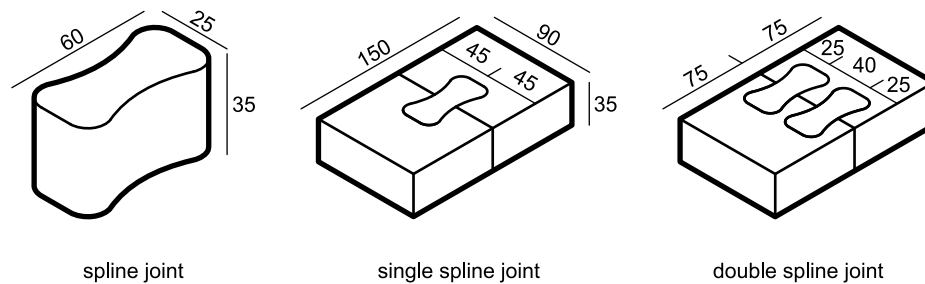

Figure 4.8: *Dimensions of the specimens.*

Two types of tests were conducted according to EN 408.[1] First, a tension strength test parallel to the grain and, second, a shear strength test perpendicular to the grain.[2] For each test, the sample size was six specimens. These were divided into two groups, with three specimens each. The first group had one spline joint and the second one had two. All of the specimens, including their joints, were made of Norway spruce with a strength class of C24.[3] The testing machine determined their maximum size limitations (see Figure 4.8). Thus, in total, they were 150 mm × 35 mm × 90 mm in size. Consequential, the test pieces with the negative joint shapes were 75 mm × 35 mm × 90 mm in size, whereas the dimensions of the spline joints were 60 mm × 35 mm × 25 mm. The joints' minimum cross-section was 17.5 mm × 35 mm. For the first group, the spline joint was located at the center of the probe. For the second group, the connection area was divided by three to determine the location of the two spline joints.

The specimens were cut by hand with a table saw. Afterward, a five-axis MAKA CNC machine milled out the joint shapes.[4] It used an end mill with a diameter of 6.0 mm. The spindle rotation speed was set

---

[1] European Committee for Standardization (CEN), *Timber structures – Structural timber and glued laminated timber – Determination of some physical and mechanical properties*, tech. rep. EN 408:2010 (Brussels, 2012).

[2] The tests were conducted at the Materials Research and Testing Institute (MFPA, Materialforschungs- und Prüfanstalt). It is a non-university research institute that is affiliated with the Bauhaus-Universität Weimar. Additionally, it is an official inspection authority for materials and products in the German state of Thuringia.

[3] The strength classes of European hard- and softwoods are standardized in EN 338:2016. It provides information about the bending, tension, compression, and shear strengths for each strength class. (European Committee for Standardization (CEN), *Structural timber – Strength classes*, tech. rep. EN 338:2016 [Brussels, 2016])

[4] Because the specific shape and structure of the spline joints were an essential part of the tests, handcrafting them was no option. Also, a very high precision was wanted for the tests. Due to time constraints, the probes had to be fabricated quickly. Therefore, it was chosen to machine them with a CNC setup already present and working.

to 9000 RPM with a step size of 4.0 mm per pass and a feed rate of 1200 mm/min. Also, a conventional milling strategy was chosen. The elements of the specimens with the negative joint shape were milled with zero tolerance. To get a strong fit, an extra 0.1 mm was milled off the spline joints. In general, the specimens were fabricated so that their grain directions align (see Figure 4.9). That is relevant for both tests since they require that specific directionality.
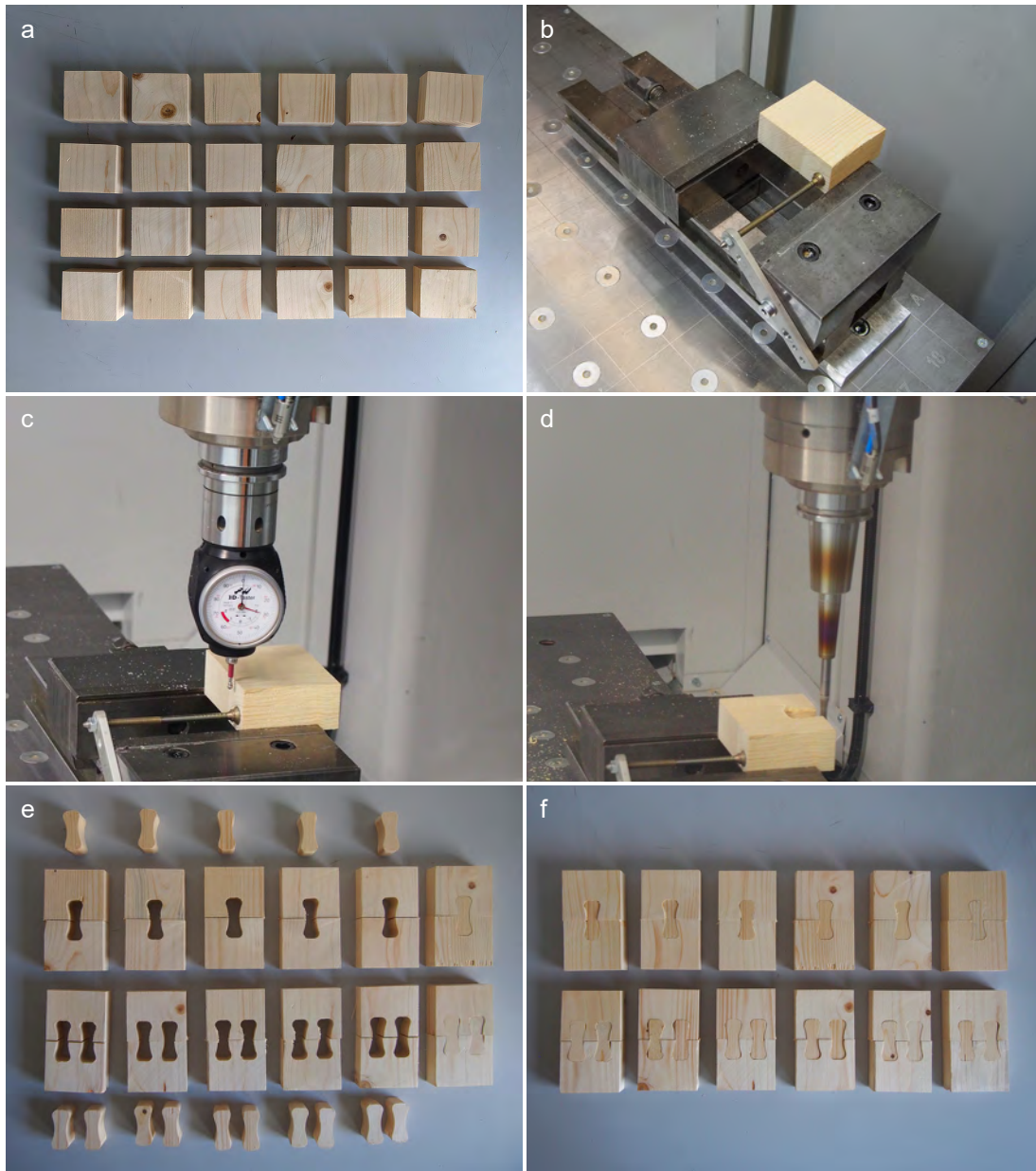

Figure 4.9: *Fabrication of the specimens: a) Raw specimens, b) Fixed specimen in the CNC machine vise, c) Measuring the coordinates of the specimen, d) Milling the joints, e) Fabricated specimens, f) Assembled specimens.*

4.2.2.1 Tension Strength Test

A universal testing machine with a standard setup conducted the tension strength tests. Its gripper jaws fixated the specimen at the top and bottom. There, small timber pieces leveled the height of the specimen to achieve a gauge length of 100 mm. Since the spline joints had a height of 60 mm, there were 20 mm between the gripper jaws and the joints left on both sides. The filling material had the same cross-section dimensions as the specimen and a height of 45 mm on both sides to ensure a perfect fit (see Figure 4.10).
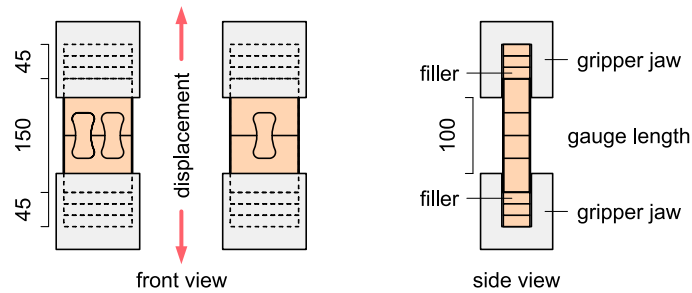
Figure 4.10: *Tension strength test setup.*

The standard testing procedure for timber tension strength prescribes reaching the maximum load in 300 s $\pm$ 120 s.[5] To reach that target, the movement speed of the machines' crossheads was 1 mm/min. Additionally, a preloading cycle with a load of 0.1 kN was performed for each test. With these settings, the testing machine pulled the specimens apart until they failed. A rapid fall in the load indicated that. Figure 4.11 portrays the results of the tension test for each specimen. There, specimens 1–3 (group two) had two spline joints, whereas specimens 4–6 (group one) had one. The values in x represent the displacement u [mm], i.e., the distance of how much a specimen was pulled apart, whereas the values in y represent the load F [kN].

A clear characteristic of tension strength tests with timber is the fluctuating graph. There, the load gradually increases until it falls off abruptly. The slippage and deformation of the timber components cause this effect. At a certain threshold, the tension is too high and any slippage is impossible. As a result, the components fail. That was different for each test. The maximum load the specimens 1–3 could endure was 2.23–2.37 kN with a displacement of 4.30–5.86 mm. On the contrary, specimens 4–6 could only endure 1.07–1.26 kN with a displacement of 3.82–5.96 mm. The tension strength parallel to the grain is calculated according to EN 408,[6] where:

$$f_{t,0} = \frac{F_{max}}{A} \tag{4.1}$$

There, F_{max} is the maximum load [N] and A is the surface area [mm²]. For each group, the median value of F_{max} had to be calculated:

---

[5] European Committee for Standardization (CEN), *Timber structures – Structural timber and glued laminated timber – Determination of some physical and mechanical properties*, 22.

[6] European Committee for Standardization (CEN), *Timber structures – Structural timber and glued laminated timber – Determination of some physical and mechanical properties*, 20.
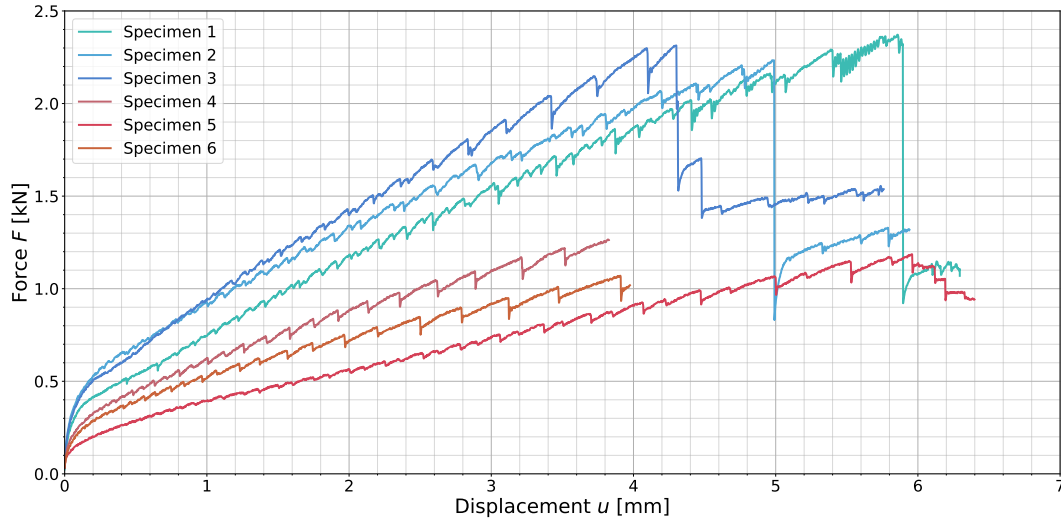
Figure 4.11: *Tension strength test graph.*

$$F_{max} = \frac{F_1 + F_2 + F_n}{n} \tag{4.2}$$

That is for group one 1174 N:

$$F_{max} = \frac{1070N + 1186N + 1266N}{3} = 1174N \tag{4.3}$$

And for group two 2306 N:

$$F_{max} = \frac{2234N + 2314N + 2372N}{3} = 2306N \tag{4.4}$$

Also, the surface area is necessary for the calculation. It is specified as the minimum cross-section of one spline joint, where l is its length [mm] and w is its width [mm]:

$$A = l \times w = 17.5 \ mm \times 35.0 \ mm = 612.5 \ mm^2 \tag{4.5}$$

For group one, the tensile strength parallel to the grain is 1.92 $\frac{N}{mm^2}$:

$$f_{t,0} = \frac{1174N}{612.5 \ mm^2} = 1.92 \frac{N}{mm^2} \tag{4.6}$$

Accordingly, the tension strength parallel to the grain for group two is 1.88 $\frac{N}{mm^2}$:

$$f_{t,0} = \frac{2306N}{2 \times 612.5 \ mm^2} = 1.88 \frac{N}{mm^2} \tag{4.7}$$

In general, the results indicate a linear relationship between the maximum load and the number of joints. The specimens with two spline joints could withstand double the load as the specimens with one spline joint. This increase is attributable to the twofold cross-section. Furthermore, both groups show the same tension strength parallel to the grain within a permissible deviation of 2%.

To set these results in context, a comparison to the standard was relevant. That is defined in EN 338: There, the tension strength parallel to the grain of the C24 softwood timber class is 14.5 $\frac{N}{mm^2}$.[7] Compared to that, the specimens of both groups had just 13% of the standardized strength. However, these differences must be interpreted critically. In general, the design of the test was unable to reproduce the exact tension strength of the timber. Rather, it presented the tension strength of the timber component and its connection. Since that consisted of three to four elements, there were a variety of forces involved. Specifically, transversal tension forces led to the failure of the specimens. Their leftover pieces indicate that clearly (see Figure 4.12 d and e). Each of them broke apart along the grain above one of the spline joints' radial transitions. As the specimens were pulled apart, the joints straddled the timber pieces until they split. That effect occurred at higher loads in specimens 1–3, indicating their greater strength. Also, the cracks only formed at their very edges. Having more material at these vulnerable spots would increase their strength. Both observations are attributable to the position of the joints. It increases the overall stability of the component. On the contrary, specimens 4–6 split close to the center of the timber. Due to its position, the joint acted as a wedge in these specimens (see Figure 4.12).
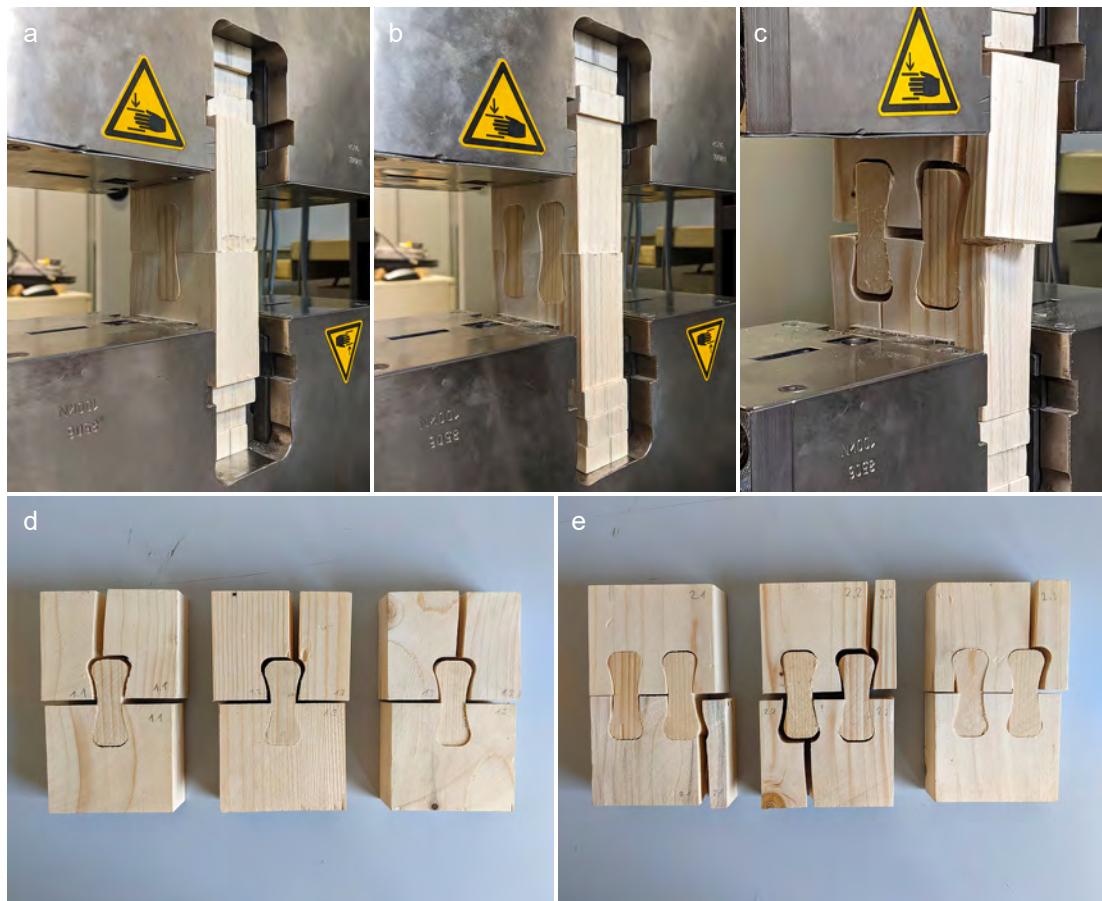

Figure 4.12: *a) & b) Specimens before the test, c) Specimen after failure, d) & e) Specimens after the tension strength tests.*

---

[7] European Committee for Standardization (CEN), *Structural timber – Strength classes*, 7.

In summary, the results indicate that an increased number of joints is beneficial for tension strength. More joints distribute the loads equally in the component. Thereby, excess forces in vulnerable areas are avoided, preventing splits. However, the number and positions of the joints must be set in relation to the overall size of the timber pieces to connect. Also, the distances to the ends of the elements should be appropriate. In general, the material is structurally still potent. As long as there are no cracks present in the timber—these are breaking points—it could be used for construction. Furthermore, it is obvious that the components have less tensile strength than solid timber. However, the structural analysis of the overall structure just has to consider these circumstances.

4.2.2.2 Shear Strength Test

The universal testing machine conducted the shear strength tests as well. For that, it had to be adjusted (see Figure 4.13). The gripping jaws were removed and replaced with a cuboid indenter at the top crosshead. Two metal plates formed a clamp to fixate the specimen. The machine's working platform was ideal to attach the bottom clamp. The top clamp sat on the specimen on one side and two timber pieces of the same height on the other. A steel profile pressed the top clamp down to prevent any movement during the tests. Finally, various screws fixated all elements (see Figure 4.14).
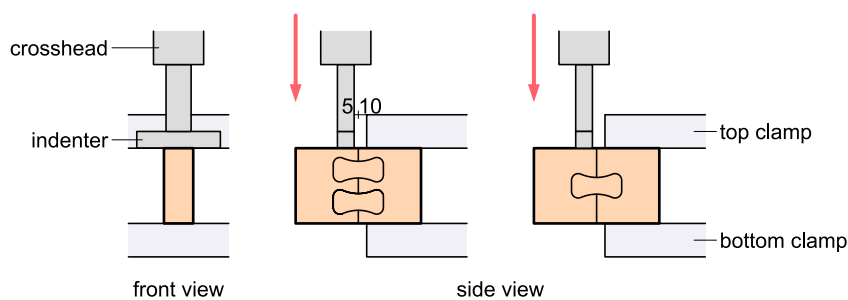
Figure 4.13: *Shear strength test concept.*

The testing procedure was similar to the tension strength test. Its duration was 300 s $\pm$ 120 s with a preloading cycle of 0.1 kN. However, the machine pressed the specimen downwards with a movement speed of 2 mm/min. That was to ensure the failure of the components within the defined timeframe. Figure 4.15 portrays the results of the shear test for each specimen. Again, specimens 1–3 (group two) had two spline joints, whereas specimens 4–6 (group one) had one. The values in x represent the displacement u [mm], i.e., the distance of such a specimen was pushed downwards, whereas the values in y represent the loads F [kN].

For all specimens, the graph shows similar characteristics. Initially, there is a steep increase in the load as the displacement rises. At a certain threshold, that trend stops. Even though the specimens are pushed apart further, i.e., the displacement increases, the load stays relatively constant. The properties of Norway spruce explain that phenomenon. Since it is softwood with high elasticity, it is difficult to reach its breaking point through shear testing. Even with a displacement of 10–14 mm, the specimens just deform without failing (see Figure 4.16 a and b). At these points, the tests were ended to avoid any damage to the machine.
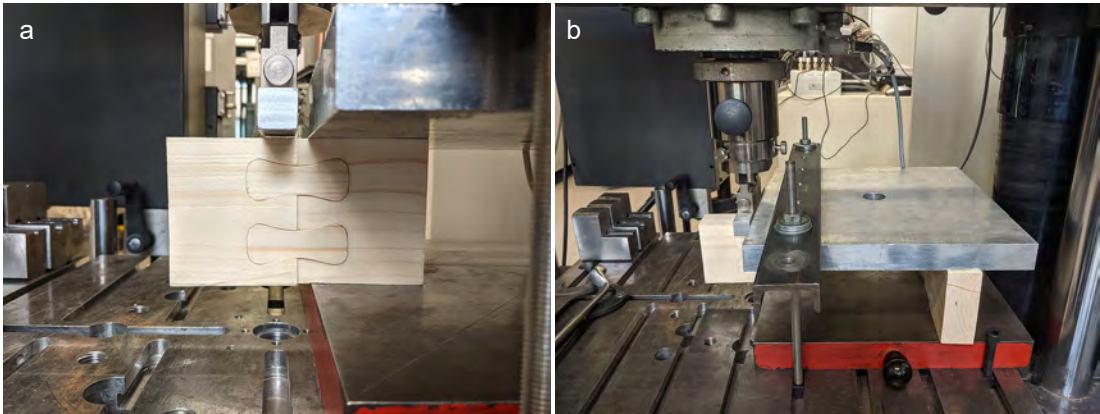
Figure 4.14: *Images of the shear strength test setup: a) Specimen positioning, b) Clamping construction.*
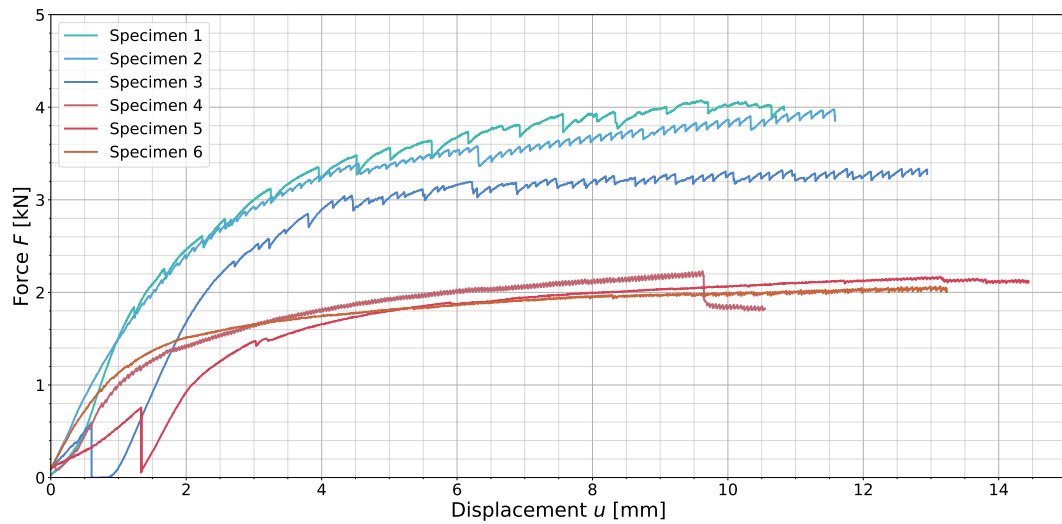
Figure 4.15: *Shear strength test graph.*

The shear force was calculated as in equation 4.1. For that, the maximum load and the surface area were necessary again. The values of the cross-section were the same as in the tension tests. On the contrary, the maximum load had to be calculated, as in equation 4.2. The result for group one is 2154 N:

$$F_{max} = \frac{2065N + 2170N + 2229N}{3} = 2154N \tag{4.8}$$

And for group two it is 3795 N:

$$F_{max} = \frac{3337N + 3977N + 4072N}{3} = 3795N \tag{4.9}$$

Accordingly, the shear strength for group one is 3.10 $\frac{N}{mm^2}$:

$$f_{t,0} = \frac{2154N}{612.5\ mm^2} = 3.10\frac{N}{mm^2} \tag{4.10}$$

And for group two it is $3.52\ \frac{N}{mm^2}$:

$$f_{t,0} = \frac{3795N}{2 \times 612.5\ mm^2} = 3.52\frac{N}{mm^2} \tag{4.11}$$

In general, the trend from the tension strength tests continues. The specimens with two spline joints endured almost double the load as the specimens with one spline joint. In group one, specimen 3 greatly deviated from the other two specimens. Due to a crack being present in the wood, specimen 3 was unable to take as much load as the rest of its group. Thereby, it distorted the result, leading to a shear strength difference of 12%. If the values of group one are adjusted by dismissing the results of specimen 3, the new median is 4025 N:

$$F_{max} = \frac{3977N + 4072N}{2} = 4025N \tag{4.12}$$

Accordingly, the adjusted shear strength for group one is $3.27\ \frac{N}{mm^2}$, that is still a difference of 7%:

$$f_{t,0} = \frac{4025N}{2 \times 612.5\ mm^2} = 3.27\frac{N}{mm^2} \tag{4.13}$$

To set these results in context, a comparison to the standard was relevant again. For C24 softwood timber, the shear strength is $4.0\ \frac{N}{mm^2}$. Compared to that, group one presented a shear strength of 82% and group two of 88% of the reference value. Even though these results were promising, the differences between groups one and two need clarification.

Again, the design of the test was unable to reproduce the exact shear strength of the timber. Rather, it presented the shear strength of the timber component and its connection. Besides, the bending strength of the specimens was of great relevance. Particularly, as the displacement increased, so did the angle the machine pushed at. Thereby, it was almost impossible to break the specimens. They only failed if they had a previous crack. However, the specimens with two spline joints got smaller—but not fatal—cracks (see Figure 4.16 c and d). More joints result in a greater stiffness, and, therefore, in a reduced capacity for the material to deform. Also, that might be the reason why group two showed a slightly higher shear strength.

In summary, the results indicate that an increased number of joints is beneficial for shear strength. More joints distribute the forces equally in the component. Also, they provided greater stability, though at the price of reduced elasticity. However, the main issue and breaking point still lies within previous cracks in the timber. However, their shear strength is close to the standard value. All of that indicates that the material is still viable for structural purposes.
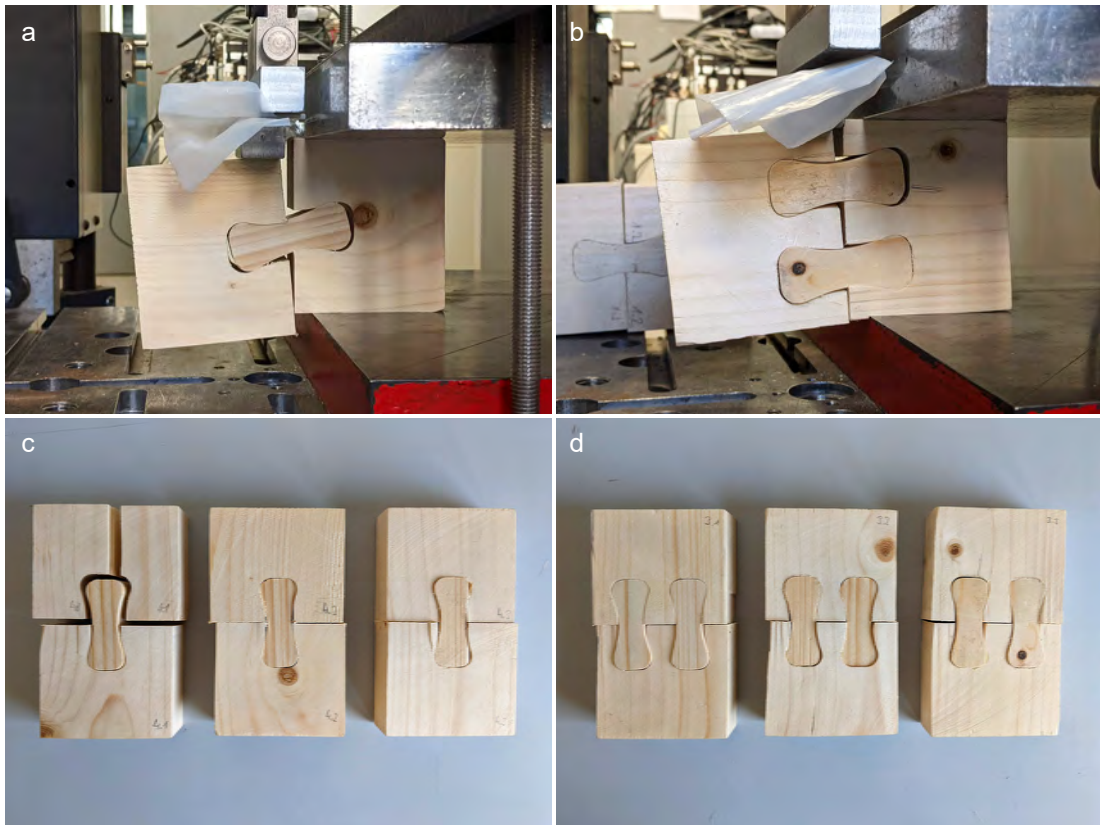
Figure 4.16: *a) & b) Specimens at maximum displacement, c) & d) Specimens after the shear strength tests.*

4.2.3 Robotic Prototypes

The complexity of the offcuts' geometries and the spatial relationship between all parts of an alignment justify the use of industrial robotic arms. The fabrication procedure emphasizes this notion further since it is unique for each offcut.

With the setup described in Chapter 3.4.1 it was possible to fabricate offcuts very precisely. The first experiments involved adjusting the fabrication setup and testing the UR10e's limits at milling operations. These insights informed the fabrication of further prototypes with the maximum stable settings. That culminated in the final prototype that acted as a demonstrator to prove the concept of the design-to-fabrication workflow.

4.2.3.1 Initial Prototypes

The fabrication of the first prototypes tested the limits of the robotic setup for milling operations. For this purpose, the settings used for the milling operations in Chapter 4.2.2 were taken as a reference. The main difference was that a CNC machine was used there instead of a robotic manipulator. It was very unlikely that the robot presented a similar performance. Therefore, the maximum settings to achieve were set to a step size of 4.0 mm per pass and a feed rate of 1200 mm/min.

The experiments began with a step size of 1.0 mm per pass, a feed rate of 600 mm/min, and a spindle rotation speed of 11000 RPM. These values were increased incrementally until the robot failed or the maximum defined was reached. The robot demonstrated a stable performance with the initial values. However, after increasing the feed rate to 1200 mm/min, the robot started oscillating when moving sideways. The internal mechanics of the UR10e might explain this phenomenon. Lateral movements, i.e., a rotation of the base joint, expose a lack of stiffness the robot has in this direction. The further the robotic arm is extended, the stronger this effect becomes. Nonetheless, it provides relatively good stiffness when it moves within the axis relative to its base, i.e., a motion similar to pulling or pushing. The oscillations increased significantly with increasing step sizes. With a step size of 2.5 mm, this still occurred even if the feed rate was reduced to 600 mm/min or lower. The presence of knots in the offcut stock exacerbated this effect further. Due to the dangerous oscillations, the robot failed and damaged the stock model (see Figure 4.17). There may be several reasons for this, such as significant deviation from the toolpath and safety precautions to prevent damage to the robot's joints. In the end, the most reliable settings with stable milling performance and adequate speed were a step size of 1.25 mm, a feed rate of 600 mm/min, a tool engagement of 4.0 mm, and a spindle rotation speed of 12000 RPM.
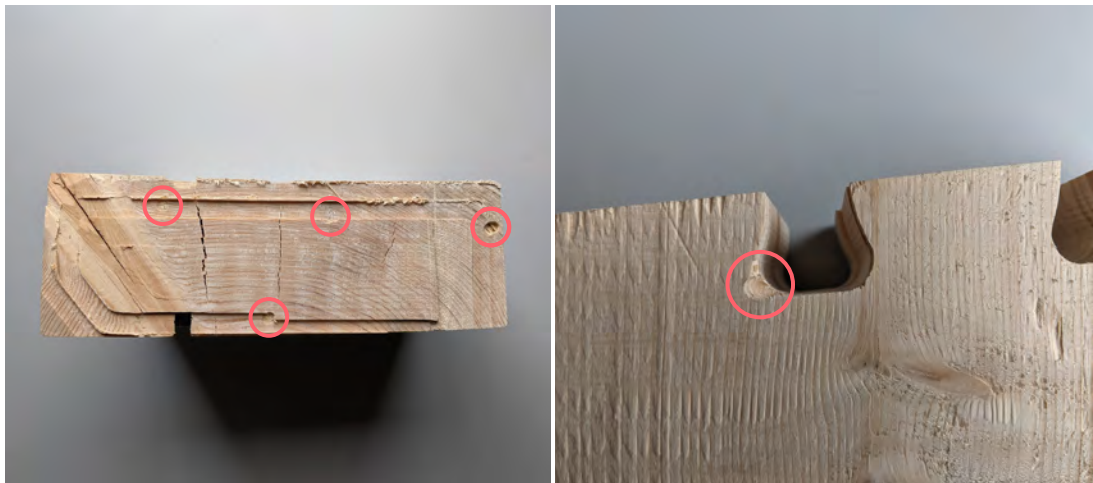
Figure 4.17: *The robot damaged the offcuts due to dangerous oscillations.*

Another significant challenge was matching the physical and digital setups (see Figure 4.18). Even though they seemed to align, there was still an inaccuracy of up to 10 mm in all directions. These inaccuracies are attributable to several reasons. First, there is a build-up of tolerance in the physical setup since it consists of multiple parts and fixtures. Second, in most cases, the offcuts' geometries are deformed and do not perfectly match their digital cuboid representations. Therefore, the setups were aligned by taking measurements with the robots' TCP. The vises served as fixed origin points from which the deviations in all directions were checked. These deviations were considered in the software environment by adjusting all toolpaths with the identified vector. This method proved to be very effective to eliminate the inaccuracies between the physical and digital setups. Also, the fixed origin point enabled a faster fabrication process because it eliminated the need for additional calibrations. However, it was still good practice to check the position of each offcut to account for larger deformations.

The mismatch between the physical and digital setups presented an additional challenge, most likely caused by the robot's mechanics. It milled the negative spline joint shapes in two steps, approaching the offcut from opposite sides (see Figure 4.19). This was necessary because the end mill was not long
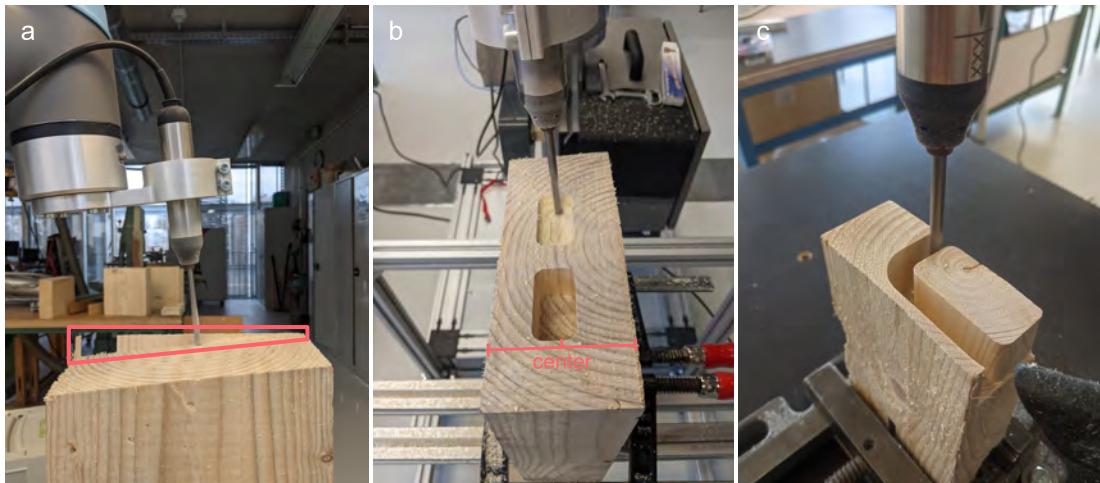
Figure 4.18: *Inaccuracies between the digital and physical setups. a) Leftover piece at the edge of an offcut. b) Incorrect position of the tenon joint pockets. c) A tenon joint that could not be milled completely.*

enough to perform the milling in one pass. Even though the toolpaths were perfectly aligned in the digital model, the joints milled by the robot had significant gaps. These gaps blocked the insertion of the spline joints, making assembly difficult. The reasons for that were inexplicable, but most likely due to the mechanics of the robot. To alleviate this issue, the toolpath for the second machining operation was shifted by the amount of the inaccuracies detected. This proved to be effective enough to achieve clean milling results. Overall, the experiments provided good insights into robotic milling with a UR10e and made it possible to adjust the setup for further fabrication.
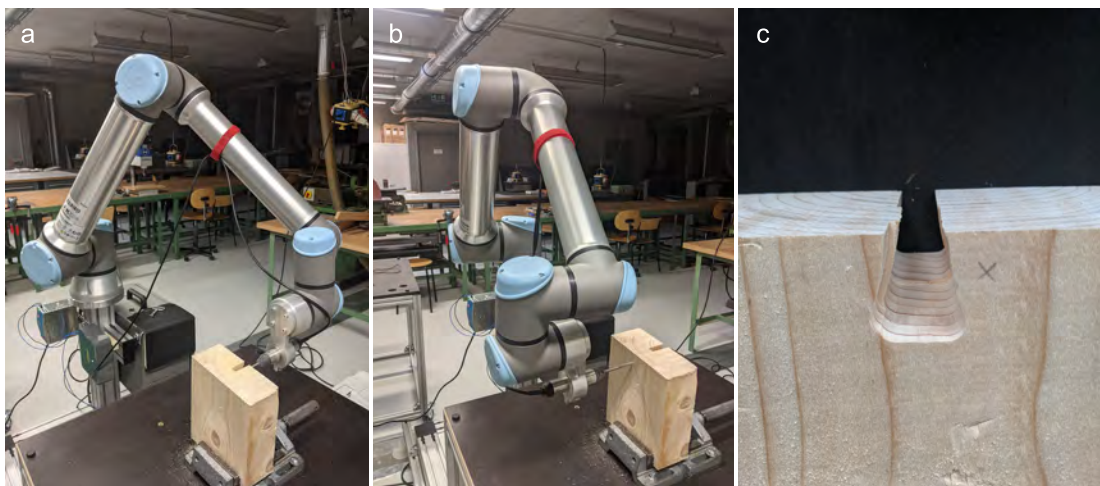
Figure 4.19: *Spline joint milling. a) & b) Milling of the first and second pockets. c) Inaccuracies that were probably caused by the robot's mechanics and had to be adjusted for.*

4.2.3.2 Demonstrator

The fabrication of the demonstrator served as a final proof of concept, i.e., the feasibility of the design-to-fabrication workflow. Due to the comparably slow milling operation and, therefore, the amount of time necessary, an alignment of only six offcuts was built. This alignment is part of the design depicted in Figure 4.3 *e* covered in Chapter 4.1.2. Figure 4.20 shows the specific offcuts chosen for the demonstrator. The alignment algorithm determined the offcuts that had the IDs 53, 66, 82, 148, 32, and 18—ordered from the bottom to the top (see Figure 4.21). Their data were defined in a database (see Table 4.1).
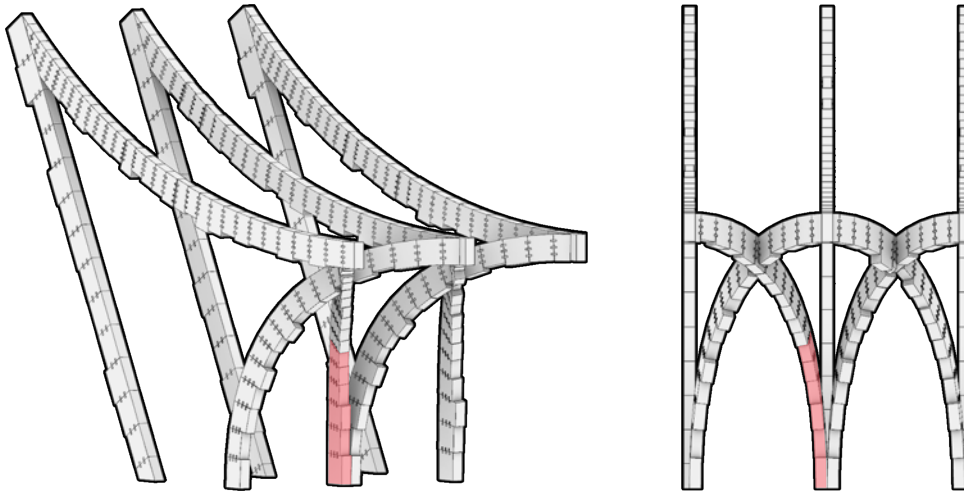
Figure 4.20: *Selected offcuts from the designed structure.*

id	x dimension	y dimension	z dimension
53	20.9	8.3	26.4
66	18.5	8.2	24.9
82	21.0	8.0	23.3
148	18.4	8.2	21.6
32	18.5	8.2	19.9
18	18.3	8.0	19.3

Table 4.1: The dimensions [cm] of the demonstrator's offcuts.

The design was adjusted to demonstrate—and test—the possibilities of the developed design tools. The specific alignment selected made use of almost all features covered in Chapter 3.2. It had a "right–bottom" positioning, a start angle of 0 degrees, and an end angle of −30 degrees. This resulted in a twisted alignment where one edge continuously followed the curve. Also, it made use of the optimization algorithm for the efficient placement of offcuts. However, the joints between the six offcuts were conceptualized differently. Here, the five connection points differed in the type or the number of joints they had. Between offcut 53 and 66, there were two tenon joints, each with a size of 50 mm × 25 mm × 60 mm. In contrast, the offcuts 66 and 82 connected with one spline joint, 82 and 148 with two, 148 and
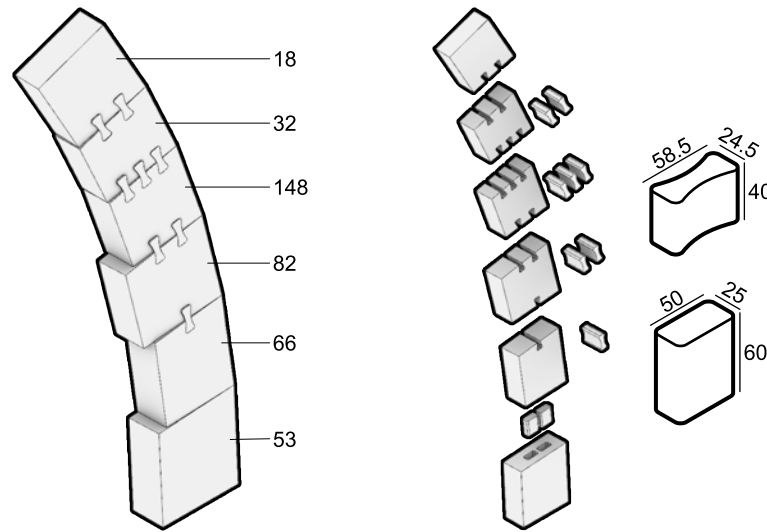
Figure 4.21: *3D Model of the demonstrator.* Left: *Assembled alignment with offcut ids.* Right: *Exploded alignment showcasing the joints with their dimensions.*

32 with three, and 32 and 18 with two. The spline joints had identical dimensions that were 58.5 mm × 24.5 mm × 40 mm. They were computed as covered in Chapter 3.3. The algorithm generated additional data necessary for the fabrication, i.e., the BReps and the planes.

Before the milling operations, the offcuts were prepared to reduce fabrication times. In particular, this meant cutting the offcuts to a specific length with a table saw. This length was determined manually, where an extra 2–5 mm was added to account for tolerances (see Figure 4.22).[8] Afterwards, the data were used to generate the toolpaths for each milling operation as described in Chapter 3.4.2. Then, the software simulated the fabrication environment and exported the machine code as covered in Chapter 3.4.3. Now, the robot could mill the offcuts to create the angular surfaces and the joints using the settings described in Chapter 4.2.3.1. The tenon and spline joints were fabricated similarly. In preparation, their stock material was cut to specific sizes to allow for an efficient milling process. It was important to consider the anisotropic property of wood so that the fibers of the joints would end up aligned with the load direction. Therefore, the spline joints were milled on the side and the tenon joints were milled on the ends of a timber slat. Figure 4.23 portrays the fabrication procedure.

The fabrication times depended on the specific milling operation. It took about 45 minutes to mill an angular surface. The pocket of a tenon joint was milled in 30 minutes, whereas half the pocket of a spline joint took 50 minutes. Furthermore, a tenon joint was milled in 50 minutes and a spline joint in 67 minutes. Accordingly, the fabrication time of (1) the ten angular surfaces was 450 minutes, (2) the four tenon pockets was 120 minutes, (3) the eight spline pockets was 800 minutes, (4) the two tenon joints was 100 minutes, and (5) the eight spline joints was 533 minutes. That culminated in a total milling time of 2003 minutes, i.e, 33.4 hours, for the demonstrator—excluding the initial tests, fails, and changes made to the setup. If broken down, this means that with the current setup the average fabrication time for one offcut is approximately 334 minutes, i.e, 5.5 hours. Concerning the design as a whole, the numbers become even more excessive. The curve of the demonstrator consists of 18 offcuts, meaning the

---

[8] If faster manufacturing methods had been available, this step would have been redundant. For instance, a CNC table saw or an end effector with a circular saw could have been used.
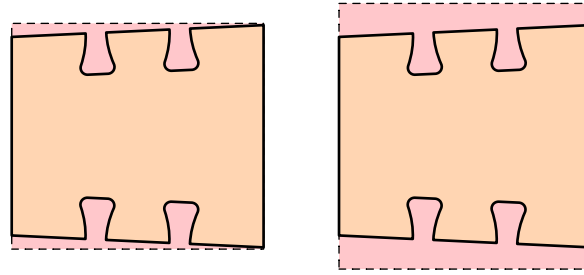
Figure 4.22: *Pre-cutting the offcuts to reduce milling times. The material to be milled is highlighted in red.* Left: *Pre-cut offcut.* Right: *Original offcut.*

fabrication times would triple to 6009 minutes. However, the complete design has 127 offcuts, resulting in approximately 42418 minutes, i.e., 707 hours or 29.5 days of milling. These numbers clearly suggest that for the fabrication to be feasible, faster methods must be employed.

Furthermore, the subtractive manufacturing of the offcuts resulted in approximately 4066 cm³ of waste. Milling the external joints produced an additional 1816 cm³ (104 cm³ for the tenon and 1712 cm³ for the spline joints) of waste but added 867.3 cm³ of material to the demonstrator. (see Table 4.2).

id	volume	fabricated volume	difference	joint volume
53	4580	3957	623	73,3
66	3780	3145	635	119
82	3910	3149	761	135
148	3260	2446	814	225
32	3020	2186	834	225
18	2830	2431	399	90
	21380	**16880**	**4066**	**867.3**

Table 4.2: Offcut volume [cm³], fabricated volume [cm³], the differences [cm³], and joint volume [cm³].

To test whether the optimization algorithm is effective in reducing fabrication waste, the volumetric values of the optimized alignment were compared to a basic alignment (see Chapter 3.2.1). For this comparison, the same curve and settings were used as described previously, resulting in an identical shape (see Figure 4.24). Also, the volumes of the joints were ignored since they would be identical in both cases. Table 4.3 portrays the results. They show that the optimization algorithm used 3350 cm³ less material and produced 2038 cm³ less waste. This relationship increases significantly with a complete alignment. In particular, the basic algorithm will result in more waste being produced if the curve has a strong curvature. Thereby, the data demonstrate that the optimization algorithm is very effective in reducing fabrication waste.

Finally, the demonstrator was successfully assembled in collaboration with the UR10e. For this purpose, the robot was equipped with a gripper with a stroke span of 85 mm. This enabled it to grip both the joints and the offcuts and thus assemble the demonstrator step by step. Figure 4.25 shows the entire process. The program used to control the robot was created using only the teach pendant. It defined how the robot would approach and grip each object. Each of these objects had a specific position so the robot always gripped them in the same place. For this purpose, a scaffold was built that served as a stop for the objects, in which two sides of an object could always be precisely aligned. The procedure was

Figure 4.23: *Robotic fabrication procedure: a) Tenon joint, b) Angular surface, c) Tenon joint pocket, d)–f) Spline joints, g)–i) Spline joint pockets.*
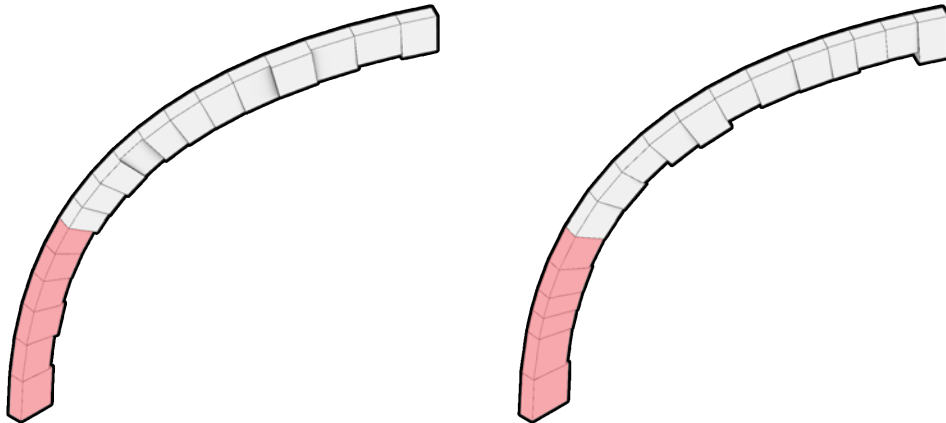
Figure 4.24: *Comparison of an optimized alignment (left) and a basic alignment (right). The relevant offcuts for the comparison are highlighted in red.*

id optimized	volume	fabricated volume	id basic	volume	fabricated volume
53	4580	4030	1	5840	4943
66	3780	3266	2	5253	4353
82	3910	3287	3	2788	2247
148	3260	2681	4	2694	2133
32	3020	2422	5	3827	2974
18	2830	2220	6	4328	3294
	21380	**17906**		**24730**	**19944**

Table 4.3: Comparison between an optimized alignment and a basic alignment. All volumetric values are in [cm³].

similar for all elements. They were approached and then picked up after the gripper closed. Then the robot moved them to their designated position in a step-wise manner. For the assembly with the tenon joints, the direction of insertion needed to be perfect. For this purpose, the joints were inserted using the free-drive option. The robot was then able to minimally move the joint out of the offcut in the direction of the z-axis of the TCP. This point was defined as the starting point of the insertion movement, which was then executed in a linear motion. For the assembly of the offcuts with spline joints, the robot moved the relevant offcuts to the designated position and aligned the angled surfaces. The spline joints were then manually inserted while the robot waited and held the offcuts in place for 10 seconds. It then released the grip and executed the next step of the program. Using these methods, the demonstrator was assembled collaboratively by humans and robots.

The final design of the demonstrator is depicted in the figures 4.26 and 4.27. It proved that the design-to-fabrication workflow is feasible and demonstrated the possibilities of the developed methods, specifically the computational design tools that informed the digital fabrication and assembly.

Figure 4.25: *Collaborative assembly procedure: a) & b) Pick and place of the first offcut, c) & d) Placing the tenon joints, e) & f) Pick and place of the second offcut, g)–j) Pick and place of the third and fourth offcuts with human collaborator inserting the spline joints.*

Figure 4.26: *Images of the final demonstrator.*

Figure 4.27: *Images of the final demonstrator.*

Chapter 5
Conclusion and Future Work

5.1 Conclusion

In the context of the concurrent sustainability and digitization challenges of the building industry, this work focused on the upcycling of timber for architectural and structural applications. For this purpo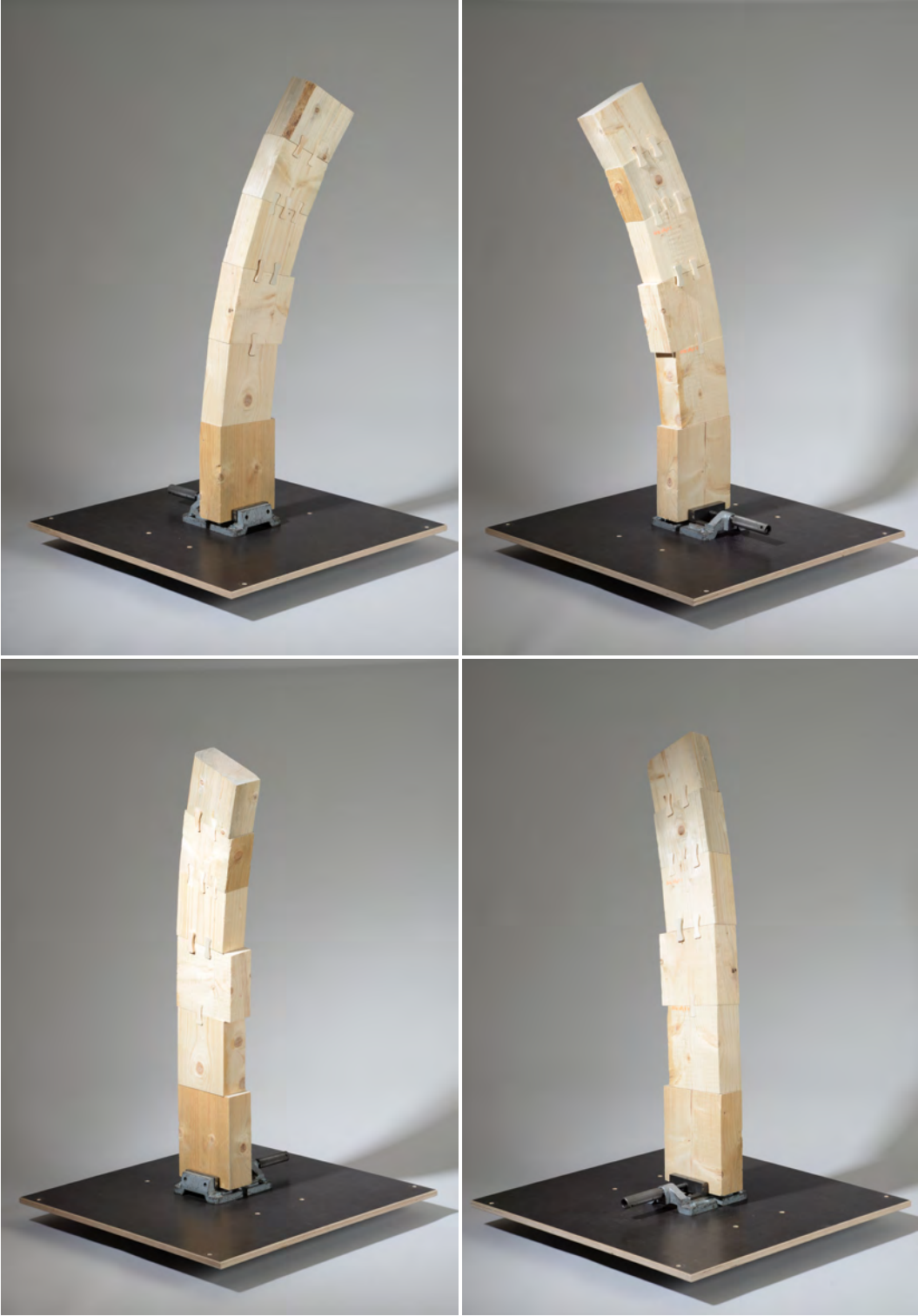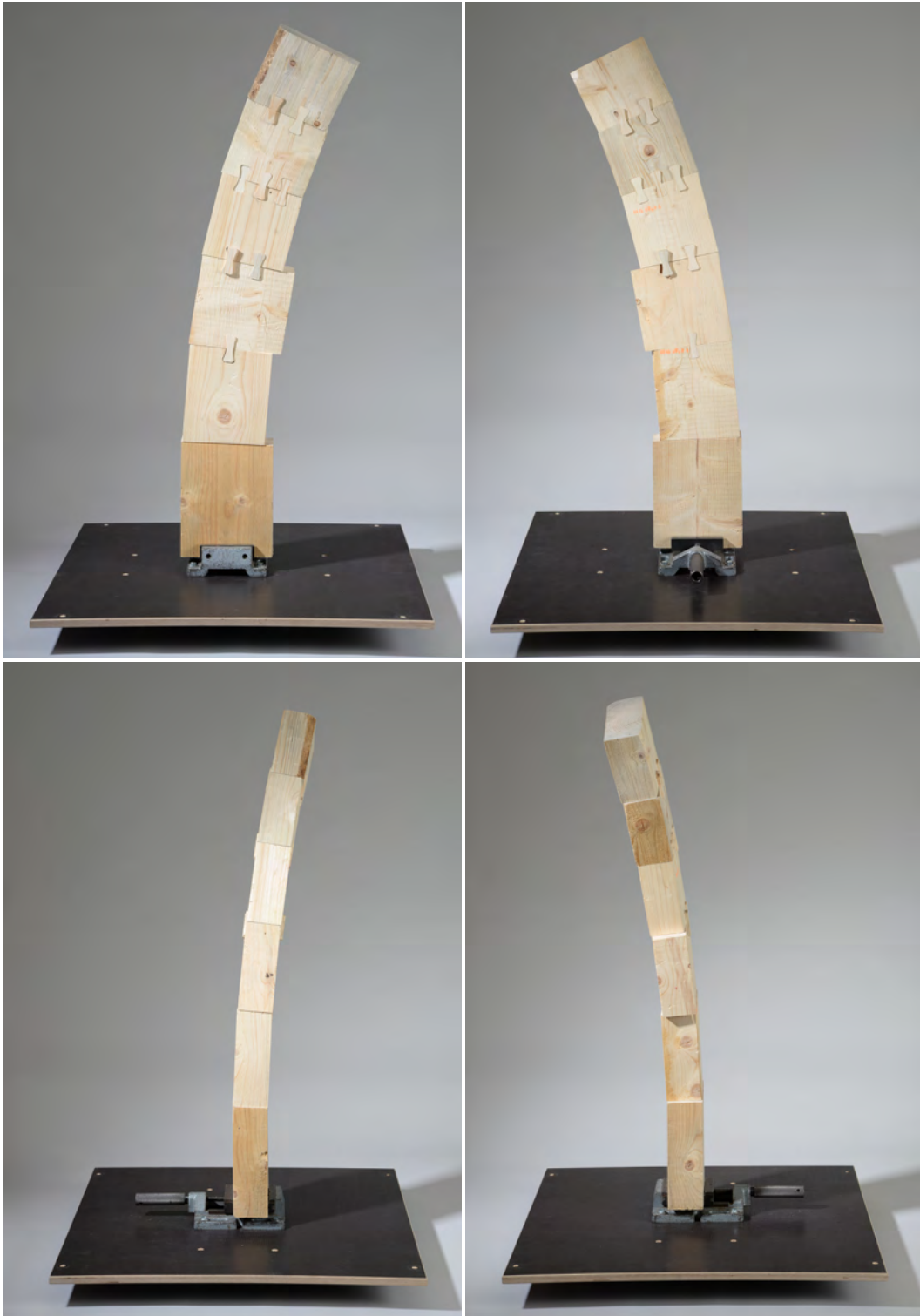se, it first explored current practices of the timber industry in the case of the German state of Thuringia (see Chapter 1.1), whereas the supply chains, waste management, and design and manufacturing practices were of particular interest. The additional site visits revealed the accumulation of a range of waste products, and, as such, timber offcuts turned out to have the most potential.

The upcycling of non-standard and low-engineered timber offcuts required computational design tools that informed the robotic fabrication. However, upcycling the offcuts is not trivial due to their non-standard geometries and the complex relationship between the parts. Due to these insights, the thesis identified three challenges: first, the upcycling of offcuts from timber production, second, the architectural and structural use of offcuts, and third, the integration into a unified design-to-fabrication workflow (see Chapter 1.2). Ultimately, addressing these challenges integratively, a digital design-to-fabrication workflow was developed. It consists of several approaches and techniques, including digital design and fabrication workflows and components. The necessity to develop and use these approaches and techniques became obvious to manage the bespoke geometry and the overall quantity of the timber offcuts. For this purpose, a .NET library was written in C# and implemented in the Rhino3d/Grasshopper software environment. Furthermore, the digital fabrication workflows and components included a five-axis CNC milling machine and a six-axis robotic arm, being equipped with a milling and a gripping end effector. The developed and implemented design-to-fabrication workflow allowed to massively expand the design and fabrication space in the realm of low-engineered timber construction and provided a basis to iteratively explore respective potentials and challenges (see Chapter 1.3).

Here, the state-of-the-art review revealed several insights (see Chapter 2). From the 1980s onward, digital fabrication practices in timber construction became very advanced in both the industry and academia. Both sectors implement cutting-edge tools, leading to new structural capacities and expressions, e.g., timber shells and free-form glulam structures. However, these structures require significant expertise and resources for their planning and construction. Also, the review revealed a research gap in the upcycling of low-engineered timber for architectural and structural applications.

Following the literature review, Chapter 3 presented the implemented methodologies. The developed software tool could work with the data from the offcut database and align the offcuts on curves (see Chapters 4.1.1 and 4.1.2). It proved to be a fast and robust tool that achieved the design of free-form offcut structures. It aligned the offcuts so that their fibers were always parallel to the principal loads. Thereby, it essentially considered the material properties of wood. Furthermore, the optimization algo-

rithm proved to be effective in reducing material waste. Also, it produced cleaner results by aligning short offcuts at places with high curvature. The tools enabled the fast and robust creation of a range of joint geometries, including spline and tenon joints (see Chapter 3.3). Furthermore, they provided the ability to control the positioning, torsion, and rotation of an alignment. Thereby, a desirable orientation could be achieved (see Chapter 3.2). That facilitated the intersections and connections between the alignments. The software provided the means to solve the intersection instances as well. In most cases, it produced fast and robust results. However, if the positioning of the alignments was unideal, the chance of the computation failing increased significantly. Therefore, it was vital to optimize the design of the curves (see Chapter 3.3.3).

The final steps of the workflow dealt with digital fabrication and the translation of digital design data into physical manipulation (see Chapter 3.4). The software created the required geometric data. Then, Fusion 360 generated the toolpaths that were imported back into Grasshopper. Finally, the tools of the HAL Robotics plugin simulated the environment and generated the machine code. The physical environment consisted of a fabrication table, a UR10e, a milling spindle, and a gripper. Overall, the robot performed the milling operations quite well and precisely milled the joint geometries (see Chapter 4.2). It further demonstrated its true capabilities at the assembly. Provided the physical and virtual environments match, it could easily place the offcuts on the table and insert the tenon joints. Additionally, the collaborative assembly with the robot holding the offcut and a human placing the spline joints was a success as well. With an automated procedure, the entire prototype was fabricated and assembled (see Chapter 4.2).

Furthermore, the strength tests revealed that the material might be viable for structural use, depending on the condition of every item. In particular, the presence of cracks was relevant. Also, the test results demonstrated that more spline joints increased the stiffness and tension strength of the connection. However, further tests with actual-sized components and multiple offcuts might provide additional insights (see Chapter 4.2.2).

In conclusion, the proposed workflow proved to be effective in the upcycling and utilization of offcuts for architectural and structural applications, and, above all, it allowed to foster new digital-material design techniques and processes. The selection, collection, measurement, and digitization of the offcuts created a database. That informed the design and alignment processes. Then, the required joints could be created. All of that led to the generation of the fabrication data. Thereby, a robot could fabricate and assemble the offcuts as designated in the design model. The assembly then closed this digital chain, which began with the selection and measurement of the offcuts. However, humans were an important component in this process, highlighting the possibilities of collaborative assembly. In this, the robot used its strengths, i.e. the precise positioning and alignment of partially heavy components at the designated location, whereas the human inserted the spline joints—a task almost impossible for the robot due to the tolerances.[1] The now closed digital chain enables the design and conception of architectures with offcuts. This non-trivial task was solved using the developed tools and serves the entire workflow from design to fabrication. Thus, the original motivation of this work—the reuse of timber waste—becomes a possible reality. It entailed the use of one of the most sustainable materials, i.e., timber, that was locally available and its integration into the circular economy. To meet these demands, the concept minimizes material waste during fabrication as much as possible. In addition, due to their wood joints, offcut structures are based on the principle of "design-for-disassembly" and can therefore be disassembled and reassembled.

Finally, full-scale automation—including multiple gantry-mounted robots working collaboratively, for instance—could enable the rapid fabrication and assembly of numerous offcuts into large components

---

[1] Currently, there are research projects that deal with the robotic assembly of wood joints and overcoming the tolerances. Machine learning is used in the process. (Apolinarska et al., "Robotic assembly of timber joints using reinforcement learning").

and structures. Due to their conception, they combine some apparent contrasts. This is particularly evident in the production of the offcuts, which takes place serially. However, although that always includes the same processes, the offcuts are bespoke because they and the spatial relationship with other elements are never the same. In addition, they combine an artisanal authenticity, i.e., working with traditional wood joints and the materiality of wood, with the digital logic of the fabrication machines. After all, the complexity of such structures would exceed what is achievable by mere woodworking handcraft. There, only the algorithms determine which offcut to place next and how to fabricate it. However, traditional woodworking knowledge is not obsolete due to these advancements, even though it was originally displaced by automation and the serialization of production. Rather, it experiences a new renaissance with the help of digital tools. Specifically, these are numerically controlled machines that act as intermediaries between humans and material, guiding the tools. In this process, the craft experience and skills are transmitted in the form of data that control the machines and describe the objects to be fabricated. These machines, e.g., industrial robots, are inherently generic and perform a multitude of operations required with a wide variety of tools. At the same time, the digital woodcraft is explicit because all operations must be described precisely. As a result, the craft knowledge of a culture is transformed and undergoes further development with the help of digital tools. This includes the adaptations to the requirements of the machines but also the inherent properties of wood.[2] That is the essence of the novel digital woodworking craft.

5.2 Future Work

The design-to-fabrication workflow for free-form timber structures with offcuts developed in this work provides a basis for future research projects, for instance, by up-scaling the fabrication system towards large-scale demonstrators to verify the capabilities of the proposed system. Concerning the computational design processes, further research would need to optimize the planning of such structures. To that end, the enhancements of the software tools would enable more efficient modes of planning and further expand the design space and decision-making process. In particular, it would be beneficial to improve the algorithm computing the intersection joints and to streamline the data transfer and the toolpath generation into a single software framework.

In addition, it is necessary to close the digital process chain, which then in turn serves the aspects of the circular economy. In this sense, the first step involves scanning the offcuts to generate precise dimensions and detect geometric irregularities. Even CT scanners could be used to detect fatal cracks and inform an improved selection process. This data enables the computational design tools to produce more accurate results and, thereby, improve the fabrication and assembly processes. The 3D model generated contains all the necessary data to monitor the offcut structures. This allows parts to be easily replaced, if necessary, and the structure to be preserved as a whole.

Additional improvements to the offcut structures imply the material of the joints. These could be made of hardwood, e.g., European beech, which provides benefits to the overall structure. In particular, their reaction to humidity is different. That causes them to soak more moisture and swell accordingly. Thereby, the strength of connection of the joints increases after a short period, while the assembly requires almost no force. Sticking with the concept, material waste from hardwood production could be processed into tenon and spline joints. Robeller and von Haaren already demonstrated the feasibility of such an approach.[3]

---

[2] Tobias Bonwetsch, Fabio Gramazio, and Matthias Kohler, "Digitales Handwerk," in *GAM Architecture Magazine 06*, ed. Urs Hirschberg, Graz Architektur Magazin Graz Architecture Magazine 6 (Springer Vienna, 2010).

[3] Robeller and von Haaren, "Recycleshell."

Additional expertise is required to preserve the plausibility of the concept as a whole. For example, calculating a life cycle assessment of such structures could provide information about the overall sustainability of the structure and thus provide relevant and holistic data. Also, structural engineers could verify the calculations from the statics software and suggest improvements. With this in mind, it is advisable to extend strength testing to entire assemblies of components. This allows conclusions to be drawn about the performance of the offcut structures, which are then in turn incorporated into the software tools. Ultimately, their performance can be evaluated in general and, thereby, lead to a better-informed design-to-fabrication workflow.

Finally, this thesis provides a basis for rethinking conventional design and planning methods. In this context, material properties, as well as detailing, manufacturing, and assembly could become part of the design phases, replacing incremental processes with integrative ones. This not only expands the design space but also facilitates and enables the upcycling of materials. The developed workflow successfully demonstrates the possibilities of such an approach with offcuts and methodically ties in with previous research, e.g. Vestartas,[4] Svilans,[5] and Apolinarksa.[6]

---

[4] Vestartas, "Design-to-Fabrication Workflow for Raw-Sawn-Timber using Joinery Solver."

[5] Svilans, "Integrated material practice in free-form timber structures."

[6] Apolinarska, "Complex Timber Structures From Simple Elements."

Appendix A
Typology Explorations

In the conceptual phase of this thesis, it was critical to understand the possibilities and limitations of various typologies when constructed with offcuts. This appendix discusses the two types that have not been considered in the end.

A.1 Planar Elements

The first concept for reusing offcuts is to construct planar elements, i.e., mass timber elements, out of them. Figure A.1 portrays a variety of the explored compositions. Since offcuts have a brick-like form, it is probably the most obvious concept. There are various advantages and disadvantages to that.

Such production of solid timber elements could reduce the amount of waste in the solid timber industry. Cutouts for windows, doors, etc., become irrelevant when walls are constructed out of small discrete elements. As in traditional brick construction, the material is easy to handle and assemble. The process could also be automated, as was shown multiple times.[1]

Though, that also means that simple forms of brick-laying are not novel. Therefore, it is questionable if proving that concept with waste timber is relevant at all. On the contrary, more sophisticated forms of puzzling the elements together are too complicated. For the elaboration of this concept, different algorithms for 3D bin packing were tested. In general, they provide good results (see Figure A.2). However, the offcuts are elements with minimal deviations in their dimensions. Therefore, they create geometrical problems that are almost impossible to solve even for advanced algorithms. In this case, the only solution would be to cut the offcuts to a specific size to allow for packaging. However, this requires a lot of time and effort.

The connections between the offcuts in the mass timber element are geometrically even more complex to solve (see Figure A.3). The joints would have to be generated and fabricated in all directions where there are neighbors. Also, the assembly might cause further issues. There, the joints would have to be designed in a way that sequential assembly is possible.

All of these constraints raise the issue of economics. Sorting the offcuts, prefabricating them to specific dimensions, fabricating the joints, and assembling the mass timber element is time and resource-demanding. Contrary to that, conventional mass timber elements are industrially produced products with high-quality standards and structural capabilities. Compared to that, the offcut-made massive timber wall takes longer to be fabricated and is potentially less capable. The industry might produce more waste in the form of cutouts, but these could still be reused (see Chapter 2.1).

---

[1] Gramazio et al., *The Robotic Touch*.
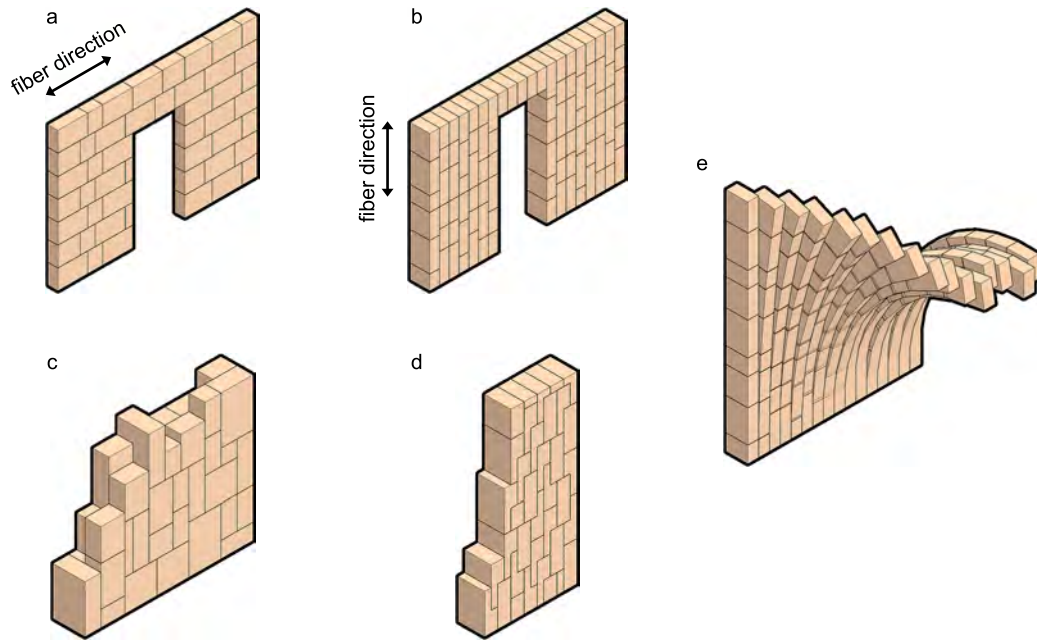
Figure A.1: *Concept of the planar elements: a) Horizontal offcuts, b) Vertical offcuts, c) Puzzled offcuts, d) Vertical puzzled offcuts, e) Vertical single-curved offcuts.*
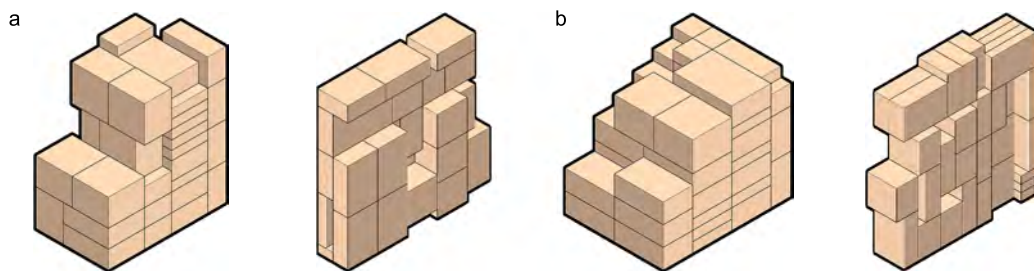
Figure A.2: *3D Bin Packing results: a) BestFit algorithm, b) EB-AFIT algorithm.*

A.2 Linear Elements

The second concept for reusing offcuts is to construct linear elements out of them. These include columns, beams, and bracings. Figure A.4 portrays a variety of the explored compositions. However, this is not a new concept. The timber industry used to do this in the past when wood was more valuable. For that, a CNC machine milled finger joints on both ends of an offcut. Then, the elements were glued together. Today, this is no longer economically viable, as there is a great demand for high-quality timber.
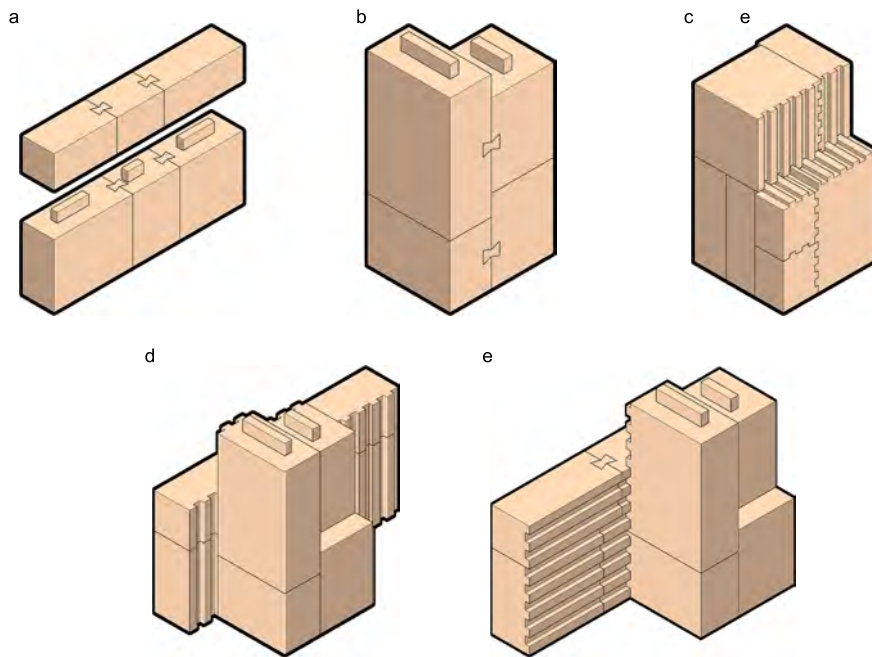
Figure A.3: *Joinery strategies for the planar elements: a) Horizontal offcuts with tenon and spline joints, b) Vertical offcuts with tenon and spline joints, c) Puzzled offcuts with finger joints on all sides, d) & e) Combination of horizontal and vertical offcuts with finger, tenon, and spline joints.*

The process of fabricating these types of elements would require the offcuts to be sorted, prefabricated, milled, and glued together. Thereby, it is more time-consuming and expensive. Compared to the low selling price of these elements, it is clear why that process was abandoned.

Furthermore, the elements are potentially structurally less capable. Due to the adhesives, the weight is higher. Also, more joints increase the number of probable weaknesses. In comparison, serially produced structural timber elements are mass products with high-quality standards. In the end, the concept did not seem to be feasible.
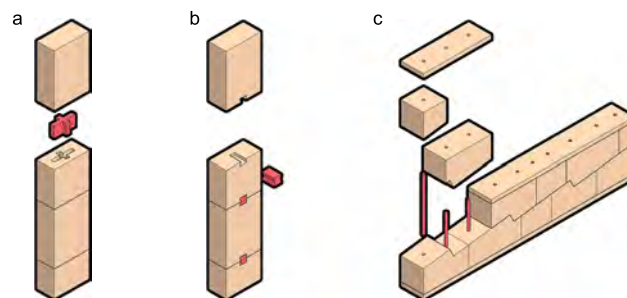
Figure A.4: *Concept of the linear elements: a) Column with cross-tenon joints, b) Column with spline joints, c) Composite indented beam with dowel joints.*

Appendix B
Software Tools

B.1 Rhino3d and Grasshopper

The chosen software framework for this thesis is Rhino3d and its plugin Grasshopper, since it is commonly used within architectural research.[1] It provides good documentation and the possibility to develop custom tools to extend its functionality. The Rhino SDK (Software Development Kit) and the RhinoCommon API (Application Programming Interface) are open source and enjoy a strong backing from the community.[2]

Rhino3d is proprietary software for CAD (Computer-Aided Design) that is based on the NURBS (Non-Uniform Rational B-splines) mathematical model.[3] Yet, it is also possible to work with mesh geometries. Grasshopper is a visual programming language running inside Rhino3d as a fixed extension.

B.2 Spruce Beetle – Designing with Offcuts

For the specified software environment, a multi-component plugin was developed within the scope of this thesis. It is implemented as a .NET library written in C#. It provides the functionality to work with timber offcuts and makes that accessible. The code is open source and available on GitHub: https://github.com/DominikReisach/Spruce-Beetle.

The current structure of the plugin was chosen on purpose. Since some of the components provide similar functions, it is possible to combine them to reduce their number. However, this would increase the complexity of the code and potentially decrease the speed of computation. Furthermore, working within the visual scripting setting of Grasshopper would also be more complicated. The components might be fewer, but their functionality and, therefore, their complexity increases. To ensure a smooth and conventional workflow within the software environment, the plugin is conceived as it is.

Furthermore, there are probably still bugs left in the code. It has been tested extensively in the scope of this thesis, though only by the author. Further use in research and teaching as well as a peer-review in the community, could reveal problems and possible enhancements. To that end, the plugin is an ongoing project.

---

[1] Robet McNeel & Associates, *Rhinoceros 3D*, https://rhino3d.com.

[2] Robert McNeel & Associates, *Rhino Developer Docs*, https://developer.rhino3d.com/api.

[3] E. Bayer and K. Dooley, *New Techniques for the Generation of Subsurface Models*, vol. All Days, OTC Offshore Technology Conference (May 1990), doi:10.4043/6295-MS.

B.3 Additional Software

Additional software was used for specific purposes. That included tools for robotic control and milling path generation.

HAL Robotics is a commercial plugin for various software—including Rhino3d—for the control of robotic arms. It was used to simulate the robot environment and to control the UR10e. Also, it generated the script that the robot used for the fabrication and assembly.[4]

Autodesk Fusion 360 is proprietary CAD and computer-aided manufacturing (CAM) software with free educational licenses. It was used to generate the milling paths for the case studies in the Sections 4.2.3.[5]

B.4 Python Code

Smaller snippets of Python code automated an array of tasks. That included the scaling of the icons of the Spruce Beetle plugin covered in Section B.2 (see Listing B.1). Additionally, it created the plots from the data generated with the strength tests in chapter 4.2.2 (see Listing B.2).

```python
import fnmatch
import cv2
import numpy
import os

# resize png files
def resize_img (png_file, png_name):

    print(png_file)

    img = cv2.imread('{}'.format(png_file), -1)
    res_img = cv2.resize(img, dsize=(24, 24), interpolation=cv2.INTER_AREA)

    print(img.item)

    print('original Size:', img.shape)
    print('rezized Size:', res_img.shape)

    status = cv2.imwrite("24x24_" + png_name, res_img)

# folder path
folder_path = os.path.dirname(os.path.realpath(__file__))

# main
for img in os.listdir(folder_path):
    if fnmatch.fnmatch(img, '*.png'):
        image = folder_path + '/' + img
        resize_img(image, img)
```

Listing B.1: Resize Icons.

---

[4] HAL Robotics, *HAL Robotics*, https://hal-robotics.com.

[5] Autodesk Inc., *Autodesk Fusion 360*, https://autodesk.com/products/fusion-360.

```python
1  import os
2  import numpy as np
3  from matplotlib import pyplot as plt
4
5  # font sizes
6  small_size = 20
7  medium_size = 25
8
9  plt.rc('font', size=medium_size) # default text size
10 plt.rc('axes', titlesize=medium_size) # font size of the axes titles
11 plt.rc('axes', labelsize=medium_size) # font size of the x and y labels
12 plt.rc('xtick', labelsize=small_size) # font size of the tick labels in x
13 plt.rc('ytick', labelsize=small_size) # font size of the tick labels in y
14 plt.rc('legend', fontsize=small_size) # font size of the legend
15 plt.rc('figure', titlesize=medium_size) # font size of the figure title
16
17 # folder path
18 folder_path = os.path.dirname(os.path.realpath(__file__))
19
20 data_list = []
21
22 # add data to list
23 for file in os.listdir(folder_path):
24     if file.endswith(r".TRA"):
25         file_path = folder_path + '/' + file
26         data = np.genfromtxt(file_path, skip_header=19,
27         delimiter=';', dtype=float)
28         data_list.append(data)
29
30 fig, axs = plt.subplots(1, 1, sharex=True, sharey=True, tight_layout=True)
31
32 # create list of colors
33 line_colors = ['#3cbbb3', '#51a7d7', '#4c81cd', '#c16570', '#d54057', '#ca643b']
34
35 for idx, data in enumerate(data_list):
36     axs.plot(data[:,2], data[:,1], label='Specimen {n}'.format(n=idx+1),
37     linewidth=2.0, color=line_colors[idx])
38
38 axs.set_xlim(0, 7)
39 axs.set_ylim(0, 2.5)
40
41 axs.set_ylabel(r'Load $F$ [kN]')
42 axs.set_xlabel(r'Displacement $u$ [mm]')
43
44 axs.grid(linewidth=1.0)
45 axs.grid(visible=True, which='minor', alpha=0.5, linewidth=0.75)
46 axs.minorticks_on()
47
48 axs.legend(loc="upper left")
49
50 fig.tight_layout()
51
52 plt.show()
```

Listing B.2: Generate Tension Strength Test Plot.

B.5 URScript

Robotic manipulators from the Universal Robots brand can be controlled on a script level with the URScript programming language.[6] It contains variables, types, and the flow control statements. Additionally, it enables monitoring and controlling the inputs, outputs, and robot movements. Listing B.3 shows an example code for a milling procedure in URScript.

In the function, the weight and TCP can be defined. The milling spindle is controlled via the *analog_out* command, where the first number is the identification of the analog output and the second number is the amount of volts, determining the rotation speed of the spindle. Furthermore *movej* determines a movement in Joint Space and *movep* a movement in Configuration Space, where *a* is the acceleration, *v* is the velocity, and *r* is the blend radius. *Movep* has six values that define the points to be moved to, specifically, the coordinates *x*, *y*, and *z* and the rotations *rx*, *ry*, and *rz*. In contrast, *movej* has six values that define the rotation of the robot's joints in radians.

```
1  def MillingPath() :
2  set_payload(0.74)
3  set_tcp(p[0.00112,-0.08964,0.1365,0,0,0])
4  movej([-1.376521,-1.98037,-2.371527,-0.360492,1.570796,0.194275], a=10,
       v=0.133333, r=0)
5  set_analog_out(1, 0.11)
6  sleep(1)
7  movep(p[-0.06267,-0.678113,-0.0545,0,3.141593,0], a=10, v=0.01, r=0.001)
8  movep(p[-0.06267,-0.678113,-0.05715,0,3.141593,0], a=10, v=0.01, r=0.001)
9  ...
10 movep(p[-0.049721,-0.735625,-0.096481,0,3.141593,0], a=10, v=0.01, r=0.001)
11 movep(p[-0.049721,-0.73604,-0.0545,0,3.141593,0], a=10, v=0.01, r=0.001)
12 set_analog_out(1, 0)
13 sleep(1)
14 movej([-1.570796,-0.785398,-2.356194,-0.907571,1.570796,0], a=0.15, v=0.133333,
       r=0)
15 end
16 MillingPath()
```

Listing B.3: Example code of a milling procedure in URScript.

[6] Universal Robots, *The URScript Programming Language G5*, https://s3-eu-west-1.amazonaws.com/ur-support-site/105198/scriptManual_SW5.10.pdf

References

Adhikari, Shankar, and Barbara Ozarska. "Minimizing environmental impacts of timber products through the production process "From Sawmill to Final Products"." *Environmental Systems Research* 7 (2018): 6. doi:10.1186/s40068-018-0109-x.

Al Bahar, Bahar, Abel Groenewolt, Oliver David Krieg, and Achim Menges. "Bending-Active Lamination of Robotically Fabricated Timber Elements." Pages 89–97 in *Research Culture in Architecture: Cross-Disciplinary Collaboration.* Edited by Cornelie Leopold. Basel: Birkhäuser, 2020. doi:10.1515/9783035620238-009.

Alvarez, Martín, Hans Jakob Wagner, Abel Groenewolt, Oliver David Krieg, Ondrej Kyjanek, Daniel Sonntag, Simon Bechert, Lotte Aldinger, Achim Menges, and Jan Knippers. "The BUGA Wood Pavilion: Integrative Interdisciplinary Advancements of Digital Timber Architecture." Pages 490–99 in *ACADIA 19: UBIQUITY AND AUTONOMY.* Proceedings of the 39th Annual Conference of the Association for Computer Aided Design in Architecture (ACADIA). Austin: The University of Texas at Austin School of Architecture, 2019.

Alvarez, Martín E., Erik E. Martínez-Parachini, Ehsan Baharlou, Oliver David Krieg, Tobias Schwinn, Lauren Vasey, Chai Hua, Achim Menges, and Philip F. Yuan. "Tailored Structures, Robotic Sewing of Wooden Shells." Pages 406–21 in *Robotic Fabrication in Architecture, Art and Design 2018.* Edited by Jan Willmann, Philippe Block, Marco Hutter, Kendra Byrne, and Tim Schork. Zurich: Springer, 2018. doi:10.1007/978-3-319-92294-2.

Apolinarska, Aleksandra Anna. "Complex Timber Structures From Simple Elements: Computational design of novel bar structures for robotic fabrication and assembly." PhD diss., Zurich: Swiss Federal Institute of Technology Zurich (ETHZ), 2018. doi:10.3929/ethz-b-000266723.

Apolinarska, Aleksandra Anna, Matteo Pacher, Hui Li an Nicholas Cote, Rafael Pastrana, Fabio Gramazio, and Matthias Kohler. "Robotic assembly of timber joints using reinforcement learning." *Automation in Construction* 125 (2021): 103569. doi:10.1016/j.autcon.2021.103569.

Baseta, Efilena. "BEND & BLOCK: a shape-adaptable system for the rapid stiffening of active-bending structures." PhD diss., Vienna: University of Applied Arts Vienna, 2019.

Bayer, E., and K. Dooley. *New Techniques for the Generation of Subsurface Models.* Vol. All Days. OTC Offshore Technology Conference. May 1990. doi:10.4043/6295-MS.

Block Research Group. *rhinoVault 2: Funicular Form Finding for Rhinoceros 6+.* 2020. https://github.com/BlockResearchGroup/compas-RV2.

Bonwetsch, Tobias, Fabio Gramazio, and Matthias Kohler. "Digitales Handwerk." In *GAM Architecture Magazine 06.* Edited by Urs Hirschberg. Graz Architektur Magazin Graz Architecture Magazine 6. Springer Vienna, 2010.

Brugnaro, Giulio, and Sean Hanna. "Adaptive Robotic Training Methods for Subtractive Manufacturing." Pages 164–69 in *ACADIA 16: POSTHUMAN FRONTIERS: Data, Designers, and Cognitive Machines.* Proceedings of the 36th Annual Conference of the Association for Computer Aided Design in Architecture (ACADIA). Ann Arbor, 2016.

Chai, Hua, and Philip F. Yuan. "Investigations on Potentials of Robotic Band-Saw Cutting in Complex Wood Structures." Pages 257–70 in *Robotic Fabrication in Architecture, Art and Design 2018.* Edited by Jan Willmann, Philippe Block, Marco Hutter, Kendra Byrne, and Tim Schork. Zurich: Springer, 2018. doi:10.1007/978-3-319-92294-2.

Churkina, Galina, Alan Organschi, Christopher Reyer, Andrew Ruff, Kira Vinke, Zhu Liu, Barbara Reck, T. E. Graedel, and Hans Joachim Schellnhuber. "Buildings as a global carbon sink." *Nature Sustainability 3*, 2020, 269–76. doi:10.1038/s41893-019-0462-4.

Colin Prentice, I., and Harry Helmisaari. "Silvics of north European trees: Compilation, comparisons and implications for forest succession modelling." Modelling Forest Succession in Europe. *Forest Ecology and Management* 42.1 (1991): 79–93. doi:https://doi.org/10.1016/0378-1127(91)90066-5.

Dinwoodie, J. M. *Timber: Its Nature and Behaviour*. London: E & FN SPON Online Taylor & Francis, 2000.

Eek, Piet Hein. "pietheineek.nl." 2022. https://pietheineek.nl/en/product-category/collection/furniture/tabels-en.

European Commission. *A new Circular Economy Action Plan: For a cleaner and more competitive Europe*. Technical report. Brussels, 2020.

European Committee for Standardization (CEN). *Eurocode 5: Design of timber structures – Part 1–1: Common rules and rules for buildings*. Technical report EN 1995-1-1. Brussels, 2004.

———. *Structural timber – Strength classes*. Technical report EN 338:2016. Brussels, 2016.

———. *Timber structures – Structural timber and glued laminated timber – Determination of some physical and mechanical properties*. Technical report EN 408:2010. Brussels, 2012.

European Construction Sector Observatory. *Analytical Report: Improving energy and resource efficiency*. Technical report. Brussels, 2018.

Eversmann, Philipp, Fabio Gramazio, and Matthias Kohler. "Robotic prefabrication of timber structures: towards automated large-scale spatial assembly." Pages 49–60 in *Construction Robotics 1*. 2017. doi:10.1007/s41693-017-0006-2.

Gandía, Augusto, Stefana Parascho, Romana Rust, Gonzalo Casas, Fabio Gramazio, and Matthias Kohler. "Towards Automatic Path Planning for Robotically Assembled Spatial Structures." Pages 60–74 in *Robotic Fabrication in Architecture, Art and Design 2018*. Edited by Jan Willmann, Philippe Block, Marco Hutter, Kendra Byrne, and Tim Schork. Zurich: Springer, 2018. doi:10.1007/978-3-319-92294-2.

Gethmann, Daniel. "Kai Strehlke (Blumer-Lehmann AG) in Conversation with Urs Hirschberg (GAM)." Pages 110–29 in *Wood: Rethinking Material*. Berlin: Jovis Verlag, 2021.

Gilly, David. *Ueber Erfindung, Construction und Vortheile der Bohlen-Dächer: mit besonderer Rücksicht auf die Urschrift ihres Erfinders*. Berlin: Friedrich Vieweg dem Aelteren, 1797.

Gramazio, Fabio, Matthias Kohler, Jan Willmann, Sandra Leittle, and Ralf Jaeger. *The Robotic Touch: How Robots Change Architecture; Gramazio & Kohler Research ETH Zurich 2005–2013*. Zurich: Park Books, 2014.

Graubner, Wolfram. *Holzverbindungen Gegenüberstellungen japanischer und europäischer Lösungen*. Munich: Deutsche Verlags-Anstalt, 2015.

Hart, Jim, and Francesco Pomponi. "More Timber in Construction: Unanswered Questions and Future Challenges." *Sustainability* 12.8 (2021): 58–70. doi:10.3390/su12083473.

Heikkinen, Pekka, and Philip Tidwell. "Designing Through Experimentation: Timber Joints at the Aalto University Wood Program." Pages 60–87 in *Rethinking Wood: Future Dimensions of Timber Assembly*. Edited by Markus Hudert. Basel: Birkhäuser, 2019.

Helm, Volker, Selen Ercan, Fabio Gramazio, and Matthias Kohler. "Mobile Robotic Fabrication on Construction Sites: dimRob*." Pages 4335–41 in *2012 IEEE/RSJ International Conference on Intelligent Robots and Systems*. Vilamoura, 2012. doi:10.1109/IROS.2012.6385617.

Höglmeier, Karin, Gabriele Weber-Blaschke, and Klaus Richter. "Evaluation of Wood Cascading." Pages 335–46 in *Sustainability Assessment of Renewables-Based Products: Methods and Case Studies*. Edited by Jo Dewulf, Steven De Meester, and Rodrigo A. F. Alvarenga. John Wiley & Sons, Ltd., 2015. doi:10.1002/9781118933916.ch22.

Hornung, Philipp. "Robotic Fabrication at the Angewandte Robotics Lab (ARL)." Pages 180–89 in *Conceptual Joining: Wood Structures from Detail to Utopia*. Edited by Lukas Allner, Christoph Kaltenbrunner, Daniela Kröhnert, and Philipp Reinsberg. Basel: Birkhäuser, 2022.

Hua, Hao, Ludger Hovestadt, and Peng Tang. "Optimization and prefabrication of timber Voronoi shells." *Structural and Multidisciplinary Optimization* 61 (2020): 1897–911. doi:10.1007/s00158-019-02445-x.

Jahn, Gwyllim, Andrew John Wit, and James Pazzi. "[BENT]." Pages 438–47 in *ACADIA 19: UBIQUITY AND AUTONOMY*. Proceedings of the 39th Annual Conference of the Association for Computer Aided Design in Architecture (ACADIA). Austin: The University of Texas at Austin School of Architecture, 2019.

Johns, Ryan Luke, and Nicholas Foley. "Bandsawn Bands: Feature-Based Design and Fabrication of Nested Freeform Sufaces in Wood." Pages 17–32 in *Robotic Fabrication in Architecture, Art and Design 2014*. Edited by Wes McGee and Monica Ponce de Leon. Cham: Springer, 2014. doi:10.1007/978-3-319-04663-1.

Kaufmann, Hermann. *Manual of Multi-Storey Timber Construction*. Munich: DETAIL, 2018.

Kramberger, Aljaz, Anja Kunic, Iñigo Iturrate, Christoffer Sloth, Roberto Naboni, and Christian Schlette. "Robotic Assembly of Timber Structures in a Human-Robot Collaborative Setup." *Frontiers in Robotics and AI* 8 (2022). doi:10.3389/frobt.2021.768038.

Krieg, Oliver David, Zachary Christian, David Correa, Achim Menges, Steffen Reichert, Katja Rinderspacher, and Tobias Schwinn. "Hygroskin: Meteorosensitive Pavilion." Pages 272–79 in *Fabricate 2014: negotiating design and making*. Edited by Fabio Gramazio, Matthias Kohler, and Silke Langenberg. London: UCL Press, 2017. doi:10.14324/111.9781787352148.

Kunic, Anja, Roberto Naboni, Aljaz Kramberger, and Christian Schlette. "Design and assembly automation of the Robotic Reversible Timber Beam." *Automation in Construction* 123 (2021): 103531. doi:10.1016/j.autcon.2020.103531.

Lee, Juney, and Tom Van Mele. *compas 3gs: 3D graphic statics package for the COMPAS framework*. 2019. https://github.com/compas-dev/compas_3gs.

Lendager, Anders. *Solution: Circular Buildings*. Copenhagen: Danish Architectural Press Arkitektens Forlag, 2020.

Leung, Pok Yin Victor, Aleksandra Anna Apolinarska, Davide Tanadini, Fabio Gramazio, and Matthias Kohler. "Automatic Assembly of Jointed Timber Structure using Distributed Robotic Clamps." Pages 583–92 in *PROJECTIONS*. Proceedings of the 26th International Conference of the Association for Computer-Aided Architectural Design Research in Asia (CAADRIA). Edited by Anastasia Globa, Jeroen van Amoijde, Adam Fingrut, Nayeon Kim, and Tian Tian Sky Lo. Vol. 1. Hong Kong: The Chinese University of Hong Kong, 2021.

Liu, Yulun, Yao Lu, and Masoud Akbarzadeh. "Kerf Bending and Zipper in Spatial Timber Tectonics: A Polyhedral Timber Space Frame System Manufacturable by 3-Axis CNC Milling Machine." In *ACADIA 21: Realignments: Toward Critical Computation*. Proceedings of the 41st Annual Conference of the Association for Computer Aided Design in Architecture (ACADIA). 2021.

Mair, Claudia, and Tobias Stern. "Cascading Utilization of Wood: a Matter of Circular Economy?" *Current Forestry Reports 3*, 2017, 281–95. doi:10.1007/s40725-017-0067-y.

Meissner, Irene. *Frei Otto: forschen, bauen, inspirieren = a life of research, construction and inspiration*. Munich: DETAIL, 2015.

Mele, Tom Van, and many others. *COMPAS: A framework for computational research in architecture and structures. COMPAS 1.14.1 (v1.14.1)*. http://compas.dev, 2022. doi:10.5281/zenodo.2594510.

Menges, Achim, and Jan Knippers. *Architecture Research Building: ICD/ITKE 2010-2020*. Basel: Birkhäuser, 2020.

Müller, Christian. *Holzleimbau = Laminated Timber Construction*. Basel, Berlin, Boston: Birkhauser, 2000.

Najari, Arman, Elliott Santos, Yuchen Chen, Ewald Jooste, Ardeshir Talaei, Eduardo Chamorro, Anuj Mittal, Alexandre Dubor, Aldo Sollazzo, Kunaljit Chadha, and Raimund Krenmüller. "Good Wood: Robotic Upcycling." 2018. https://www.iaacblog.com/programs/good-wood-robotic-upcycling/.

Nii, Koichi. *The Complete Japanese Joinery*. Point Roberts, WA: Hartley & Marks, 1995.

Ormondroyd, Graham Alan, Morwenna Spear, and Campbell Skinner. "The Opportunities and Challenges for Re-use and Recycling of Timber and Wood Products Within the Construction Sector." Pages 45–103 in *Environmental Impacts of Traditional and Innovative Forest-based Bioproducts*. Edited by Andreja Kutnar and Subramanian Muthu. Vol. 12. Environmental Footprints and Eco-design of Products and Processes 8. Singapore: Springer, 2021. doi:10.1007/978-981-10-0655-5_3.

Österlund, Toni, and Markus Wikar. "Freeform Timber Structures: Digital Design and Fabrication." Pages 132–49 in *Rethinking Wood: Future Dimensions of Timber Assembly*. Edited by Markus Hudert. Basel: Birkhäuser, 2019.

Pastrana, Rafael, Patrick Ole Ohlbrock, Pierluigi D'Acunto, and Stefana Parascho. *COMPAS CEM: The Combinatorial Equilibrium Modeling framework for COMPAS*. 2021. doi:10.5281/zenodo.5705740.

———. *Constrained Form-Finding of Tension-Compression Structures Using Automatic Differentiation*. 2021. doi:10.48550/arXiv.2111.02607.

Piker, Daniel. "Kangaroo: Form Finding with Computational Physics." Pages 136–37 in *Computation Works: The Building of Algorithmic Thought*. Edited by Brady Peters. London: John Wiley & Sons, 2013.

Poteschkin, Viktor, Jürgen Graf, Stefan Krötsch, and Wenchang Shi. "Recycling of Cross-Laminated Timber Production Waste." Pages 100–12 in *Research Culture in Architecture: Cross-Disciplinary Collaboration*. Edited by Cornelie Leopold. Basel: Birkhäuser, 2020. doi:10.1515/9783035620238-010.

Raith, Karin. "Wood Construction – On the Renewal of an Ancient Art." Pages 96–107 in *Conceptual Joining: Wood Structures from Detail to Utopia*. Edited by Lukas Allner, Christoph Kaltenbrunner, Daniela Kröhnert, and Philipp Reinsberg. Basel: Birkhäuser, 2022.

Reinhardt, Frank, and Franz Makeschinr. "Historische Waldumbauversuche mit Rotbuche in Form der „Grünen Augen" im Thüringer Forstamt Hummelshain: Entstehungsgeschichte und aktuelle Bedeutung." *Forstwissenschaftliches Centralblatt vereinigt mit Tharandter forstliches Jahrbuch 120*, 2001, 318–30. doi:10.1007/BF02796103.

Rippmann, Matthias, and Philippe Block. "Funicular Shell Design Exploration." Pages 337–46 in *ACADIA 13: Adaptive Architecture*. Proceedings of the 33rd Annual Conference of the Association for Computer Aided Design in Architecture (ACADIA). Cambridge, 2013.

Robeller, Christopher, and Niklas von Haaren. "Recycleshell: Wood-only Shell Structures Made From Cross-Laminated Timber (CLT) Production Waste." *Journal of the International Association for Shell and Spatial Structures* 61 (2020): 125–39. doi:10.20898/j.iass.2020.204.045.

Robeller, Christopher, and Yves Weinand. "Integral joints for timber folded plate structures." Pages 73–83 in *Advancing Wood Architecture: A computational approach*. Edited by Achim Menges, Tobias Schwinn, and Oliver David Krieg. New York: Routledge, 2017.

Robeller, Christopher, Yves Weinand, Volker Helm, Andreas Thoma, Fabio Gramazio, and Matthias Kohler. "Robotic Integral Attachment." Pages 92–97 in *Fabricate 2017: rethinking design and construction*. Edited by Achim Menges, Bob Sheil, Ruairi Glynn, and Marilena Skavara. London: UCL Press, 2017. doi:10.14324/111.9781787350014.

Roswag-Klinge, Eike. "Designing Natural Buildings." Pages 236–46 in *Research Culture in Architecture: Cross-Disciplinary Collaboration*. Edited by Cornelie Leopold. Basel: Birkhäuser, 2020. doi:10.1515/9783035620238-023.

Salas, Jasser, Soroush Garivani, Elena Kavtaradze Amin Ziaie Bigdeli, Yasmina El Helou, Timothy Magara, Lars Erik Elseth, Alexandre Dubor, Aldo Sollazo, Kunaljit Chadha, and Raimund Krenmüller. "Sourced Wood." 2018. https://www.iaacblog.com/programs/sourced-wood/.

Satterfield, Blair, Alexander Preiss, Derek Mavis, Graham Entwistle, Marc Swackhamer, and Matthew Hayes. "Bending the Line: Zippered wood creating non-orthogonal architectural assemblies using the most common linear building component (THE 2x4)." Pages 58–65 in *Fabricate 2020: making resilient architecture*. Edited by Jane Burry, Jenny Sabin, Bob Sheil, and Marilena Skavara. London: UCL Press, 2020. doi:10.14324/111.9781787358119.

Schindler, Christoph. "Ein architektonisches Periodisierungsmodell anhand fertigungstechnischer Kriterien, dargestellt am Beispiel des Holzbaus." PhD diss., Zurich: Swiss Federal Institute of Technology Zurich (ETHZ), 2009.

Schleicher, Simon, Riccardo La Magna, and Jan Knippers. "Bending-Active Plates: Planning and Construction." Pages 242–49 in *Fabricate 2017: rethinking design and construction*. Edited by Achim

Menges, Bob Sheil, Ruairi Glynn, and Marilena Skavara. London: UCL Press, 2017. doi:10.14324 / 111.9781787350014.

Schwinn, Tobias. "Landesgartenschau Exhibition Hall." Pages 111–24 in *Advancing Wood Architecture: A computational approach*. Edited by Achim Menges, Tobias Schwinn, and Oliver David Krieg. New York: Routledge, 2017.

Shapiro, Vadim. "Chapter 20 - Solid Modeling." Pages 473–518 in *Handbook of Computer Aided Geometric Design*. Edited by Gerald Farin, Josef Hoschek, and Myung-Soo Kim. Amsterdam: North-Holland, 2002. doi:https://doi.org/10.1016/B978-044451104-1/50021-6.

Søndergaard, Asbjørn, Oded Amir, Philipp Eversmann, Luka Piskorec, Florin Stan, Fabio Gramazio, and Matthias Kohler. "Topology Optimization and Robotic Fabrication of Advanced Timber Space-Frame Structures." Pages 190–203 in *Robotic Fabrication in Architecture, Art and Design 2016*. Edited by Dagmar Reinhardt, Rob Saunders, and Jane Burry. Zurich: Springer, 2016. doi:10.1007/978-3-319-26378-6.

Stehling, Hanno, Fabian Scheurer, and Jean Roulier. "Bridging the Gap from CAD to CAM: Concepts, Caveats and a new Grasshopper Plug-In." Pages 52–60 in *Fabricate 2014: negotiating design and making*. Edited by Fabio Gramazio, Matthias Kohler, and Silke Langenberg. London: UCL Press, 2017. doi:10.14324/111.9781787352148.

Stehling, Hanno, Fabian Scheurer, Jean Roulier, Hélori Geglo, and Mathias Hofmann. "From Lamination to Assembly: Modelling the Seine Musicale." Pages 258–63 in *Fabricate 2017: rethinking design and construction*. Edited by Achim Menges, Bob Sheil, Ruairi Glynn, and Marilena Skavara. London: UCL Press, 2017. doi:10.14324/111.9781787350014.

Stehling, Hanno, Fabian Scheurer, and Sylvain Usai. "Large-Scale Free-From Timber Grid Shell: Digital Planning of the new Swatch Headquarters in Biel, Switzerland." Pages 210–17 in *Fabricate 2020: making resilient architecture*. Edited by Jane Burry, Jenny Sabin, Bob Sheil, and Marilena Skavara. London: UCL Press, 2020. doi:10.14324/111.9781787358119.

Strehlke, Kai. "Aspekte der Geometrie in der Planung von Vor- und Bauprojekt." Pages 59–65 in *Architektur fertigen: Konstruktiver Holzelementbau*. Edited by Mario Rinke and Martin Krammer. Zurich: Triest Verlag, 2020.

Sunshine, Gil. "Medium Resolution." 2021. https://marchthesis.mit.edu/Medium-Resolution.

Svilans, Tom. "Integrated material practice in free-form timber structures." PhD diss., Copenhagen: The Royal Danish Academy of Fine Arts, 2020.

Takabayashi, Hiroki, Kado Keita, and Gakuhito Hirasawa. "Versatile Robotic Wood Processing Based on Analysis of Parts Processing of Japanese Traditional Wooden Buildings." Pages 222–32 in *Robotic Fabrication in Architecture, Art and Design 2018*. Edited by Jan Willmann, Philippe Block, Marco Hutter, Kendra Byrne, and Tim Schork. Zurich: Springer, 2018. doi:10.1007/978-3-319-92294-2.

Thoma, Andreas, Arash Adel, Matthias Helmreich, Thomas Wehrle, Fabio Gramazio, and Matthias Kohler. "Robotic Fabrication of Bespoke Timber Frame Modules." Pages 448–59 in *Robotic Fabrication in Architecture, Art and Design 2018*. Edited by Jan Willmann, Philippe Block, Marco Hutter, Kendra Byrne, and Tim Schork. Zurich: Springer, 2018. doi:10.1007/978-3-319-92294-2.

Thoma, Andreas, David Jenny, Matthias Helmreich, Augusto Gandia, Fabio Gramazio, and Matthias Kohler. "Cooperative Robotic Fabrication of Timber Dowel Assemblies." Pages 77–87 in *Research Culture in Architecture: Cross-Disciplinary Collaboration*. Edited by Cornelie Leopold. Basel: Birkhäuser, 2020. doi:10.1515/9783035620238-008.

Thüringer Ministerium für Infrastruktur und Landwirtschaft (TMIL). *Waldzustandsbericht 2019: Forstliches Umweltmonitoring in Thüringen*. Technical report. Erfurt, 2020.

Tutsch, Joram F. "Weitgespannte Lamellendächer der frühen Moderne: Konstruktionsgeschichte, Geometrie und Tragverhalten." PhD diss., Munich: Technical University of Munich, 2020.

Vamza, Ilze, Fabian Diaz, Peteris Resnais, Antra Radzina, and Dagnija Blumberga. "Life Cycle Assessment of Reprocessed Cross Laminated Timber in Latvia." *Environmental and Climate Technologies* 25.1 (2021): 58–70. doi:10.2478/rtuect-2021-0005.

Vercruysse, Emmanuel, Zachary Mollica, and Pradeep Devadass. "Altered Behaviour: The Performative Nature of Manufacture: Chainsaw Choreographies + Bandsaw Manoeuvres." Pages 309–19 in *Robotic Fabrication in Architecture, Art and Design 2018*. Edited by Jan Willmann, Philippe Block, Marco Hutter, Kendra Byrne, and Tim Schork. Zurich: Springer, 2018. doi:10.1007/978-3-319-92294-2.

Vestartas, Petras. "Design-to-Fabrication Workflow for Raw-Sawn-Timber using Joinery Solver." PhD diss., Swiss Federal Institute of Technology Lausanne (EPFL), 2021.

Vestøl, Geir, Carolin Fischer, Ludvig Fjeld, and Audun Øvrum. "Bending Properties and Strength Grading of Norway Spruce: Variation within and between Stands." *Canadian Journal of Forest Research* 44 (February 2014): 128–35. doi:10.1139/cjfr-2013-0187.

Wagner, Hans Jakob, Martin Alvarez, Ondrej Kyjanek, Zied Bhiri, Matthias Buck, and Achim Menges. "Flexible and transportable robotic timber construction platform – TIM." *Automation in Construction* 120 (2020): 16–23. doi:10.1016/j.autcon.2020.103400.

Weinand, Yves. *Advanced Timber Structures: Architectural Design and Digital Dimensioning*. Basel: Birkhäuser, 2017.

Wenzel, Anett, Nico Frischbier, Jürgen Schwerhoff, and Frank Wittau. *Bundeswaldinventur 3 im Freistaat Thüringen*. Technical report. Erfurt: ThüringenForst – Anstalt öffentlichen Rechts, 2015.

Willmann, Jan. "Digitale Revolution im Holzbau: Roboter, Narration, Entwurf." Pages 137–42 in *Architektur fertigen: Konstruktiver Holzelementbau*. Edited by Mario Rinke and Martin Krammer. Zurich: Triest Verlag, 2020.

Willmann, Jan, Fabio Gramazio, and Matthias Kohler. "New paradigms of the automatic: Robotic timber construction in architecture." Pages 13–27 in *Advancing Wood Architecture: A computational approach*. Edited by Achim Menges, Tobias Schwinn, and Oliver David Krieg. New York: Routledge, 2017.

Willmann, Jan, Michael Knauss, Tobias Bonwetsch, Anna Aleksandra Apolinarska, Fabio Gramazio, and Matthias Kohler. "Robotic timber construction: Expanding additive fabrication to new dimensions." *Automation in Construction* 61 (2016): 16–23. doi:10.1016/j.autcon.2015.09.011.

Wójcik, Marcin, and Jan Strumiłło. "Behaviour-based Wood Connection as a Base for New Tectonics." Pages 170–84 in *Proceedings of the 20th Annual International Sustainable Development Research Conference*. Edited by Martina Keitsch. Resilience: the New Research Frontier. Trondheim: Norwegian University of Science; Technology, June 2014. doi:https://doi.org/10.21427/D71R50.

Wood, Dylan, Philippe Grönquist, Simon Bechert, Lotte Aldinger, David Riggenbach, Katharina Lehmann, Markus Rüggeberg, Ingo Burgert, Jan Knippers, and Achim Menges. "From Machine Control to Material Programming: Self-Shaping Wood Manufacturing of a High Performance Curved CLT Structure – Urbach Tower." Pages 50–57 in *Fabricate 2020: making resilient architecture*. Edited by Jane Burry, Jenny Sabin, Bob Sheil, and Marilena Skavara. London: UCL Press, 2020. doi:10.14324/111.9781787358119.

Yuan, Philip F., Hua Chai, Chao Yan, and Jin Jiang Zhou. "Robotic Fabrication of Structural Performance-based Timber Gridshell in Large-Scale Building Scenario." Pages 196–205 in *ACADIA 16: POSTHUMAN FRONTIERS: Data, Designers, and Cognitive Machines*. Proceedings of the 36th Annual Conference of the Association for Computer Aided Design in Architecture (ACADIA). Ann Arbor, 2016.

Zwerger, Klaus. *Wood and Wood Joints: Building Traditions of Europe, Japan, and China*. Basel: Birkhäuser, 2011.